THE DESIGN, DEVELOPMENT AND OPTIMIZATION OF MECHANICAL CONNECTION SYSTEMS IN SANDWICH PANEL CONSTRUCTION

Adham M. Khalil

A THESIS

in the

Faculty of Engineering

Presented in Partial Fulfilment of the Requirements for the Degree of Doctor of Engineering at
Sir George Williams University
Montreal, Canada

September, 1973

To my wife NEVINE,

and my children NIHAL and MOHAMED,

without whose encouragement, patience and sacrifice, this work would not have been done.

A B S T R A C T

THE DESIGN, DEVELOPMENT AND OPTIMIZATION OF MECHANICAL CONNECTION SYSTEMS IN SANDWICH PANEL CONSTRUCTION

by

Adham M. Khalil

A B S T R A C T

This work is concerned with the design and development of mechanical connection systems for load-bearing sandwich panels used in frameless construction. In order to overcome the disadvantages of the existing connection systems, the Laced Connection was proposed.

The development of a process, by which an invention of a connection could be taken from its conceptual stage to the stage of its application, was part of this study.

In the process of optimizing the Laced Connection System, four new concepts were developed as alternate solutions to the problem of connections.

New techniques for the determination of fringe values in photoelasticity were introduced when optimizing the sections of the Laced Connection System.

ACKNOWLEDGEMENTS

A C K N O W L E D G E M E N T S

The author wishes to express his gratitude to his thesis supervisor, Dr. P.P. Fazio, Chairman of the Civil Engineering Department and Director of the Systems Building Center at Sir George Williams University, who provided the guidance, stimulus and valuable advice throughout the course of the research work.

The financial support of La Formation de Chercheurs et d'Action Concertée du Quebec, and The National Research Council of Canada, Account No: A-4770, is also gratefully acknowledged.

The author wishes to thank all the members of the Systems Building Group, the staff of the Structures Laboratory and the Machine Shop for their assistance, and wishes to thank Mrs. M. Schoofs, and Miss M. Stredder for typing his thesis.

TABLE OF CONTENTS

TABLE OF CONTENTS

LIST OF TABLES

L I S T O F T A B L E S

LIST OF FIGURES

L I S T O F F I G U R E S

NOTATIONS

NOTATIONS

A_c	Effective Cross-Section of Cable
D	Maximum Deviation of External Dimensions
E_c	Modulus of Elasticity of Cable Material
K	Constant
L	Original Length of Panel
L_{cc}	Length of Cable per Cycle
L_{co}	Initial Length of Cable
L_{ec}	Length of Cable Ends
L_{ef}	Maximum Change in Cable End Length
L_{em}	Maximum Change in Length of Extrusion
L_{fc}	Maximum Change in Cable Length per Cycle
L_{ib}	Total Increase in Cable Length
L_{oc}	Maximum Change in Length of Cable per Joint
L_{rcl}	Relative Change in Cable Length
N	Fringe Order
P	Applied Load
S_{su}	Minimum Opening Between Panels
S_w	Maximum Opening of Joint
S_{wp}	Increase in Distance Between Rows of Pins
T_c	Change in Cable Tension
T_{ct}	Total Change in Length Due to Thermal Effects
T_d	Design Tension in Lacing Cable
T_i	Installation Tension of Cable

T_{ib}	Total Change in Length Due to Bending Alone
T_{wd}	Increase in Tension Due to Wind
c	Relative Optic Coefficient
d	Permissible Deviation in Dimension of Building
f_σ	Material Fringe Value
f	Frequency of Light
h	Material Thickness
l	Typical Length Dimension
n	Number of Panels in One Run
p	Permissible Deviation in Panel Size
t_c	Temperature at Centre of Panel
t_i	Temperature at Inner Surface of Panel
t_{in}	Minimum Inside Temperature of Building
t_{ix}	Maximum Inside Temperature of Building
t_o	Temperature in Outer Surface of Panel
t_{os}	Maximum Outside Summer Temperature
t_{ow}	Minimum Winter Temperature
t_s	Installation Temperature
$\hat{t}_{cm}$	Maximum Predicted Cable Temperature
$\hat{t}_{cn}$	Minimum Predicted Cable Temperature
x_p	Distance Between Rows of Pins in Connection

α_p	Coefficient of Thermal Expansion of Panel Surface
α_c	Coefficient of Thermal Expansion of Cable
α_e	Coefficient of Thermal Expansion of Extrusion Material
α	Coefficient of Thermal Expansion of Panel Material
Δt	Maximum Possible Change in Temperature
Δ	Relative Retardation
δ_o	Increase in Length of Outer Surface of Panel
δ_i	Decrease in Length of Inner Surface of Panel
δ_L	Total Change in Length due to Temperature Change
θ	Bending Angle of Panels
λ	Wave Length of Light
σ	Stress at a Point
∇^2	The Operator $[\frac{\partial^2}{\partial x^2} + \frac{\partial^2}{\partial y^2}]$

SUBSCRIPTS

G	Green
R	Red
Y	Yellow
x	Point "x"
c	Point "c"
m	Model
p	Prototype
x, y	Directions
1, 2	Directions of Principal Stresses

C H A P T E R I

INTRODUCTION

CHAPTER I

INTRODUCTION

One of the main factors why the advantages of panelized sandwich construction has not been more fully exploited in the past has been the lack of effective connection systems. To overcome the disadvantages of the existing connection systems the Laced Connection was introduced by Fazio [1]. Because of the drawbacks that are usually associated with the first prototype, a need was recognized for:

(i) The establishment of a process whereby an invention of a connection could be taken from its conceptual stage to the stage of application, and

(ii) The creation of an environment whereby new ideas on connections would develop.

This study was undertaken to develop and create the process and environment referred to above. A series of tests were established to assess the performance of a new connection. These tests were carried out on the Laced Connection System. The results were used to revise the arrangements and optimize the components of that connection. The optimization was carried out using the photoelastic method - in the course of the optimization new techniques on the evaluation of fringe values were introduced.

In the process of optimizing the Laced Connection System, four new concepts were developed as alternative solutions. The particular solution to be adopted for a specific application can be determined after having compared the requirements of the application and the merits of the connections. This last step could form the basis of further detailed studies.

Some of the problems with joints are discussed and the requirements of an ideal system are given in Chapter II. Available connection systems are described in Chapter III.

A description of the tests performed on the Laced Connection System and the techniques used in the optimization of this connection is given in Chapter IV.

Four new connection systems are introduced in Chapter V.

C H A P T E R II

PROBLEMS AND REQUIREMENTS OF JOINTS

C H A P T E R II

PROBLEMS AND REQUIREMENTS OF JOINTS

2.1 GENERAL

Some of the problems in joints are discussed in this Chapter. Among these problems are the effect of tolerances in the individual components on the final size of the building, problems with seals and the effect of internal and external temperatures of buildings on joints. The requirements of connection systems are also given.

2.2 TOLERANCES AND THEIR EFFECT ON BUILDING SYSTEMS

When standardized sandwich panels are mass produced, they will have to be manufactured with low tolerances so that these will be assembled with a minimum of dimensional problems. Fortunately, with structural sandwich panels, a conventional frame is not present in the building and therefore, the panels are not manufactured to fill up the gaps between the various components in space. The procedure in the assembly is of the additive locational type. This type of assembly is discussed by Eden and Seymour-Walker [2]. It offers the advantage that the components are assembled to one another to form the resulting structure rather than fill up the gap between points. The joint for each component is

pulled up tight before the next component is added, and the overall size of the assembly is the sum of the size of the components.

The overall maximum deviation in the external dimension of a building is given in [3] as

$$D = \sqrt{np^2 + d^2} \qquad (2.1)$$

where D is the maximum deviation in external dimension.

n is the number of panels in one run.

$\pm$ p is the permissible deviation in panel size.

$\pm$ d is the permissible deviation in the dimension of building.

2.3 JOINT MOVEMENT

In panelized buildings having a frame, the joints have to be designed not only to be able to have the panels fit into the frame as described by Bonshor et al [3], but also to allow for movements. In frameless panelized buildings however, only the joint movements have to be taken into consideration in the design of the seals.

There are two types of movements in buildings: one reversible and one irreversible. The settling of a building is an irreversible movement and its deflection under permanent load and its creep fall under this category. Reversible

movements include thermal changes and wind loads. If the irreversible movements are very small, they may not affect the sealant, especially if they occur slowly and can be neglected. The reference by Skempton [4] may be used as a guide to determine movements due to settlement. Deformations due to wind load are normally evaluated when a building is designed, Lewicki [5] is one among many references that show how these deformations are evaluated.

2.4 THERMAL DEFORMATIONS

Two types of thermal deformations occur in buildings.

(i) Length change

(ii) Bending

2.4.1 Length Change

A panel such as the one shown in Figure 2.1 undergoes a longitudinal change in length due to a change in temperature in the surrounding air. This change in length has no effect on the sealant of the joint since the panels are not restrained from motion by intermediate frames.

The total change in length due to temperature change as given in [6] is

$$\delta_L = L. \alpha. \Delta t$$

where δL is the total change in length

L is the original length of the panel

α is the coefficient of thermal expansion of the panel

Δt is the maximum possible change in temperature

2.4.2 Bending

Due to the difference between the temperature of the two surfaces of a panel one of the surfaces will elongate more than the other, as shown in Figure 2.2.

This bending will cause the seals in the joint either to be compressed more than when installed or will cause some of the compressive force to be released or may even produce tension in the seal. The outer surface of the building is the important surface to be considered in the design of seals. Referring to Figure 2.2 and assuming that the panels are symmetrical about a central axis a-a, and that the temperature distribution in the panel material follows a linear relationship, the temperature at the centre of the panel would be

$$t_c = \frac{t_o - t_i}{2} + t_i \qquad t_o > t_i$$

where t_c is the temperature at the centre of the panel

t_i is the temperature at the inner surface of the panel

t_o is the temperature at the outer surface of the panel

The increase in length of the outer surface of the panel is

$$\delta_o = L.\ \alpha_p(t_o - t_s)$$

where δ_o is the increase in length of the outer surface of the panel

α_p is the coefficient of thermal expansion of the surfaces of the panel

t_s is the temperature of the atmosphere when the panels are installed

and

$$\delta_i = L.\ \alpha_p(t_s - t_i)$$

where δ_i is the decrease in length of the inner surface of the panel

The maximum opening of the outer surface would occur in winter when the temperature inside the building would be greater than that outside. The maximum opening is

$$S_w = (\delta_i - \delta_o).$$

or

$$S_w \triangleq L.\ \alpha_p(t_{ix} - t_{ow}) \qquad (2.2)$$

where S_w is the maximum opening of the joint

T_{ow} is the minimum winter temperature

t_{ix} is the maximum inside temperature of the building

If the minimum opening occurs in summer, this would be "S_{su}".

$$S_{su} = (\delta_o - \delta_i)$$

or

$$S_{su} = L.\ \alpha_p (t_{os} - t_{in}) \qquad (2.3)$$

where t_{os} is the maximum outside temperature in summer

t_{in} is the minimum inside temperature in the building

In selecting an external seal for the building, one should check that the seal will be effective with the movements. Karpati [7] gives the movement capabilities of some generic seals.

In placing the seal, special attention should be made to the adhesion of the seal to the panels. The manufacturer's recommendations have to be followed in surface preparation and priming to ensure proper sealing when the seal is in tension.

When selecting the seal for a building, one should make sure that the seal will be effective and maintain its flexibility when the temperature is low.

The temperature at which the seal is installed is another important factor in obtaining an efficient seal.

Manufacturer's recommendations should be followed for best results. If the temperature, when installing the seal, is lower than recommended the sealant will mainly work in compression. In this case the seal will probably not fail in tension since its ultimate tensile stress will not be reached. In the case of higher temperatures than recommended the size of the joint has to be increased by a factor depending on the excess of the temperatures of the environment over the recommended range of installation temperatures.

2.5 REQUIREMENTS OF CONNECTION SYSTEMS

The connections between sandwich panels are a problem of paramount importance. A design should not diminish the advantages that the sandwich construction offers.

Structurally, connecting systems should be designed as given in [1], to carry and transmit:

(i) Transverse and longitudinal shears
(ii) Direct tension and compression
(iii) Stresses between load-bearing panels
(iv) Bending moments.

In designing the connections one should note

(v) The different positions of the connections in the system as shown in Figures 2.3 and 2.4

and emphasis should be made on

(vi) Aesthetics

(vii) Insulation from weather factors (water and vapour)

(viii) Sound insulation

(ix) Thermal insulation

(x) Fire resistance

(xi) Ease in erection

(xii) Economy of production.

Connection systems were introduced in the past in an attempt to resolve the above problems. A number of typical examples are reviewed in the next chapter.

C H A P T E R III

REVIEW OF TYPICAL CONNECTION SYSTEMS

C H A P T E R III

REVIEW OF TYPICAL CONNECTION SYSTEMS

Connection systems may be classified as discrete or continuous. In the discrete system, the connecting mechanisms are placed at certain points along the sides of the panels. Stresses are transmitted through these points from panel to panel. In the continuous system, the connecting mechanism acts along the entire edge of the panels. Stresses are transmitted from panel to panel through the entire connecting edge.

3.1 DISCRETE CONNECTIONS

The system patented by Adams [8] in 1907 is one of the earliest. This system, shown in Figure 3.1, was used to connect partition panels. The hook-shaped element placed along the edge of one panel hooks into a plate with an opening on the mating panel edge. To unlock the panels a rod is introduced through the hole shown on the side. Among the disadvantages of this system are:

(i) The panels must be brought in contact before they may be connected.

(ii) There is little control on the joining force between the panels.

(iii) When the panels are joined, the walls will have protrusions at the junctions.

The connection patented by Thelander [9] in 1953, is shown in Figure 3.2. In this connection, a series of inter-connected spring loaded hooks placed on one panel hook onto pins on the mating panel edge. In this sytem, a rod accessible at the corners of the panels is used for mounting or dismantling of the panels. The disadvantages here, lie in:

(i) The complexity of the parts and the precision required in their manufacturing process.

(ii) The panels must be brought in contact before they can be connected.

(iii) Little control over the joining force between the panels.

Jones [10] patented a simple version of the hook mechanism. This is shown in Figure 3.3. A key, introduced from the panel facing, is used to turn the hook which fits into a spring loaded part with a hole which is fixed to the mating panel. Some of the disadvantages here are:

(i) The panels must be brought into contact with each other before they may be connected.

(ii) No control over the joining forces between the panels exist.

(iii) Perforations are visible along the edges of the panels to allow for the introduction of the key.

Figure 3.4 shows the fastener patented by Palfey et al [11] which also utilizes a hook in one panel that grips onto a pin on the mating panel. This is another version of the mechanism patented by Jones [10]. It has the same disadvantages as those in the Jones mechanism.

3.2 CONTINUOUS CONNECTIONS

The connector patented by Logan [12] and shown in Figure 3.5 falls into the category of continuous connection systems. This connection makes the mounting and dismantling of non-load-bearing panels a relatively simple matter. Parts 24 and 26 are bent to allow the edge of the panels (Parts 34) to fit into the connection. This connection system has the disadvantages that:

(i) It offers no resistance to tension or bending at the joint.

(ii) It has a low resistance to shear.

(iii) It may be used only for non-load-bearing panels.

Figure 3.6 shows the connection system patented by Harvey [13]. This system is used for interlocking decks or mating surfaces for roadways and airfields. Some modifications must be made to have this connection suitable for buildings. In its present state, this system is very sensitive to bending, simple shear and tension. In the second part of his patent, (Fig. 3.7), Harvey [13] introduces another alternative. In the modified system, the extrusion shown in the upper part of the figure, is the connecting element between the panels. The panels have to be brought into contact with one another before the extrusion may be introduced. The connection will still be sensitive to bending but will be able to resist tensile, as well as shear loads. A groove on the surfaces at the connecting edge, will be visible. This might have an effect on the aesthetics of a wall. A thermal bridge between the outer surfaces of the panels exist in this system.

The connection system patented by Morgan et al [14] and shown in Figure 3.8, is a modified version of that patented by Harvey [13]. This former system connects the surfaces of the adjoining panels, improving the resistance of the joint to bending stresses. In this system, the panels have to be

brought into contact before the outer extrusions will be able to be introduced. There are two main disadvantages in this connection: lack of tolerance and lack of a mechanism to provide prestress between the panels.

Fazio et al [15] have introduced a number of continuous connection systems. Some of these are shown in Figures 3.9 to 3.12. In these connections, the edges of the panels are covered by metallic extrusions extending to the sides of the panels below the skin, plates or angles are placed at the junctions. These plates are bolted to the metallic extrusions. In these connection systems, the loads are carried entirely by the joining angles. The exposed angles are not aesthetically pleasing.

Fazio et al [16] have also introduced the Channel Connection System shown in Figure 3.13. In this connection, the panels are introduced into the extrusion shown. Staples are used to form the junction between the panels and the extrusions. In this system, a thermal bridge exists between the surfaces of the panels. Some tests were carried out on a model building using the Channel Connection System stapled to sandwich panels [17]. Other connection systems may be found in References [18] and [19].

The above connection systems have many drawbacks. Among these are:

(i) The need to bring the panels into contact before the connection can be made, (in some cases the panels must be pushed towards each other).

(ii) The discrete connections cause stress concentrations.

(iii) The continuous connections have a thermal bridge and an external connecting member.

In an attempt to improve over the existing systems, Fazio [1] has introduced the Laced Connection System.

3.3 THE LACED CONNECTION SYSTEM

This connection was introduced originally for sandwich panels. These panels usually have reinforcing frames along their edges to stiffen the peripheral area against delamination and to facilitate the connections between adjacent panels. This frame was used to house the Laced Connection System.

A metallic extrusion is integrated into the frames of the panels. Figure 3.14 shows the cross-sections of the female extrusion proposed by Fazio [1]. Figure 3.15 shows the cross-section of the male extrusion. Two male extrusions are connected to each other by a cable, or lace, passing

over pins placed in the extrusions. Figure 3.16 shows the edges of two panels being drawn to each other by the lacing cable. The cable is anchored at one end of a panel, it is laced back and forth between the two panels and is pulled outwards from the other end of the panel. Figure 3.17 shows a cross-section through the edges of adjacent panels. A prestressing force is created at the joint by increasing the tension in the lacing cable. It should be noted that with this system there is no thermal bridge between the faces of each panel.

Intersections may occur between walls or between floors and walls (Figures 2.3 and 2.4). In such cases, an intermediate member also called the cross-member embodying a special extrusion (Figure 3.18) is used to connect the intersecting panels. Figures 3.19 and 3.20 show how intersecting members may be connected.

A number of drawbacks, such as the high friction between cable and pins and the large quantity of material required, were associated with the prototype of this proposed connection system. A need was recognized to establish the performance and optimize the connection. This process is described in the next chapter.

C H A P T E R IV

PERFORMANCE AND OPTIMIZATION OF THE LACED CONNECTION SYSTEM

CHAPTER IV

PERFORMANCE AND OPTIMIZATION OF THE LACED CONNECTION SYSTEM

4.1 GENERAL

To determine the performance of the connection and to optimize its cross-section, three groups of tests were carried out on the prototype of the Laced Connection System.

In the first group of tests the following parameters were optimized: cable, pin configuration, bushing and friction-reducing agent.

A second set of tests was carried out on the prototype having the above parameters optimized to determine the ultimate value of the following stresses: tension, compression, single shear, double shear, transverse shear and bending. At this stage the creep and the effect of vibrations on the connection were also determined. The results of the tests were compared to the charactaristic strengths of a sandwich panel.

The third series of tests dealt with the optimization of the shapes of the different components of the proposed connection.

4.2 THE TEST MODEL

Panels 6 ft x 6 ft x 3½ in. were made to test the system. These panels were formed of a wooden frame made of

$2\frac{1}{2}$ x $2\frac{1}{2}$ in cross-section bars, with two reinforcing bars placed at each third of the length of the panels. The extrusion and all the components were bonded together. Nails were used to reinforce the bond. Several cross members were also made.

One type of female extrusion was used in the test model. This was done to reduce the cost in manufacturing the extrusions.

The panels themselves, were made so rigid in order to determine the characteristics of the connection itself, without introducing the effect of the flexibility of the panels.

A number of cross members and panels were also made with tongues and grooves cut along their edges. Figure 4.1 shows the tongue and groove arrangement on two cross members.

4.3 CABLES, PINS AND BUSHINGS

4.3.1 Cables

The male extrusion shown in Figure 3.15, was designed with a space of 0.25^{+}in. allowed for the cable. Cable C of Table 4.1, was selected for preliminary calculations and tests. The price of this cable was the major factor influencing this selection. Aluminum pins were placed 4 inches apart along each side of the male extrusions. Figure 4.2 shows the initial arrangement of the pins and cable. With 5,000 lbs

tension in the cable, the diameter of the pins was 3/8 ins. This dimension was determined from shear strength calculations. Ideally, the angle θ in the initial arrangement should be as big as possible to maximize the force F, but due to the stiffness of the cable this angle had to be 40.5° to transmit any tension from one end of the cable to the other.

With the arrangement described above, a pull of 1,140 lbs on the cable at one end of the panel after winding over 36 pins, transmitted 342 lbs at the other end of the panel. The loss in tension was 70%.

This loss in tension was attributed to:

(i) The high stiffness of the cable which yielded as it was bent over the pins. Figure 4.3 shows the cable after its extraction from the tested panel connection.

(ii) The relative hardness of the steel cable and the aluminum pins. The cable scored the pins when tension was applied. Figure 4.4 shows scored pins after a test.

With the results of the preliminary tests in mind, it was decided to determine the best type of cable and optimum pin configuration on a specially made connection system formed of two angle sections. This connection is described in

Appendix I.

Table 4.1 gives the properties of some of the cables that were tested with this connection system. Cable A gave the best results due to its high strength and its flexibility, because of the small size of the individual wires forming the cable.

4.3.2 Pins

Due to the scores incised in the aluminum pins, these were replaced by case hardened steel dowel pins.

A set of pins was placed in the two-angle connection. A cable was passed over the pins. Attached to either end of the cable were the C-shaped members, load cells and the eye bolts described in Appendix I.

Tension was applied to the cable by tightening the eye bolts. The load monitored by the load cells was recorded. Close observation of the deformation of the cable as the tension was increased revealed that beside the flattening of the cable over the pins, it (the cable) moved towards the sides of the connection scoring it. This increased the loss due to friction.

4.3.3 Bushings

Brass bushings were placed over the pins. These had

TABLE 4.1

PROPERTIES OF CABLES

Cable	Type & Grade	Size in	Strands	Core	Minimum Breaking Strength lbs	Manufacturer
A	Galvanized Type 302 Alloy U.S.Mil.Spec. MIL-C-5424A	3/16	7 x 19	Wire Rope	4200	Wire Rope Industries of Canada (WRI)
B	Grade 110/120 Improved Plow	3/16	6 x 19	Steel	3200	WRI
C	Grade 110/120 Improved Plow	1/4	6 x 7	Fibre	5000	WRI
D	Nylon Rope	3/16		Nylon Rope	1100	Gourock-Bridgeport Gundry Ltd. (GBG)
E	Manila Rope	9/16		Manila Rope	450	GBG

a groove machined to accommodate the cable. This was done to prevent the cable from touching the sides of the connection.

Several friction reducing agents were applied to the bushings to reduce the friction between the bushings and the pins and between the bushings and the sides of the connection. Thrust bearings were also used for this purpose. Oil, grease and graphite were used with little success. A Teflon-based spray, commercially known as Xylan-2 [20] was applied to the bushings and the connection was tested. The results of these tests are given in Figure 4.5. In the same figure, the results of tests using the thrust bearings, to reduce friction, are also shown.

4.3.4 Pin Configuration

The pin configuration plays an important role in the efficient functioning of the laced connection system. As a result of the preliminary tests, the angle through which the cable bent was found to be critical. A series of tests were carried out, using the two-angle connection previously described to determine the optimum cable inclination. In that connection, the pins can have their positions varied by placing the pins in different holes, as can be seen in Figure A-8 of Appendix I. The first step in resolving the problem of yielding of the cable was to have the cable pass over two consecutive pins on each side of the connection

before it went to the other side, as shown in the schematic diagram in Figure 4.5. The reduction in bending angles of the cable reduced yielding.

With this configuration and with the bushings, thrust bearings and Xylan-2 coating, a study of the bending angle of the cable with load was conducted. The results of this study are also given in Figure 4.5. It can be seen from that figure that using the thrust bearings the loss in transmission was reduced to 3.2%, with a 3,000 lb tensile force in the cable, using 16 pins on a 6 ft connection. With the same configuration as has just been described, using Xylan-2 in the place of the thrust bearings, the loss in transmission was 6%.

The high price of the thrust bearings and the time spent in assembling them, as compared to the low price of the Xylan-2 spray and the ease in its application, makes the latter more practical for this system.

The mean loss in transmission per pin, with the Xylan-2 coating brushings, was 0.4 % on the 6 ft connection.

4.4 PERFORMANCE TESTS

The optimum set-up was found in the previous section and the model of the Laced Connection System was tested under different loading conditions to determine its perfor-

mance characteristics.

4.4.1 Tension Tests

Two cross-members were interconnected by the optimum cable-pin arrangement and fixed to the loading frame described in Appendix I. Figure 4.6 shows the set-up used for these tests. The upper cross-member was fixed to the frame while the lower one was connected to a series of cables to create a distributed load, as described in Appendix I. While the load was applied, the tension in the lacing cable was monitored and the relative displacement of the mid-point of the connection system was measured with the increase in load.

Table 4.2 gives the results of such a test.

Figure 4.7 gives a plot of the measurements taken during the tension test. At point "A" on this Figure, the cable failed at one end, at the clamps. This failure was due to overtightening of the clamp.

4.4.2 Test for Compression

No tests for compression were carried out since these would only determine the crushing strength of the wooden frame and would not reveal any information on the connection system.

TABLE 4.2

RESULTS FROM TENSION TESTS

Parameters	Values
Initial tension in lacing cable	3,000 lbs
Tension in lacing cable before failure	3,100 lbs
Tensile force on connection	7,280 lbs
Tensile force per unit length	101 lbs/in
Maximum separation between members	0.001 in

4.4.3 Single Shear Tests

In these tests, two cross-members were inter-connected by the lacing cable. A shear load was applied by the arrangement shown in Figures A.3 and A.6 of Appendix I. The shearing force and the resulting displacements were measured. Figure 4.8 shows the effect of varying the tension in the lacing cable on the shear force. Table 4.3 gives the results of the final tests with 3,000 lbs tension in the lacing cable.

4.4.4 The Double Shear Tests

Three cross-members were connected to one another as shown in Figure 4.9. The Pulley connection described in Appendix I rested on the central cross-member with a cable running through it. This cable was connected to the hydraulic ram through a load cell. The ram rested on the middle portion of a U-shaped member. The ends of this member rested on the outer two cross-members. By actuating the ram, a double shear force was applied to the system. The relative displacement of the cross-members was measured with dial indicators.

The results obtained from these tests for 1,890 lbs and 3,000 lbs tension in the lacing cable are given in Figure 4.10. The results with 3,000 lbs tension in the lacing cable are given in Table 4.4.

TABLE 4.3

RESULTS FROM SINGLE SHEAR TESTS

Parameters	Values
Initial tension in lacing cable	3,000 lbs
Ultimate shear force	2,400 lbs
Ultimate shear force per unit length	33 lbs/in
Shear displacement	0.103 in

TABLE 4.4

RESULTS FROM DOUBLE SHEAR TESTS

Parameters	Values
Initial tension in lacing cables	3,000 lbs
Ultimate double shear force	6,650 lbs
Ultimate double shear force per unit length	93 lbs/in
Shear displacement	0.064 in

4.4.5 Transverse Shear Tests

Figure 4.11 shows the arrangement used for the transverse shear tests. A 120-kip Tinus Olsen Loading Machine was used to load the connection. Two I-beams were used as supports for the outer two members while the central member was loaded by lowering the head of the machine onto a box section placed onto the central cross-member. The relative displacement of the cross-members were recorded.

Two tests were carried out on this connection system. The first one was done by applying a load of 3,000 lbs to the connection, then releasing the load. The shear displacement at mid-span of the connection at that load was 0.048 in. When the load was released, the displacement was totally recovered. On the second loading, the displacement was measured up to 0.05 in, then the load was increased until failure of the connection (see Figure 4.12). The results of these tests are plotted in Figure 4.13.

Table 4.5 gives a summary of the results of the ultimate transverse shear characteristics of the Laced Connection System.

4.4.6 The Bending Tests

Figure 4.14 shows a schematic diagram of the arrangement used in the bending tests. A distributed load was

TABLE 4.5

RESULTS FROM TRANSVERSE SHEAR TESTS

Parameters	Values
Initial tension in cable	3,000 lbs
Ultimate transverse shear load	45,000 lbs
Ultimate transverse shear load per unit length	630 lbs/in

TABLE 4.6

RESULTS FROM BENDING TESTS

Parameters	Values
Initial tension in cable	3,000 lbs
Maximum bending moment applied	440 lb-in
Bending angle "θ"	34^{o}

applied at the edge P. The displacements of the edge P were recorded.

The results from these tests are given in Table 4.6 and shown in Figure 4.15.

4.4.7 The Creep Test

This test was aimed at determining the effect of time on the tension in the lacing cable. A load cell attachment was fixed to one end of the lacing cable. The lacing cable was subject to 3,000 lbs tensile force. The tension in the cable was recorded at different times until there was no more detectable change in tension.

The results of this test show that creep is negligible (see Table 4.7 for results) .

4.4.8 Vibration Tests

To complete this series of tests on the connection system, the effect of subjecting the connection system to vibrations of different amplitudes at the natural frequency of the connection system was studied., A 3,000 lb tension was applied to the lacing cable and the connection was subjected to vibrations. The tension in the lacing cable was measured after the test.

TABLE 4.7

RESULTS FROM CREEP TEST

Parameters	Values
Duration of test	70 hrs
Initial tension in lacing cable	3,000 lbs
Final tension in lacing cable	2,998 lbs
Percentage loss in cable tension	0.07 %

TABLE 4.8

RESULTS OF VIBRATION TESTS

Parameters	Values
Initial tension in cable	3,000 lbs
Loss in tension immediately after start of test	28 lbs
Exciting frequency in initial test	109 Hz
Duration of initial test	15 mins.
Number of cycles used for final test	10,000 cycles
Maximum exciting frequency	10 KHz
Final tension in cable	2,972 lbs
Total percentage loss in tension	0.94 %

Figures 4.16 and 4.17 show the set-up for the vibration tests. Table 4.8 gives the results of these tests.

4.5 COMPARISON OF RESULTS

The resulting strengths from the above tests are compared to values of strengths of a standard sandwich panel. The sandwich panel had 0.025 in-thick aluminum facings and a 3.5 in-thick polystyrene core [22]. The values for these strengths assume complete stability of facings. The failure, however, would be governed by buckling.

It can be seen from Table 4.9 that some modifications should be made of the system to increase its shear capacity.

An increase in shear strengths of the joint can be achieved by using interlocking keys or introducing dowel pins in the edges of the panels. The Laced Connection System showed little resistance to bending, but this is not considered a critical deficiency since buildings can be designed with moment-free connections.

4.6 OPTIMIZATION OF SECTIONS

The stresses in the metal extrusions were analyzed using the photoelastic technique. This technique was selected because the stresses may be viewed over the entire tested model enabling the investigator to determine directly the areas of stress concentrations. Material was taken away from

TABLE 4.9

CHARACTERISTIC STRENGTHS OF THE LACED CONNECTION SYSTEM AND A STANDARD SANDWICH PANEL (WITH 0.025 IN-THICK ALUMINUM FACINGS AND 3.5 IN-THICK POLYSTYRENE CORE)

		Capacity of Panel at Yield	Capacity of Connection. Experimental Values
Tensile Strength lb per lineal in.		500	101
Longitudinal Shear Strength lb per lineal in.	Single	300*	33
	Double	600*	93
Transverse Shear Strength lb per lineal in.		158**	630

* Values assume instability of facings or glue line at 50% of yield/strength of aluminum.

** Value taken from Reference [22] and based exlusively on core shear strength

Note: Values in columns 1 and 2 can be matched by varying the thickness of the facings and the diameter of the cable.

the understressed areas in a section, while material was added to the overstressed areas. This was done to allow a reasonable flow of stresses over the entire model. This technique is described by Heywood [23] and others. The photoelastic theory and the method for the determination of stresses at different points on a model may be determined by either the methods described in References [23 - 32] or by the methods introduced in Appendix II of this work.

A full-scale drawing of the two-dimensional model of the male extrusion that was tested is shown in Figure 4.18. Figure 4.19 shows a full-scale drawing of the model of the four-way female extrusion embodied in a model of a wooden frame. Figure 4.20 shows a photograph of the loaded model in a polariscope. It should be noted here that the male extrusion is understressed relative to the stresses in the female extrusion.

4.6.1 Optimization of Male Extrusion

Shown in Figure 4.21 is the optimized shape of the model of the male extrusion. This model was supported on two blocks while a load was applied, as shown in Figure 4.21. Figure 4.22 shows the dimensions of the optimized male extrusion.

4.6.2 Panel-to-Panel Female Extrusion

Figure 4.23 shows a photograph of the observed stress patterns in an intermediate step before the optimized shape is reached. Figure 4.24 shows the stress patterns in the supporting end of the female extrusion after its shape has been optimized. Figure 4.25 gives the dimensions of the optimized female panel-to-panel extrusion.

4.6.3 Four-Way Female Extrusion

Figures 4.26, 4.27 and 4.28 are photographs of the stress patterns in different four-way extrusions loaded by the equivalent of 3,000 lbs scaled according to Equation II.10 of Appendix II are given in Figure 4.29.

4.6.4 Results of the Optimization of Sections

Table 4.10 gives a comparison between the areas of the different cross-sections according to their original design and according to their optimized shape. It can be seen that reductions in material up to 48% have been achieved in the optimized design.

TABLE 4.10

COMPARISON BETWEEN CROSS-SECTIONAL AREAS
IN ORIGINAL AND FINAL DESIGNS

Extrusion	Cross-Sectional Area of Original Design by Fazio [1] in^2	Cross-Sectional Area in Optimized Design in^2	Percentage Reduction in Cross-Sectional area
Female (Fig. 3.14)	0.80	0.42	47.8
Male (Fig. 3.15)	0.75	0.46	38.6
Cross-Member (Fig. 3.18)	1.44	1.43	0.7

4.6.5 The Optimized Laced Connection System

The optimized Laced Connection System is reported in [33].

Figures 4.30 to 4.36 show the different components of the optimized version of the Laced Connection System in various assemblies. Some of the methods of sealing the joints that may be used with this system are given in [34] and [35]. An appropriate position for the seal is in the space between the tongue and the groove which should be modified to fit the chosen seal.

4.7 EFFECT OF JOINT MOVEMENTS ON TENSION IN LACED CONNECTION CABLE

The tension in the cable of the Laced Connection system will be affected by the changes in temperature. The tension in the cable must be checked for the various temperature conditions in the building and in the atmosphere. The maximum tension predicted must not exceed the maximum safe tension of the cable. The minimum tension however, must not be lower than the design tension.

Defining a cycle in the cable as being the length ABCDE, shown in Figure 4.37, which is the repeated arrangement of the cable and pins along the length of the connection, the change in length of one cycle is

$$L_{fc} = L_{cc} \cdot \alpha_c \cdot (\hat{t}_{cm} - \hat{t}_{cn}) \qquad (4.1)$$

where L_{fc} is the maximum change in cable length per cycle

L_{cc} is the length of cable in one cycle at installation temperature

α_c is the coefficient of thermal expansion of cable

$\hat{t}_{cm}$ is the maximum predicted temperature of cable

$\hat{t}_{cn}$ is the minimum predicted temperature of cable

In the arrangement shown in Figure 4.37, L_{cc} = 16.40 ins. For a 10 ft wall, we would have 6 cycles and two ends to be used for clamping the ends of the cable. These ends would have a total length of 24 inches. The maximum change in length of the cable ends is

$$L_{ef} = L_{ec} \cdot \alpha_c \cdot (\hat{t}_{cm} - \hat{t}_{cn}) \qquad (4.2)$$

where L_{ef} is the maximum change in length of the cable ends

L_{ec} is the length of the cable ends at installation temperature.

The maximum change in cable length per joint is

$$L_{oc} = n \cdot L_{fc} + L_{ef} \qquad (4.3)$$

The male extrusion will also change in dimensions due to the change in temperature. If we assume that there is no clearance between the mating surfaces of the male extrusion (this assumption is reasonable because the clearance is so small relative to the lengths under consideration in the extrusions), then the changes in lengths considered would be those along which the cable passes.

The lengths considered in the extrusion are $(L_{ec} + n\ L_{cc})$, and the maximum change in length is

$$L_{em} = (L_{ec} + n\ L_{cc}) \cdot \alpha_e \cdot (\hat{t}_{cm} - \hat{t}_{cn}) \qquad (4.4)$$

where L_{em} is the maximum change in the length in the extrusion

α_e is the coefficient of linear expansion of the material of the extrusion

The relative change in the length of the cable due to temperature change is

$$L_{rcl} = L_{em} \pm L_{oc} \qquad (4.5)$$

where L_{rcl} is the relative change in cable length due to temperature change

Assuming elastic deformations in the cable, the change in cable tension due to the change in length L_{rcl} is

$$T_c = \frac{L_{rcl} \cdot E_c \cdot A_c}{L_{co}} \qquad (4.6)$$

where T_c is the change in cable tension

E_c is the modulus of elasticity of material of cable

A_c is the effective cross-sectional area of the cable

L_{co} is the initial length of the cable

$L_{co} = n\, L_{cc} + L_{ec}$

There is a further change in cable length due to the bending of the panel due to the change of temperature, as described in Section 2.4. The pins in the male extrusion will move a distance S_{wp} apart

$$S_{wp} = (X_p) \cdot \alpha_e \cdot (t_{ix} - t_{ow}) \qquad (4.7)$$

where S_{wp} is the increase in distance between the rows of pins due to thermal bending

X_p is the distance between the rows of pins

Referring to Figure 4.37, the distance (X_p) will increase to $(X_p + S_{wp})$ and the length of the cable per cycle will increase by $(2\, S_{wp} \cdot \sin \hat{\theta})$. The increase in length of the cable for the whole connection is

$$L_{ib} = 2 \cdot n \cdot S_{wp} \cdot \text{Sin}\ \hat{\theta} \qquad (4.8)$$

where L_{ib} is the total increase in cable length due to bending of panel

$$\hat{\theta} = \text{Sin}^{-1} \left[\frac{X_p + S_{wp}}{b} \right]$$

or

$$L_{ib} = 2 \cdot n \cdot S_{wp} \cdot \left[\frac{X_p + S_{wp}}{b} \right] \qquad (4.9)$$

and the increase in tension due to thermal bending is

$$T_{ib} = \frac{L_{ib} \cdot E_c \cdot A_c}{L_{co}} \qquad (4.10)$$

The maximum change in tension due to thermal effects is

$$T_{ct} = \sqrt{(T_{ib}^2 + T_c^2)} \qquad (4.11)$$

In the Laced Connection System, the installation tension in the cable at a specified installation temperature may be calculated from

$$T_i = T_d - (T_{ct} + T_{wd}) \qquad (4.12)$$

where T_i is the installation tension in the cable

T_d is the design tension of the Laced Connection System

T_{wd} is the increase in tension due to wind loads and other deformations

T_{wd} is calculated from the drformations due to the applied loads and the stiffness of the building.

A general equation is derived giving the loss of tension due to the combination of both pure and bending thermal effects. This equation is

$$T_c = E_c \cdot A_c \cdot \left[(\hat{t}_{cm} - \hat{t}_{cn})(\alpha_e - \alpha_c) + \right.$$

$$\left. \frac{1}{2} \cdot n \cdot x_p^2 \cdot \alpha_e^2 \cdot \frac{(t_{ix} - t_{ow})\left[\left(\frac{1}{\alpha_e}\right) + t_{ix} - t_{ow}\right]}{b(n L_{cc} + \frac{1}{2} L_{ec})} \right] \quad (4.13)$$

Tables 4.11 and 4.12 were computed to study the effect of variations of temperature on the tension of the lacing cable. These tables were computed for the following set of data:,

Height of Panel	16 ft
Design Tension in Cable	3,000 lbs
L_{cc}	16.4 in
L_{ec}	24 in
n	6
E_c	20.5×10^6 lb/in^2
A_c	0.0261 in^2

α_c	3.73×10^{-6}	in/in/^oF.
α_e	7.80×10^{-6}	in/in/^oF.
x_p	1.75	in
b	6.65	in

Table 4.11 was computed for the value of $(t_{ix}-t_{ow}) = 100^oF$.

It was noted in calculating Table 4.11 that the effect on the tension due to changes in temperature in the extrusions may be neglected. The last term of Equation 4.13 can thus be omitted and the equation may be written as

$$T_c = E_c \cdot A_c \cdot (\hat{t}_{cm}-\hat{t}_{cn}) (\alpha_e-\alpha_c) \qquad (4.14)$$

4.8 DISCUSSION AND COMMENTS

The following observations can be made from the foregoing study and in particular from Table 4.9 :

(i) The optimization resulted in reductions of material in different components of up to 48 %.

(ii) The connection system provides relatively high transverse shear carrying capacity and low tensile and longitudinal shear carrying capacity. The ultimate shear capacity of the core is 158 lb/lineal in versus 630 lb/lineal in provided by the connection. It should be noted however that the framing around the panel will contribute

TABLE 4.11

PERCENTAGE LOSS IN CABLE TENSION DUE TO CHANGE IN ITS TEMPERATURE

$(\hat{t}_{cm}-\hat{t}_{cn})$ ^{o}F	Loss in Tension lbs	Percentage loss in tension lbs
10.0	21.8	0.7
20.0	43.6	1.5
30.0	65.3	2.2
40.0	87.1	2.9
50.0	108.9	3.6
60.0	130.7	4.4
70.0	152.5	5.1
80.0	174.2	5.8
90.0	196.0	6.5
100.0	217.8	7.3

considerably to the transverse shear strength of the panel.

The tension carrying capacity of the connection can be increased by providing a larger diameter cable. The shear capacity will increase with larger tension. It can be concluded that with the proper proportioning of panel and connection components, it is possible to exploit the strengths of the panel with this connection system.

(iii) The moment carrying capacity is relatively low but it is not of prime importance since a building can be designed so that there are no bending moments at the connection of panels.

(iv) Long term tests have shown that creep is negligible.

(v) The connection system remains stable under severe vibration loading.

(vi) An increase in temperature of 100 ^{o}F after installation of the cable will reduce the tension in the cable by 7.3 %. The change in cable tension due to the effect of temp-

erature on the pin spacing may be neglected. One can conclude that the joint is stable with severe temperature changes.

(vii) The connection remains concealed and provides two seals against weather conditions, and has no thermal bridge.

(viii) The connection system is completely incapsuled in the frame and is protected against fire. It provides a secondary structure after the panel deteriorates in case of fire.

The course of study that is given in this chapter to determine the optimum set-up, charactaristic strengths and the study of the thermal effects on the Laced Connection System gave rise to a number of alternate solutions to the problem of connections. Four of these are treated in the next chapter.

C H A P T E R V

CONNECTION SYSTEMS DEVELOPED DURING THE OPTIMIZATION OF THE LACED CONNECTION SYSTEM

C H A P T E R V

CONNECTION SYSTEMS DEVELOPED DURING THE OPTIMIZATION OF THE LACED CONNECTION SYSTEM

5.1 GENERAL

During the performance and optimization studies on the Laced Connection System, alternate solutions to the connection problem were realized. Some of these solutions offer different advantages and disadvantages over the Laced Connection. Four of these new connection systems are described in this Chapter. The advantages and disadvantages of each system are included. It should be noted that no single solution is foreseen for all panel connections. A variety of solutions will allow an appropriate choice for individual applications.

5.2 THE SLOTTED BAR CONNECTION

5.2.1 General

With the progress in the experiments carried out on the Laced Connection System, other connection systems were designed. The Slotted Bar Connection described in [36] is one such connection system.

5.2.2 The Panels

These are similar to the ones used with the Laced Connection System with the same female extrusion integrated into the panels, as shown in Figure 4.30.

5.2.3 The System

Male extrusions, similar to the optimized design of the Laced Connection System described earlier, are used in this connection system. Figure 5.1 shows the assembly of the male extrusions and the slotted bar. Part 2 is the slotted bar which runs along all the length of the panel. At one end of the bar there is a threaded rod which is welded to the bar. The bar itself, has inclined slots cut into it. Pins (Part 3) are introduced in the sides of the male extrusions. These pins pass through the appropriate slots of the bar. The slotted bar assembly, which is composed of two male extrusions, the bar and an appropriate number of pins, is introduced into the adjoining female extrusions of the mating panels. The joining force is created after the washer and nut (Parts 4 and 5 - Figure 5.2) are threaded onto the rod at the end of the bar and the nut is tightened. The male extrusions will be forced to move towards each other, as shown in Figure 5.2. When this assembly is introduced into the female extrusions, the tightening of the nut will force the panels towards each other. The joining force is

controlled by tightening the nut.

Panels in different planes may be connected to each other, using an intermediate member. Such a connection is shown in Figure 5.3. The situations requiring the use of an intermediate member are shown in Figure 2.3 and 2.4. These positions are marked by A, B, C, D and E.

Figure 5.4(a) shows a view of four panels (1, 2, 3 and 4) connected to intermediate members (5, 6, 7 and 8) to form the joint. The space marked 9 is closed with a plug after assembly, as shown in Figure 5.4(b). A typical corner of a panel is shown in Figure 5.4(d). The intermediate member to be used on the outside of the building is shown in Figure 5.4(c). This intermediate member has one side blocked. The blocked side is longer than the member. This is to cover the end connection.

A prototype of this connection system was built and tested at Sir George Williams University. Figures 5.5 and 5.6 show this prototype.

This connection system offers not only the same advantages as the Laced Connection System, but also it is

(i) a simple mechanism to install in the panels

(ii) an easily controlled method of loading the connection, and

(iii) easily dismantled

The disadvantages of this system are

(i) quantity of material needed

(ii) accuracy in manufacture

(iii) the panels should be brought into contact with each other, before the slotted bar assembly is introduced in the panels

5.3 THE ZIG-ZAG BAR CONNECTION

5.3.1 General

This connection was developed in an attempt to reduce the material used in the connection systems discussed above. This connection system is described by Fazio and Khalil [37].

5.3.2 The System

The female extrusions "1" shown in Figure 5.7 are fixed into the edges of the panels by nuts and bolts. After the panels are brought into contact with each other, the bars "3" and pins "2" shown, are introduced into the female extrusions, as shown in Figure 5.8 and 5.9. The bars go from panel to panel. These bars are fixed to the pins that are free to move along the female extrusions.

In Figure 5.8, the first bar introduced into the edge of the panel is anchored to the panel by a retaining plate "4" also shown in Figure 5.10, the threaded rod and bolt. The last bar introduced is pulled out of the panel assembly. This last bar also has a threaded rod welded to its end. Due to the fixed lengths of the bars and to the restriction imposed on the motion of the pins when the last bar is pulled out, the panels will be forced towards each other.

Figure 5.9 shows a section in the joint after assembly. Figure 5.8 shows a section of the two panels when the last bar is released.

Loading the bars is done by connecting part "5", shown in Figure 5.8, to the end of the threaded bar of the last member and pulling this bar outwards. Figure 5.11 shows the loading mechanism used for pulling the last bar.

The procedure to load this system is as follows:

(i) the nut (part "6") is loosely screwed onto the rod

(ii) the pulling accessory (part"5") is screwed to the end of the bar

(iii) the tightening bridge (part "8") is introduced onto the edge of the panels

(iv) the nut (part "9") is tightened. This will pull the rods creating the tightening force

(v) when the required tightening force is reached, the retaining plate (part "7") is introduced

(vi) the nut (part "6") is then tightened

(vii) the nut (part "9") is released

(viii) the pulling accessory (part "5") and the tightening bridge (part "8") are removed

(ix) a predetermined torque is applied to the nut (part "6") to create the design prestress to the connection

Figure 5.12 shows a different arrangement of the zig-zag bar connection system.

The advantages of this system over the previous ones are many, among them

(i) less material is utilized in this connection than in the previously discussed systems

(ii) the joining force is easily controlled

(iii) the material of the female extrusion must be made of a hard material or rails of a hard material may be used as rails for the pins. In the latter case, the extrusion may be made of a less hard material.

5.4 THE ROD CONNECTION

5.4.1 General

The rod connection system is one that uses standard on-the-market components. This connection system is described by Fazio and Khalil [38].

5.4.2 The Connection System

The basic components of this connection system are shown in Figure 5.13. The parts marked "1" are standard steel box sections. These are fastened to the adjoining panels by screws, as shown in Figure 5.14. In Figure 5.13, the panels are simulated by wooden bars (part "2"). Short lengths of the box sections are fastened to the panels, as shown. A square rod (part "3") is used to connect the panels, as shown in Figure 5.14. The joining force is created by turning part "3" so that the corners of the rod push onto the inner surfaces of the box sections. This is shown in Figure 5.15. To retain the position of the rod after assembly, two circular rods (parts "4" - Figure 5.17) are introduced in the spaces between the square rod and the box sections.

The connection itself, may be totally concealed, as shown in Figure 5.17.

Figure 5.18(a) shows a typical corner connection formed with the aid of an intermediate member (Part IM), also shown in Figure 5.18(c). Figure 5.18(b) shows three walls meeting at a point joint with the help of the intermediate member. In Figure 5.18(c) the intermediate member to connect four panels is shown.

The advantages of this system are

(i) use of standard components

(ii) ease in loading. The rod may be loaded by twisting both ends

The disadvantages are

(i) the panels must be brought into close contact with each other before the introduction of the rod

(ii) to increase the joining force, the contact wooden surfaces of the panels should be shimmed. This shim may be placed along grooves cut along the edges of the panels. The intermediate members have the box sections embedded in them. Control over the joining force is achieved by shimming the box-section-panel surface. This operation would have to be done on-site.

5.5 THE BOLTED CONNECTION SYSTEM

5.5.1 Introduction

This connection system described by Fazio and Khalil [39] basically utilizes two types of panels. One type which is large and completely prefinished is referred to as the basic panel. The other type, which is much smaller than the basic panel, called the joining panel, is partly finished before assembling on the structure site. The joining panels are those used to connect the basic panels.

5.5.2 The Basic Panels

These are sandwich type panels that are pre-assembled and finished before reaching the construction site. The frames of these panels are made of a non-metallic material. These are formed of four members placed along the edges of the panel, every member may be connected to its neighbouring one with corrugated fasteners. Figure 5.19 shows an exploded view of a basic panel.

It can be seen from that figure that the non-metallic frame which is formed of four members is joined by corrugated fasteners and has a number of holes drilled along its sides. A nut assembly is secured along the internal side of the frame in front of each hole.

The different components of such a panel are bonded together to form the panel assembly.

5.5.3 The Joining Panels

These are of a much smaller size than the size of the basic panels. Figure 5.20 shows a joining panel placed in a structure assembly. In this Figure, Part "3" is a metallic frame formed of U-shaped members welded together. Layers of wood are bonded to the frame, these are Parts "2" and "4". This wood is used to break the thermal bridge between the two sides of the panel. Part "1" is an outer skin or facing bonded to one side of the panel. Holes are drilled along the edges of the semi-finished panels to allow bolts (Part "5") to be introduced through them and through the holes in the basic panels previously described. When assembling a complete system the bolts introduced are fastened to the nuts in the basic panels and are tightened to the required torque. The insulations (Parts "6" and "7") are then introduced in the space of the panel and the outer facing. Part "8" is then placed to complete the assembly of this panel. The contact surfaces of the parts to be assembled are to be covered with an adhesive that is pre-applied to the surfaces that will be in contact. A protective sheet is placed over the layer of adhesive so that on final assembly, this sheet is removed and the parts joined, thus completing the assembly.

5.5.4 The Building System

Figure 5.21(a) shows the method of connecting four intersecting walls or two walls and two floors. A corner connection is formed by connecting a basic panel to a joining panel, as shown in Figure 5.21(b). The T-connection is for the joining of two walls and a floor or three intersecting walls. In the T-connection two basic panels are bolted to a joining panel.

In a wall assembly such as that shown in Figure 5.22, the horizontal joining panels are interconnected at a point half-way along the edge of the basic panel. This increases the rigidity of the system.

When the joining panels are located away from the outer shell of the building, the space for the insulation may be utilized for the passage of the electrical and minor mechanical systems. The frame of the joining panel would have to have openings to accomodate these systems.

The frames of the joining panels, when interconnected, may act as an emergency frame to the building system. This feature is especially useful when a basic panel has to be changed in the building system and in case of a fire, this will increase the lapse of time before the entire building collapses.

In Figure 5.22, the basic panels are one-storey high with the edge of the joining panel placed such that these are not visible at the ceiling level, however at the floor level, an opening may be seen. This opening may be covered after the panel assembly is completed. Horizontal electrical and mechanical systems may pass through these horizontal joining panels and the outputs may be placed at any position along the floor level.

In a building system of this type, the main electrical and mechanical systems must be placed in vertical core-shafts which feed the systems in the horizontal joining panels.

This system is totally different from all the previously discussed ones.

The advantages here, are

(i) utilization of standard pieces

(ii) the existence of a form of secondary frame to assist in emergencies

(iii) simplicity in mounting

The disadvantages are

(i) more work to be done on-site

(ii) the possibility of using bonding agents on-site

The performance and optimization of the connection systems described in this chapter can be established, using the procedures developed in Chapter IV. This process was not repeated here, due to lack of resources. It is hoped that industrial interests will wish to pursuit some of these concepts and provide the necessary funding.

C H A P T E R VI

SUMMARY AND CONCLUSIONS

C H A P T E R VI

SUMMARY AND CONCLUSIONS

In this research project a standard process for assessing the performance of connection systems has been established. In the course of assessing the performance of the Laced Connection System four new connection systems have been devised.

In this established process a model would be subjected to

(i) tension
(ii) single shear
(iii) double shear
(iv) transverse shear
(v) bending moments
(vi) vibrations

and the effect of creep would also be determined.

The Laced Connection showed, in general, good strength characteristics. It can be used to exploit the capacity of the panel by properly proportioning panel and connection components (see discussion in Section 4.8).

The new connection systems offer alternate solutions

to the problem of joining of panels. The performance of these new connection systems should be assessed by the standardized process described. A complete economic study comparing the different connection systems described should form part of the assessment.

The techniques for the evaluation of fringe orders introduced in this work proved to be successful, although not necessary for this application.

REFERENCES

REFERENCES

[1] Fazio, P., "Panel Connection System", Sir George Williams University, Declaration FP-1, Patent Pending, (1970).

[2] Eden, J.F. and Seymour-Walker, K., "Joints in the Context of an Assembly Process", Building, Vol. 219, No. 6648, pp.155-163, (1970).

[3] Bonshor, R.B. and Harrison, H.W., "The Relationship Between Component Size and Joint Dimension", Building, Vol. 219, No. 6652, pp.141-150, (1970).

[4] Skempton, A.W. and MacDonald, D.H., "The Allowable Settlements in Buildings", Proc. Instr. Civ. Engrs., Part III, Vol. 5, (1956).

[5] Lewicki, B., "Building With Large Prefabricates", Elsevier Publishing Company, New York, (1964).

[6] Gunther, R.C., "Refrigeration, Air-Conditioning, and Cold Storage", Chilton Company Inc., Philadelphia, (1957).

[7] Karpati, K.K., "Guide for Sealed Joint Design", Technical Paper No. 385, Div. Building Research, National Research Council, Canada, (1973).

[8] Adams, A., "Interchangeable Partition Section", United States Patent No. 856,198, (1907).

[9] Thelander, A.F., "Building Construction", United States Patent No. 2,629,139, (1953).

[10] Jones, F.M., "Locking Mechanism", United States Patent No. 2,647,287, (1953).

[11] Palfey, A.J. et al, "Building Panels and Fastener Means Therefore", United States Patent No. 3,280,522, (1966).

[12] Logan, N.J., "Wall Fixing Connector", Canadian Patent No. 727,846, Class 20-40, (1966).

[13] Harvey, L.M., "Interlocking Mating and Coupling Bar Therefore", United States Patent No. 3,348,459, (1967).

[14] Morgan, E.L. et al, "Connector Structure for Modular Panels and the Like", United States Patent No. 3,512,819, (1968).

[15] Fazio, P. and Mikler, J., "Modular Panelized Buildings", Sir George Williams University, Technical Report No.II, (1970).

[16] Fazio, P. and Mikler, J., "Modular Panelized Buildings", Sir George Williams University, Technical Report No. III, (1970).

[17] Fazio, P. and Ha, H.K., "Analysis of Three-Dimensional Orthotropic Sandwich Plate Structures By Finite Element Method", Report No. SBC XX CE 72-4, Sir George Williams University, (1972).

[18] "Structural Sandwich Composites" - United States Department of Defence - MIL - HDBK - 23-A, (1968).

[19] Wachsmann, K., "The Turning Point of Building", Reinhold Publishing Company, New York, (1961).

[20] "Xylan-2", Whitford Corporation, West Chester, Pa., 19380, U.S.A.

[21] Fazio, P., "Experimental and Theoretical Study of Aluminum Sandwich Elements and in Particular Aluminum Folded-Sandwich-Plate Structures", Thesis, University of Windsor, (1968).

[22] Allen, H., "Analysis and Design of Structural Sandwich Panels", Pergamon Press, New York, (1969).

[23] Heywood, R.B., "Photoelasticity for Designers", Pergemon Press, New York, (1969).

[24] Coker, E.G. and Filon, L.N.G., "A Treatise on Photoelasticity", London: Cambridge University Press, (1931).

[25] Hetenyi, M., "Photoelastic Stress Analysis Made in ThreeDimensions", Machine Design, Vol. 10, pp.40-41, (1938).

[26] Jenkins, F. and White, H., "Fundamental of Optics", 95 McGraw-Hill Book Company, Inc., New York (1957).

[27] Holister, G.S., "Experimental Stress Analysis", Cambridge at the University Press, Cambridge, (1967).

[28] Dally, J.W. and Riley, W.F., "Experimental Stress Analysis", McGraw-Hill Book Company, New York, (1965).

[29] Frocht, M.M., "Photoelasticity", Vol. 1 and 2, New York: John Wiley and Sons, (1948).

[30] Dolan, T.J. and Murray, W.M., "Photoelasticity", Handbook of Experimental Stress Analysis, M. Hetenyi (ed). New York: John Wiley and Sons, Inc. (1950).

[31] Born, M. and Wolf, E., "Principles of Optics", Pergamon Press, New York (1964).

[32] Oppel, G., "Photoelastic Investigation of Three-Dimensional Stress and Strain Conditions", National Advisory Committee, Aeronautics Memorandum 824, (1937).

[33] Fazio, P. and Khalil, A.M., "Optimized Laced Connection System", Sir George Williams University, Civil Engineering, Report FP-1-R, Patent Pending, (1973).

[34] "Weathertight Joints for Walls", Report NBR1-51C, Norwegian Building Research Institute, Oslo, Norway, January (1968).

[35] Gillette, H.G. and Everett, M.H., "Elastomeric O-Rings", Machine Design, Vol. 41, No. 14, pp.73-75, (1969).

[36] Fazio, P. and Khalil, A.M., "The Slotted Bar Connection", Declaration FP-4, Sir George Williams University, Civil Engineering, Patent Pending, (1973).

[37] Fazio, P. and Khalil, A.M. "The Zig-Zag Bar Connection System", Declaration FP-5, Sir George Williams University, Patent Pending, (1973).

[38] Fazio, P. and Khalil, A.M., "The Rod Connection", Declaration FP-8, Sir George Williams University, Patent Pending, (1973).

[39] Fazio, P. and Khalil, A.M., "The Bolted Connection System", Declaration FP-9, Sir George Williams University, Patent Pending, (1973).

[40] Enerpac Hydraulic Ram. No. RWP-25 Catalogue E-202, Enerpac and Applied Power Industry, Butler, Wisconsin, U.S.A. (1972).

[41] Gilmore Loading System, Catalogue A.29117, Gilmore, Cleveland, Ohio, (1969).

[42] Tinus Olsen Machine, Catalogue 61-4, Tinus Olsen Testing Machine Company, Willogrove, Pennsylvania, (1968).

[43] Fazio, P. and Khalil, A.M., "Displacement Transducer Type FP-2", Sir George Williams University, Civil Engineering, Report FP-2, (1973).

[44] "Autodensidater", Publication 11/67 Joyce, Loebel & Co. Ltd., London, (1972).

[45] Sciammarella, C.A. and Doddington, C.W., "Effect of Photographic Film Nonlinearities on the Processing of Moiré-Fringe Data", Experimental Mechanics, 388-402, (1967).

[46] Khalil, A.M. and Fazio, P., "On the Application of Correction Factor Equations of Lenses to the Resulting Scans of Photoelastic Models", talk given at meeting of the Montreal Section of the Society of Experimental Stress Analysis, (March 5, 1973).

[47] Khalil, A.M., and Fazio, P., "L'Equation de la Distortion Générale des Lentilles et la Photoélasticité". Paper submitted for the Fifth International Conference on Stress Analysis in Udine-Italy, (1974).

[48] Khalil, A.M. and Fazio, P., "Lens Distortion Equation Using Moiré", Applied Optics, Vol. 12, pp. 972-975, (May 1973).

[49] Khalil, A.M. and Fazio, P., "Moiré-Fringe Measurements", Experimental Mechanics, Vol. 13, No. 6, (1973).

[50] Barer, R. and Cosslett, V.E., "Advances in Optical and Eléctron Microscopy", Vol. 1, Academic Press, New York, (1966).

[51] "Kodak Filters for Scientific and Technical Uses", Kodak Publication No. B-3, Eastman Kodak Company, Rochester, New York, (1972).

[52] Jerrard, H.G., "Examination and Calibration of a Babinet Compensator, J.Sci. Instr. Vol. 27, pp.62-66, (1950).

[53] Jerrard, H.G., "Examination and Calibration of Soleil Compasators", J.Sci. Instr. (1950).

[54] Photoelastic Inc., "Materials for Photoelastic Coatihgs-Photoelastic Models", Bulletin P-1120-1, (1970).

A P P E N D I X I

TESTING EQUIPMENT AND METHODS

A P P E N D I X I

TESTING EQUIPMENT AND METHODS

AI.1 THE LOADING FRAME

Figure A.1 shows the frame that was used to test the performance characteristics of the Laced Connection System. In designing this frame, the need for complete versatility of the size of the encompassing model was a major factor considered. This frame is used for different testing procedures making only little modifications. It is formed of stiff steel members interconnected by bolts.

AI.2 LOADING MECHANISMS

AI.2.1 Two-Ton Hydraulic Ram

The Enerpac pull type hydraulic ram [40] shown in Figure A.2 is used here, to pull the lacing cable.

AI.2.2 Gilmore Electrohydraulic Closed Loop Testing Machine

This is a standard Gilmore Testing Machine [41] with a 3,000 lb linear actuator fixed to its frame. Figure A.3 shows a connection system being tested on this machine. The Gilmore Machine is used for both static, as well as for dynamic loading tests.

AI.2.3 120,000 lb Tinus Olsen Testing Machine [42]

AI.2.4 C-Shaped End Piece With Nut

This attachment shown in Figure A.4, was designed to have one end resting on the edge of a panel and allowing the lacing cable to pass through it. The cable was connected to an eye bolt. To produce tension in the cable, the nut at the end of the eye bolt was tightened.

AI.2.5 Cable and Pulley System

Figure A.5 shows the method by which a distributed load was applied. The tension in the cable was produced by actuating the pull ram shown.

AI.3 LOAD MEASUREMENT

AI.3.1 Static Load

This may be measured using either a load cell designed and made at Sir George Williams University or by reading the indicator on the testing machine used in the test.

AI.3.2 Distributed Load

The magnitude of the distributed load was calculated from the tension in the cable and Pulley System described above and the geometrical configuration of the cable system.

AI.3.3 Dynamic Load

The amplitude and the frequency of the dynamic load applied by the Gilmore Machine can be determined from its console.

AI.4 MEASURING DISPLACEMENTS

AI.4.1 Dial Gages

These are standard Starrett dial gages. Figure A.6 shows the arrangement used to measure the displacement due to shear in a test.

AI.4.2 Displacement Transducers

Figure A.7 shows two such transducers used to monitor displacement. These transducers were designed, made and calibrated at Sir George Williams University [43].

AI.5 AUXILIARY EQUIPMENT

AI.5.1 Two-Angle Section Connection

The different components of the two-angle section connection are shown in Figure A.8. This connection was used to determine the optimum pin type and configuration, the best type of cable to be used and to allow the inspection of the movements of the cable and the bushings.

AI.5.2 The Pulley Connection

Figure A.9 shows this connection. It consists of two pulleys mounted on pins fixed to a steel frame.

A P P E N D I X II

METHODS FOR THE DETERMINATION OF FRINGE VALUES IN PHOTOELASTICITY, AND MODELING

A P P E N D I X II

METHODS FOR THE DETERMINATION OF FRINGE VALUES IN PHOTOELASTICITY, AND MODELING

AII.1 GENERAL

The stresses in the metal extrusions were analyzed using the photoelastic technique. This technique was selected because the stresses are viewed over the entire tested model enabling the investigator to determine directly the areas of stress concentrations. Enlarged models of the different sections were made of birefringent sheets. Material was taken away from the understressed areas in a section, while material was added to the overstressed areas. This was done to allow a reasonable flow of stresses over the entire model. This technique is described by Heywood [23] and others.

AII.2 DETERMINATION OF STRESSES ON PHOTOELASTIC MODELS

The relation between the difference between the principal stresses and fringe order, as given by Heywood [23] may be rewritten as

$$\sigma_1 - \sigma_2 = Nf_\sigma/h \qquad \text{(II.1)}$$

where $\sigma_{1,2}$ are the principal stresses

$N = \Delta/2\pi$ is the fringe order

Δ is the relative retardation

$f_\sigma = \lambda/c$ is the material fringe value, psi-in

h is the material thickness, in

λ is the wavelength of light

c is the relative optic coefficient of the material

It is evident that the stress difference may be evaluated at every point on a model when the fringe order is determined.

Many methods have been used for the determination of fringe orders. References [23-32] are among those describing most of the methods used.

Scanning methods may be divided into two groups depending on whether the actual model is scanned or a photographic plate of the stressed model is used as the object to be scanned.

AII.2.1 Scanning a Photographic Plate

Scanning of a photographic plate by an Autodensidater [44] gives reliable results of the fringes recorded on the photograph. The photographic plate however shrinks unevenly during processing, giving rise to non-linearities

in the photograph. Non-linearities also arise due to film response, as described by Sciammarella et al [45].

Among the other problems arising from the use of photographic plates is the infidelity of the recorded image of the object model. This infidelity is due to the inherent distortions in the lens used in producing the photographic plate.

AII.2.2 Scanning of the Model Itself

Two techniques that may be used were described by Khalil and Fazio [46] and [47]. The position of the imaging lens in relation to the scanning system decides on the technique used to determine accurately the fringe position.

AII.2.3 Lens Moving With Scanning Device

Figure A.10 shows a schematic diagram of the set-up. The light source (DLS) emits diffused light which passes through the polariser (POL), Quarter Wave Plate (QWP1), model, Quarter Wave Plate (QWP2) and the analyser (ANA), through which the isochromatic patterns are seen. The projecting lens (PL) magnifies the isochromatic pattern and images this pattern onto a screen with a pinhole (PH). The rays passing through the pinhole are collected by the lens (CL) which is placed so that its focus is at the pinhole and the rays collimated are projected onto a Cadmium Sulphide photo-

cell (PC) connected to a differential amplifier, RC filter and the Y-terminal of an X-Y electronic recorder. The lens (PL), pinhole (PH), lens (CL) and the photocell (PC) are all mounted on a transverse stage that has a motion in a direction that is parallel to the plane of the model. The motion of this stage is monitored by a displacement transducer whose output is connected to the X-terminal of the X-Y electronic recorder.

It is imperative that all the components be firmly mounted on the transverse stage holding them. The focal lengths of the lenses in the scanning devices are chosen to be as large as possible to reduce errors in focusing. Due to the long focal lengths, the different components on the transverse stage are placed a large distance apart. This increases the sensitivity of the scanning components to vibrations, which increase the errors in the measurements.

AII.2.4 Stationary Lens and Moving Scanning Device

This set-up is shown in Figures A.11 and A.12. It is similar to that described in the previous section except that in this one, the projecting lens is stationary with respect to the scanning device. This set-up has the advantage that the moving parts are all concentrated in a small area. This decreases the vibration problems. The disadvan-

tages of this system are in the errors in the image due to the inherent distortion in the projecting lens system. These errors will be present in the X-axis of the X-Y plot. Correction factors obtained from the previous calibration of the projecting lens using moiré are used. This technique is described by Khalil and Fazio [48], [49] . With these correction factors, the errors in the measurements are nearly eliminated.

AII.3 DETERMINATION OF FRINGE VALUES

Figure A.13 shows an example of a resulting scan of a stressed model. To determine the position of an integer fringe order (the point of minimum intensity on the curve also called the extinction point) is extremely difficult; since this point is not distinctively defined,as can be seen by close examination of Figure A.13. Barer and Cosslet [50] give a complete analysis of the errors in determining the extinction points.

The following are methods for determining fringe values:

AII.3.1 Use of Two-Band Pass Filters

The spectrophotometric curves for two superimposed band pass filters are shown in Figure A.14. The data for these curves was taken from reference [51] for number 25 (Red Filter) and number 58 (Green Filter). It can be seen

from these superimposed curves that they intersect at 5893 Å which is the wavelength of Yellow Light. From these superimposed curves, it can be noted that the band of transmittence is very narrow.

In photoelasticity, using white light, a fringe is present when the yellow colour (5893 Å) is extinguished from the spectrum of colours. On a stressed model, this point is determined by determining the point where the colour changes from red to green.

From the observations mentioned above, a theory was established and a test was made to verify this theory. In this test, the stressed model was illuminated with white light passed through a yellow band pass filter. A recorded scan of the model was made; this resulted in the upper curve of Figure A.15. The integer fringe orders would occur at points A' and C' of that curve. Points B' and D' would be half fringe orders. Two more scans along the same points as the first scan were made. The latter scans are made with the yellow filter replaced once by a green filter and once by a red filter. The plots of these scans are shown in Figure A.15. The points of intersection of the latter two scans when projected onto the former curve give the exact location of the points A', B', C' and D'.

The fringe order at any point on the stressed model

illuminated with yellow light may be evaluated by determining the partial fringe order with a red filter and with a green filter with the aid of a compensating device and using the relation derived below.

The phase shift at a particular point on a stressed model may be determined by the following equation taken from Reference [30]

$$\Delta = \frac{K}{\lambda} (\sigma_1 - \sigma_2) \qquad \text{(II.2)}$$

Using the subscripts Y, R, and G for yellow, red and green, respectively, we can rewrite Equation (II.2)

$$\Delta_Y = \frac{K}{\lambda_Y} (\sigma_1 - \sigma_2) \qquad \text{(II.3)}$$

$$\Delta_R = \frac{K}{\lambda_R} (\sigma_1 - \sigma_2) \qquad \text{(II.4)}$$

$$\Delta_G = \frac{K}{\lambda_G} (\sigma_1 - \sigma_2) \qquad \text{(II.5)}$$

The above are the equations relating the relative retardation to the wavelength of light, at a particular point on a stressed model. Subtracting Equation (II.4) from (II.5) gives

$$\Delta_G - \Delta_R = K(\sigma_1 - \sigma_2)\left[\frac{1}{\lambda_G} - \frac{1}{\lambda_R}\right] \qquad \text{(II.6)}$$

and replacing $K(\sigma_1 - \sigma_2)$ from Equation (II.3) gives

$$\Delta_G - \Delta_R = \Delta_Y \lambda_Y \left[\frac{1}{\lambda_G} - \frac{1}{\lambda_R}\right]$$

which when rearranged becomes

$$\Delta_Y = \frac{(\Delta_G - \Delta_R)(\lambda_G \cdot \lambda_R)}{\lambda_Y(\lambda_R - \lambda_G)} \qquad \text{(II.7)}$$

This equation is very useful in the verification of the correctness of the values of the partial fringe orders measured.

AII.3.2 Superposition of Background Intensity Onto the Scan of an Isochromatic Pattern

An accurate method for determining the partial fringe orders may be achieved by superimposing a scan of the intensity of the unstressed model onto the scan made with the yellow filter described in the previous section.

To determine the fringe order at any point along the scan with the yellow filter, the vertical distance from the point under investigation to the background intensity scan is measured. The vertical distances from the points of maximum and minimum intensities, as determined using the method described in the previous section, to the scan of the background intensity are also measured. From these measurements the partial fringe order at the point under investigation may be determined, using the following observations:

(i) A curve giving the relationship between the relative intensity of light and the inclination of the analyzer to the polarizer is given in Figure A.16. In that same figure, the square roots of the relative intensities versus the relative inclination of the analyzer to the polarizer are also given. It can be assumed here, that since the second curve is a straight line, then the first one could be a parabola, approximately.

(ii) Figure A.17 is one which gives the different plots described earlier. "X" is the point at which the partial fringe value is to be determined.

(iii) The fringe value increases from point "C" to "A" since the colour changes from red to green.

(iv) Assuming that at point "C", we have an N_C order fringe, then at point "X" the fringe order would be

$$N_X = [N_C + (\frac{c'c'' - x'x''}{c'c'' + B'B''})^{\frac{1}{2}}] \qquad (II.8)$$

It should be noted that the second term of the above expression represents a fraction of half a fringe. The validity of the above expression was checked by determining the partial fringe order using a Babinet-Soleil compensator [52, 53]

and the described theory. The results differed by less than 3%.

AII.3.3 Point-By-Point Detection

The Babinet-Soleil Compensator is one of the most used instruments to determine partial fringe orders. This instrument suffers from its reliance on the ability to sense and locate the exact point of extinction on the compensator. To locate this point accurately, a photosensitive element is placed on the viewing side of the compensator; the output of this element is connected to the Y-terminal of an X-Y recorder. The change in the optical path length of the compensator is monitored. The output voltage of the monitory device is connected to the X-terminal of that recorder. Two scans are recorded, one with a red filter in front of the compensator and one with a green filter. Using the same procedure described in Section A.II.3.1, above, the point of extinction of light is determined. The fractional fringe order may be determined immediately from the calibrated X-axis of the plot.

AII.4 MODELLING AND SCALING

Two-dimensional models of the metal extrusions were cut from plastic birefringent sheets, Type PS-8-A, supplied by Photoelastic Incorporated [54]. Models of the wooden parts

of the connection were cut from PS-3-A birefringent sheets, also supplied by Photoelastic Incorporated.

The stress compatibility equation for plane strain in the absence of body forces is

$$\nabla^2(\sigma_x + \sigma_y) = 0 \qquad \text{(II.9)}$$

where ∇^2 is the operator $(\partial^2/\partial x^2 + \partial^2/\partial y^2)$

σ_x and σ_y are stresses

It is to be noted that Equation (II.9) is independent of the modulus of elasticity and Poisson's ratio.

For the case of a two-dimensional model with an applied load P, the dimensionless ratio for stresses is $\frac{\sigma h l}{P}$. Thus, the stresses in the prototype may be written as

$$\sigma_p = \sigma_m \frac{P_p}{P_m} \frac{h_m}{h_p} \frac{l_m}{l_p} \qquad \text{(II.10)}$$

where σ is the stress at a given point

P is the applied load

h is the thickness

l is a typical length dimension and

subscripts p and m refer to prototype and model

The process of optimization of sections is to reduce the material in the portions of the part that are understressed

and to redesign the portions that are overstressed. It should also be noted that cracks usually start from the periphery of a section. At the boundary, one of the principal stresses is zero. Thus, Equation (II.1) may be rewritten as

$$\sigma = \frac{N F_\sigma}{h} \qquad \text{(II.11)}$$

and it is thus only necessary to determine the stresses at the boundaries of the model.

AII.5 CONCLUSIONS

The new methods described in this appendix, show that the fringe orders, at specified points on a stressed birefringent specimen placed in a polariscope, can be detected with greater accuracy. The method for determining partial fringe orders using the background intensity scan needs further improvement. The use of the fringe multiplication technique, as given by Heywood [23] and others, will improve further the accuracy of the results as obtained by the methods described in this work.

Determination of partial fringe orders using compensator techniques as described here, needs further study and refinements.

F I G U R E S

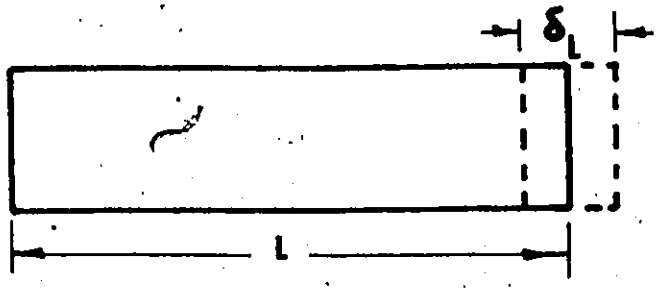

FIGURE 2.1 LONGITUDINAL THERMAL DEFORMATIONS IN PANELS

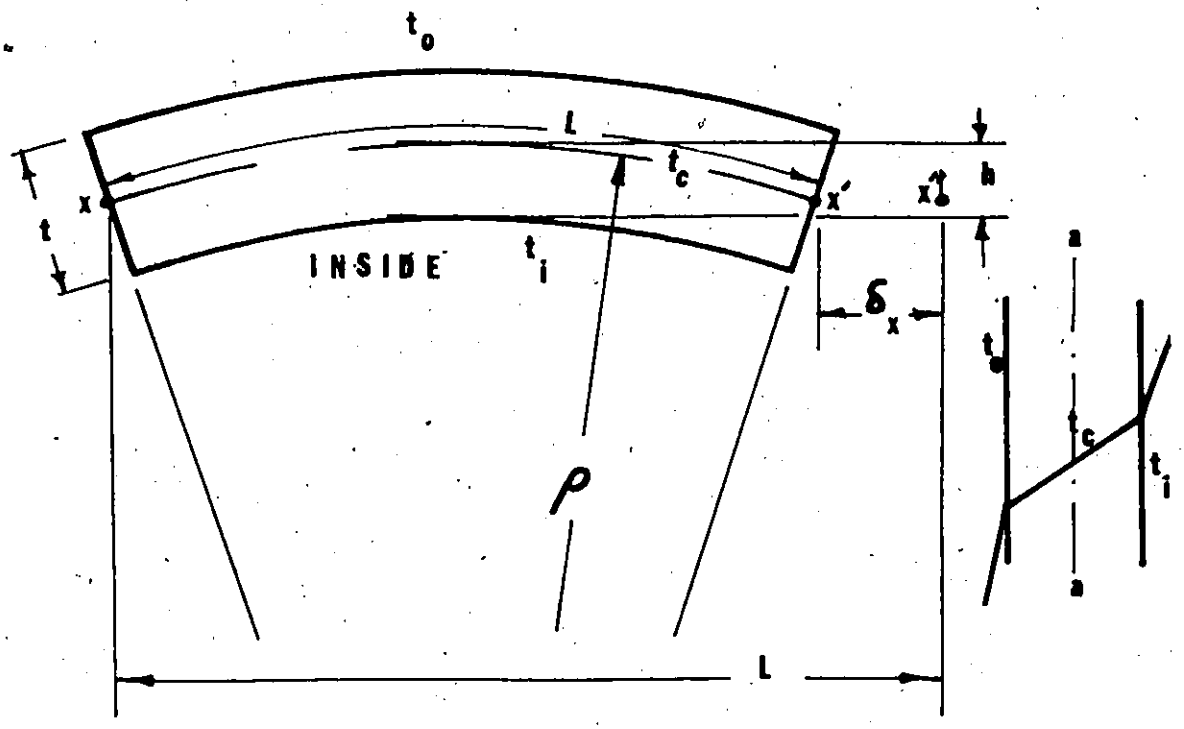

FIGURE 2.2 BENDING DEFORMATIONS

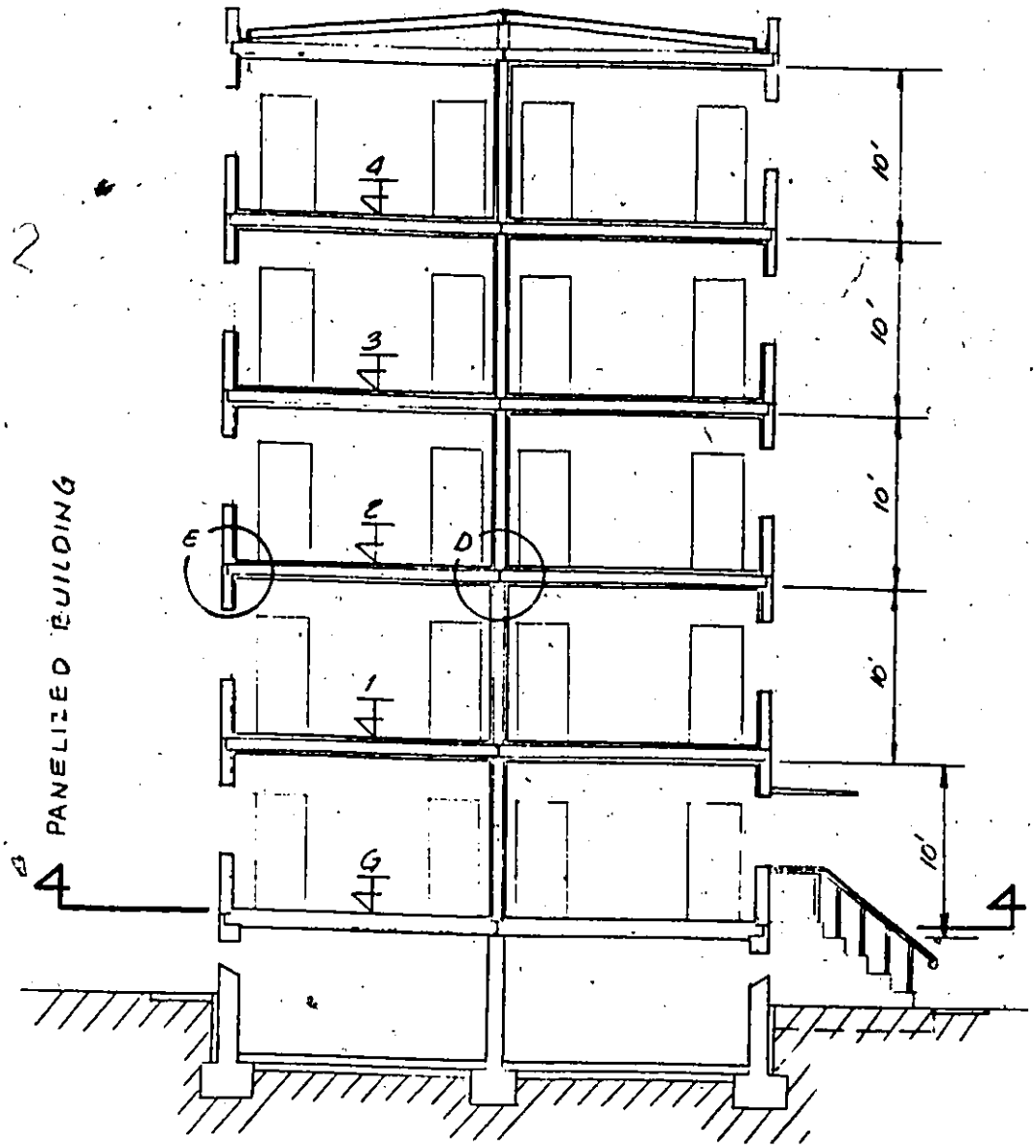

FIGURE 2.3 ELEVATION OF TYPICAL PANELIZED BUILDING (REPRODUCED FROM [15]*)

* Numbers in Square Brackets Refer to Reference Numbers

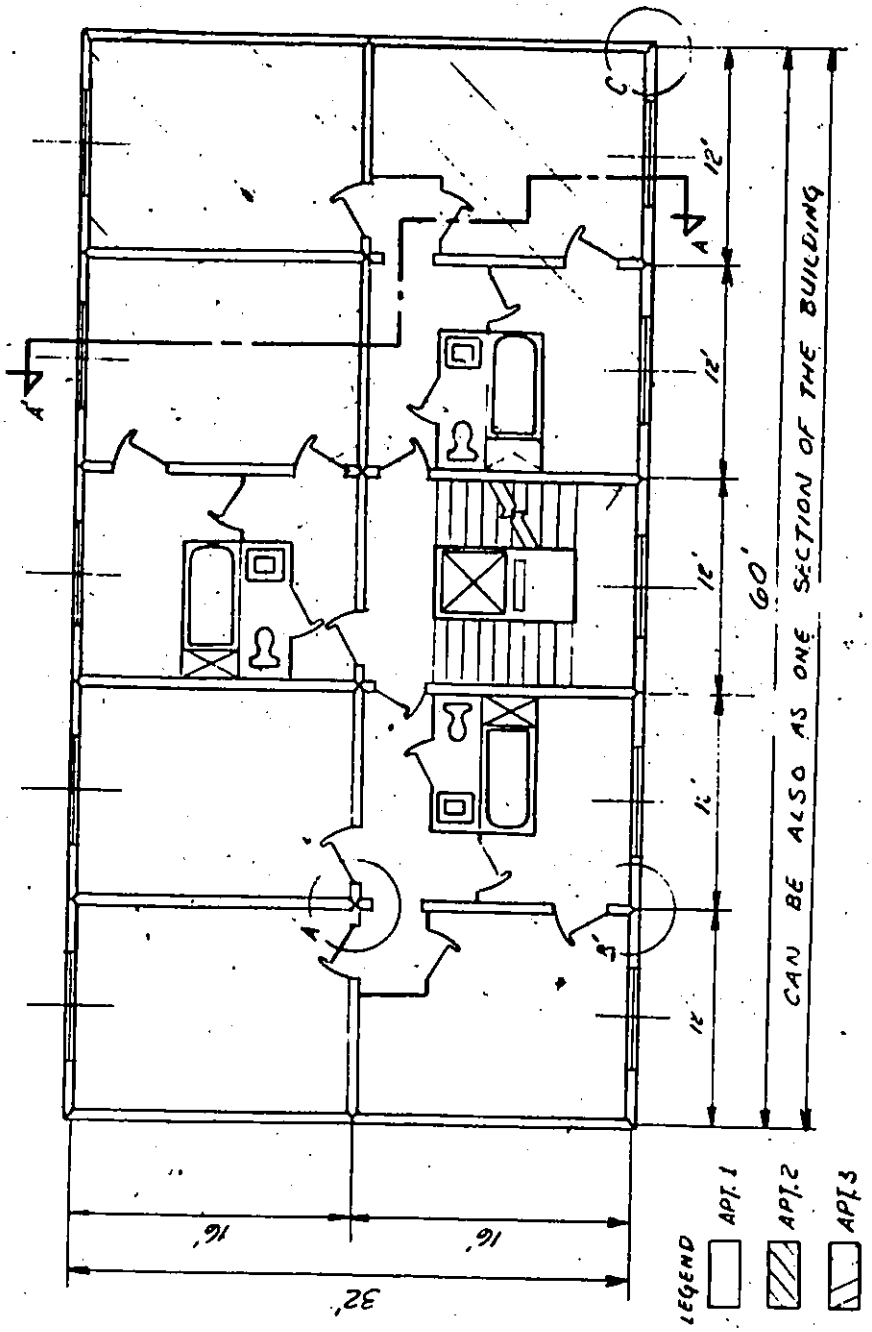

FIGURE 2.4 PLAN OF TYPICAL FLOOR OF PANELIZED DWELLING BUILDING
(REPRODUCED FROM [15])

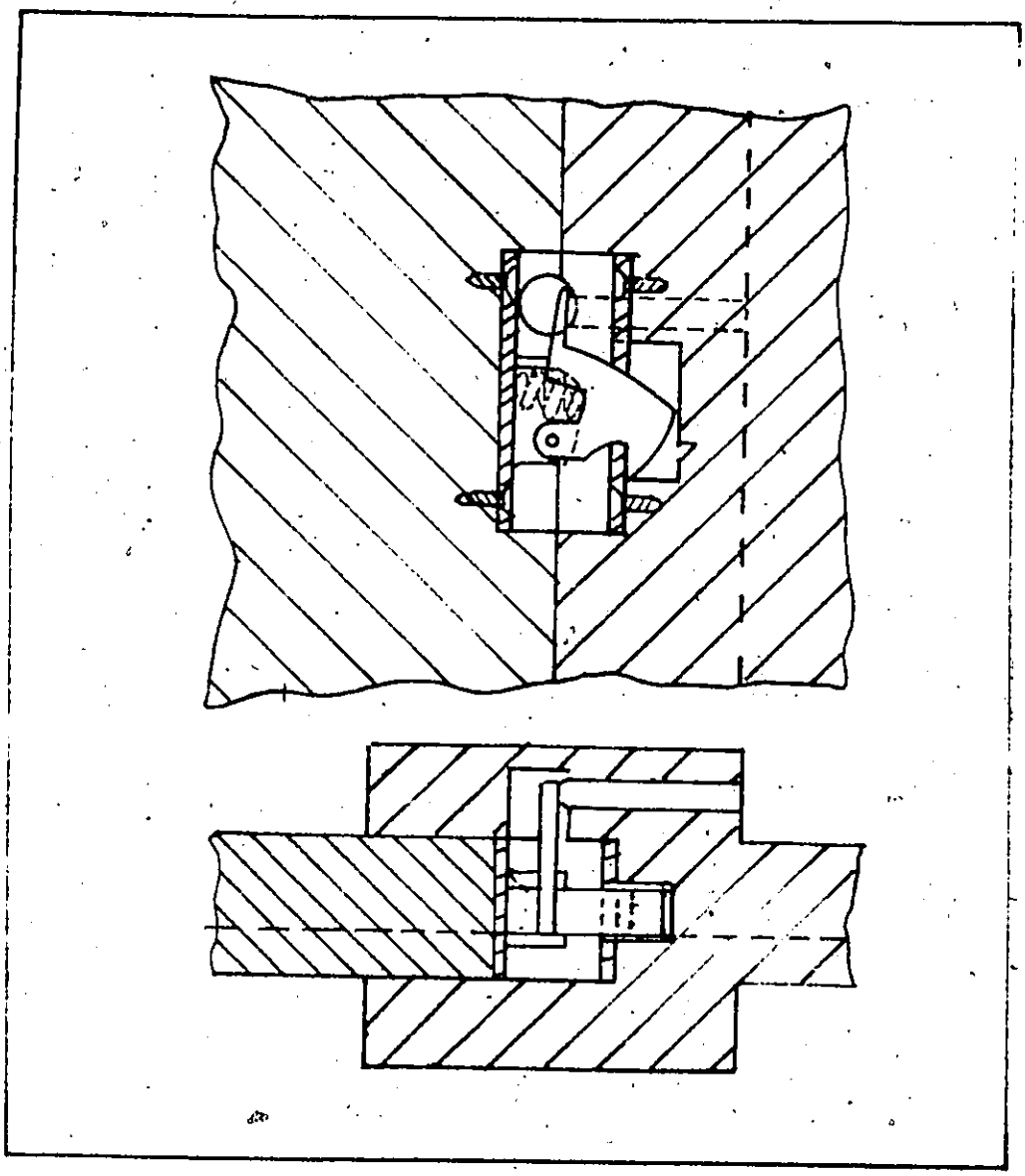

FIGURE 3.1 ADAM'S CONNECTION SYSTEM
(REPRODUCED FROM [8])

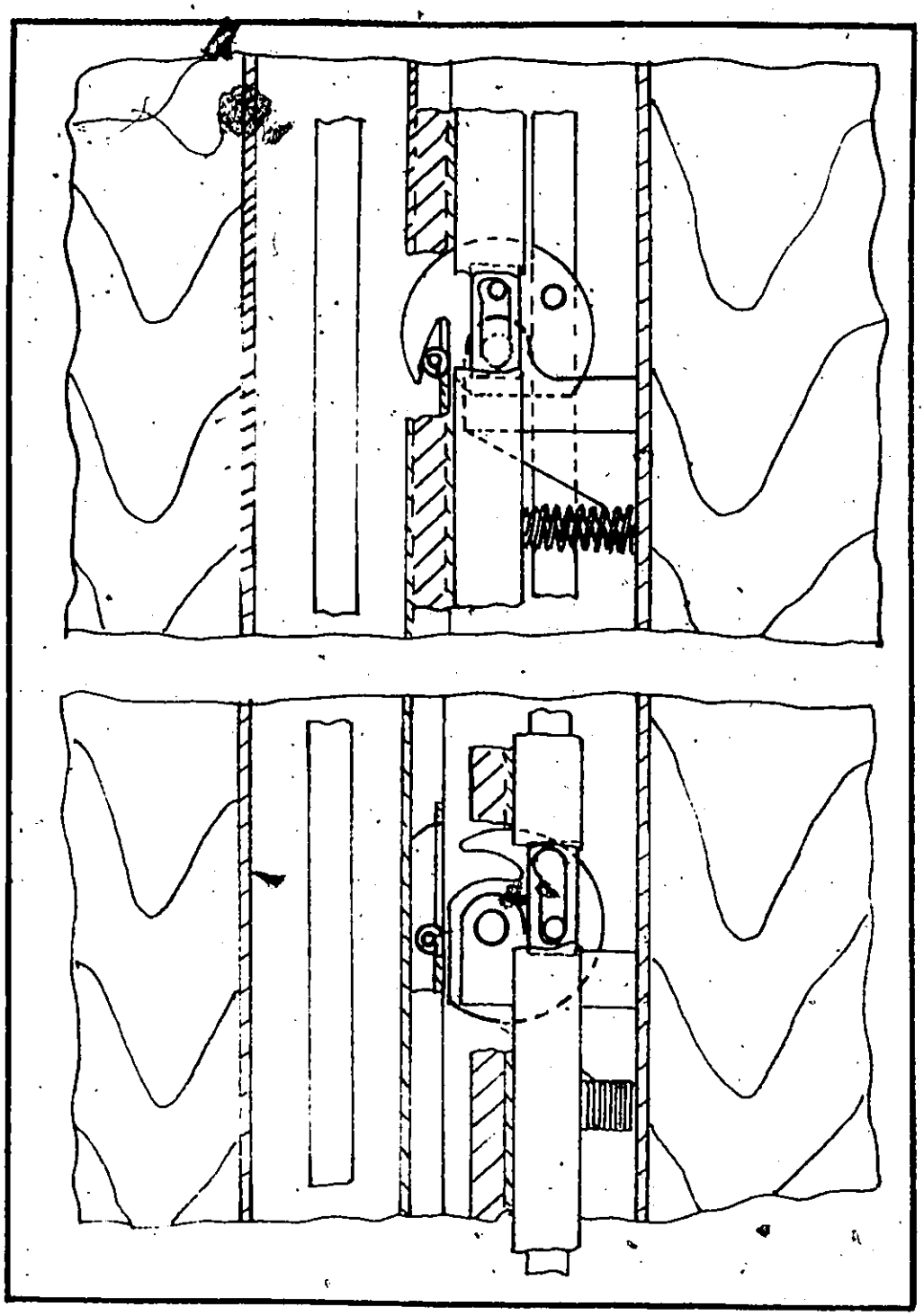

FIGURE 3.2 THE THELANDER CONNECTION

(REPRODUCED FROM [9])

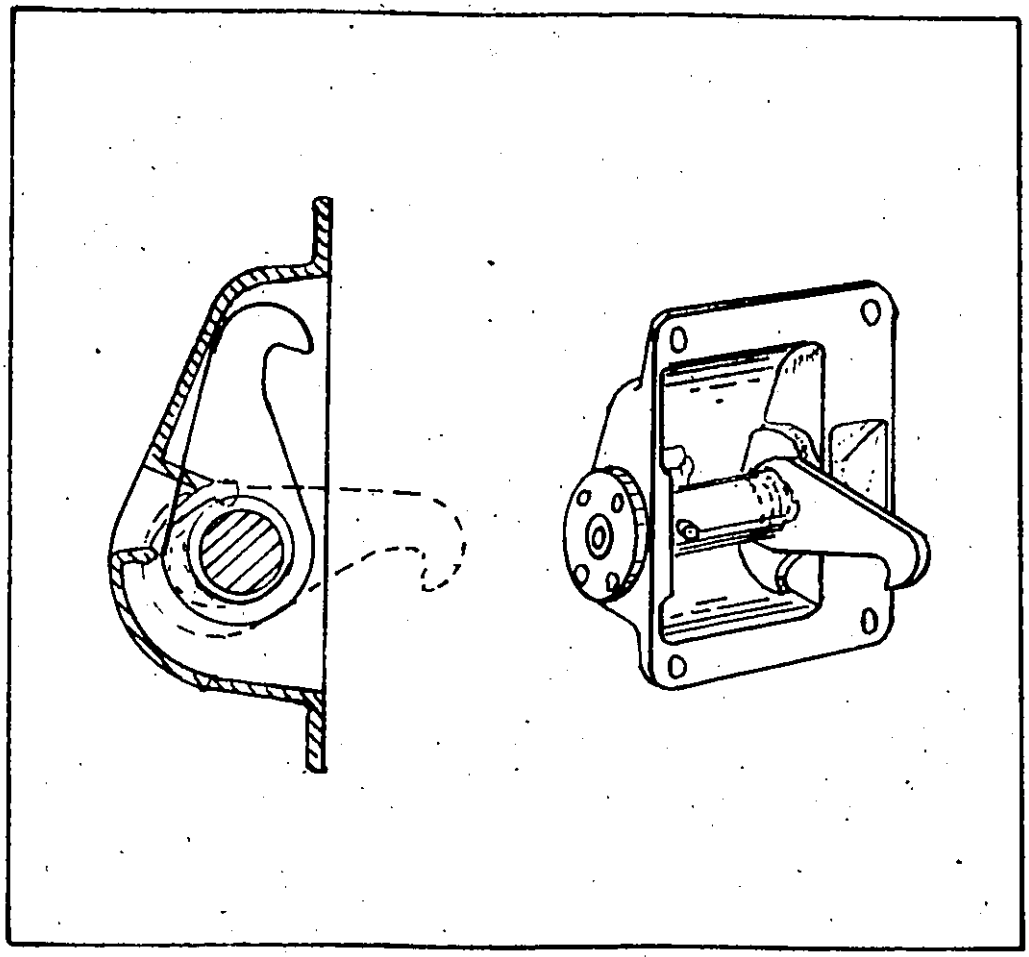

FIGURE 3.3 THE LOCKING MECHANISM BY JONES
(REPRODUCED FROM [10])

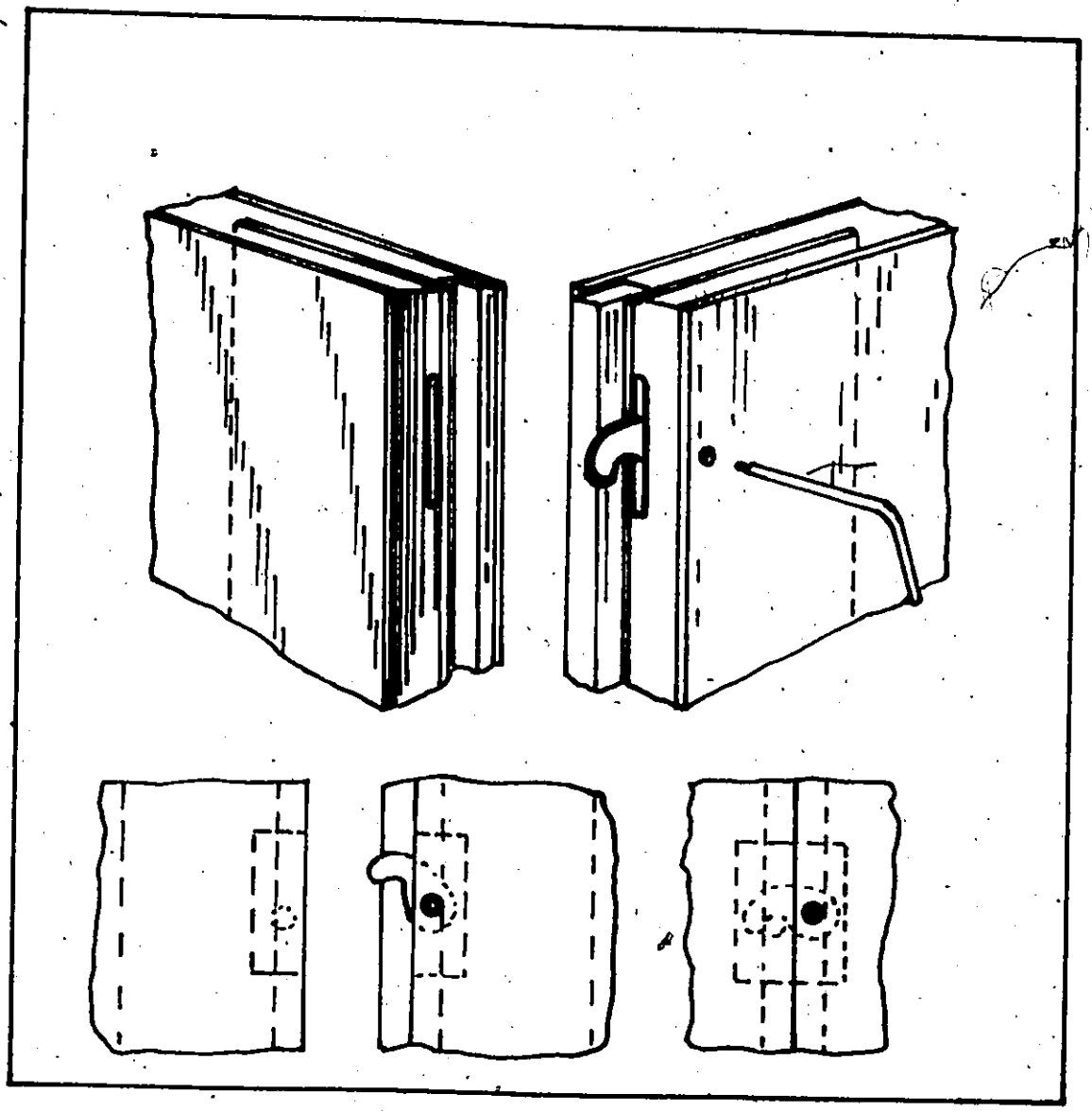

FIGURE 3.4 PALFEY ET AL FASTENER

(REPRODUCED FROM [11])

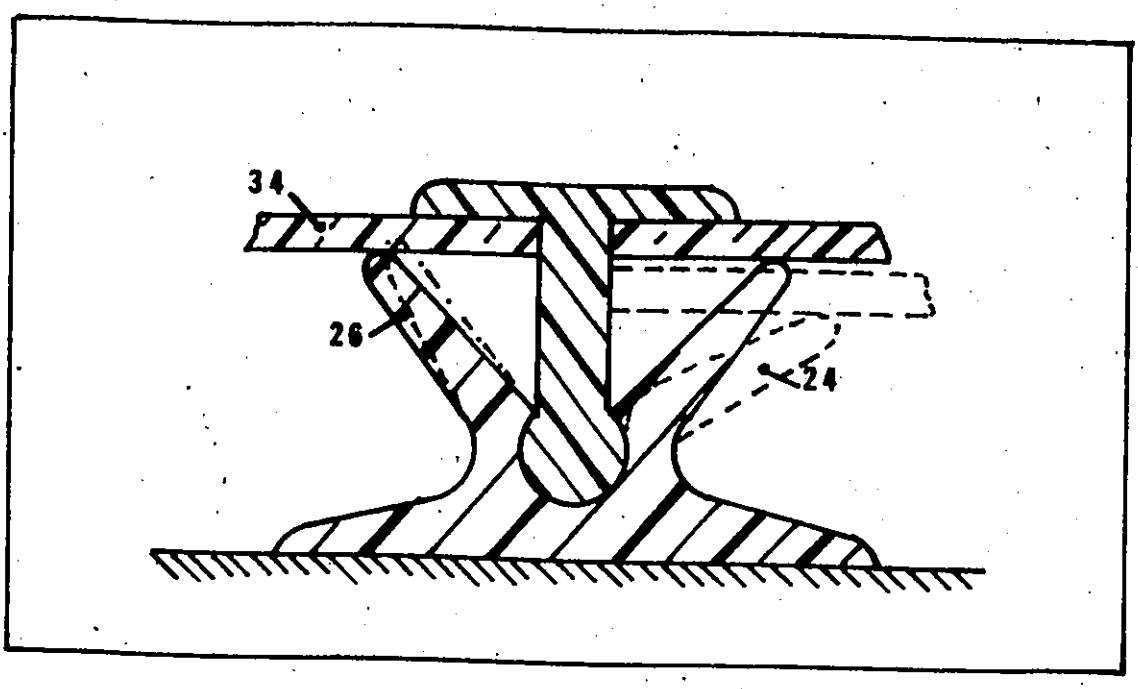

FIGURE 3.5 WALL FIXING CONNECTOR BY LOGAN
(REPRODUCED FROM [12])

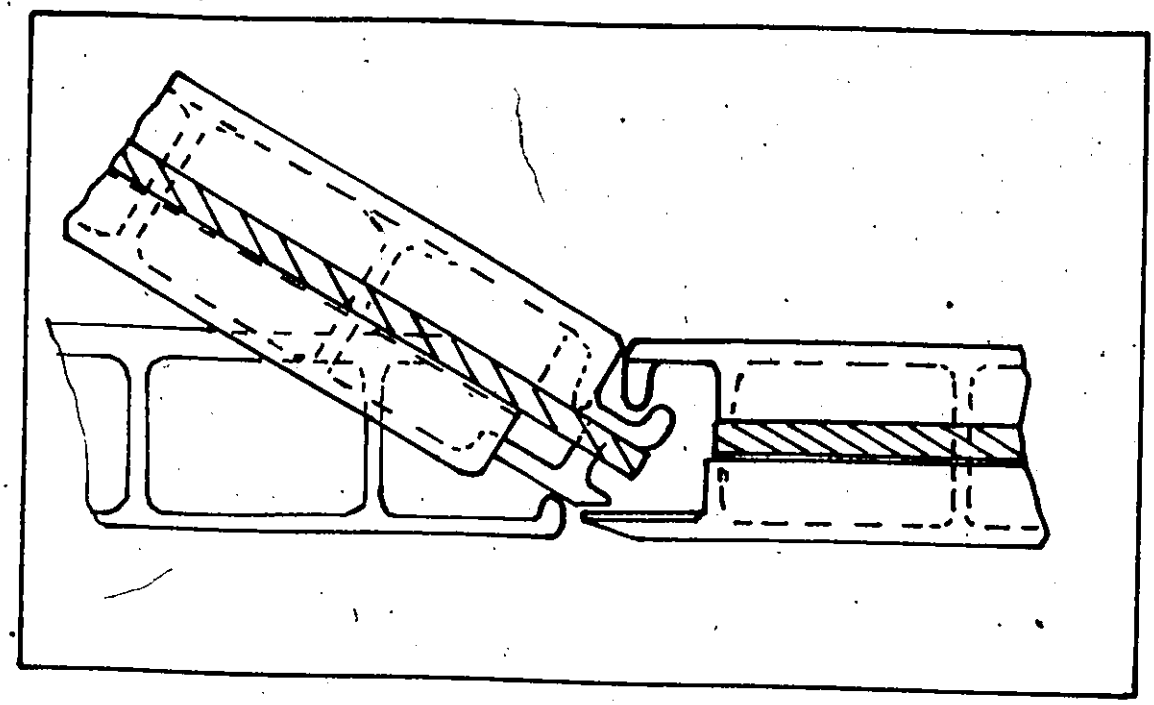

FIGURE 3.6 THE CONNECTION PATENTED BY HARVEY
(REPRODUCED FROM [13])

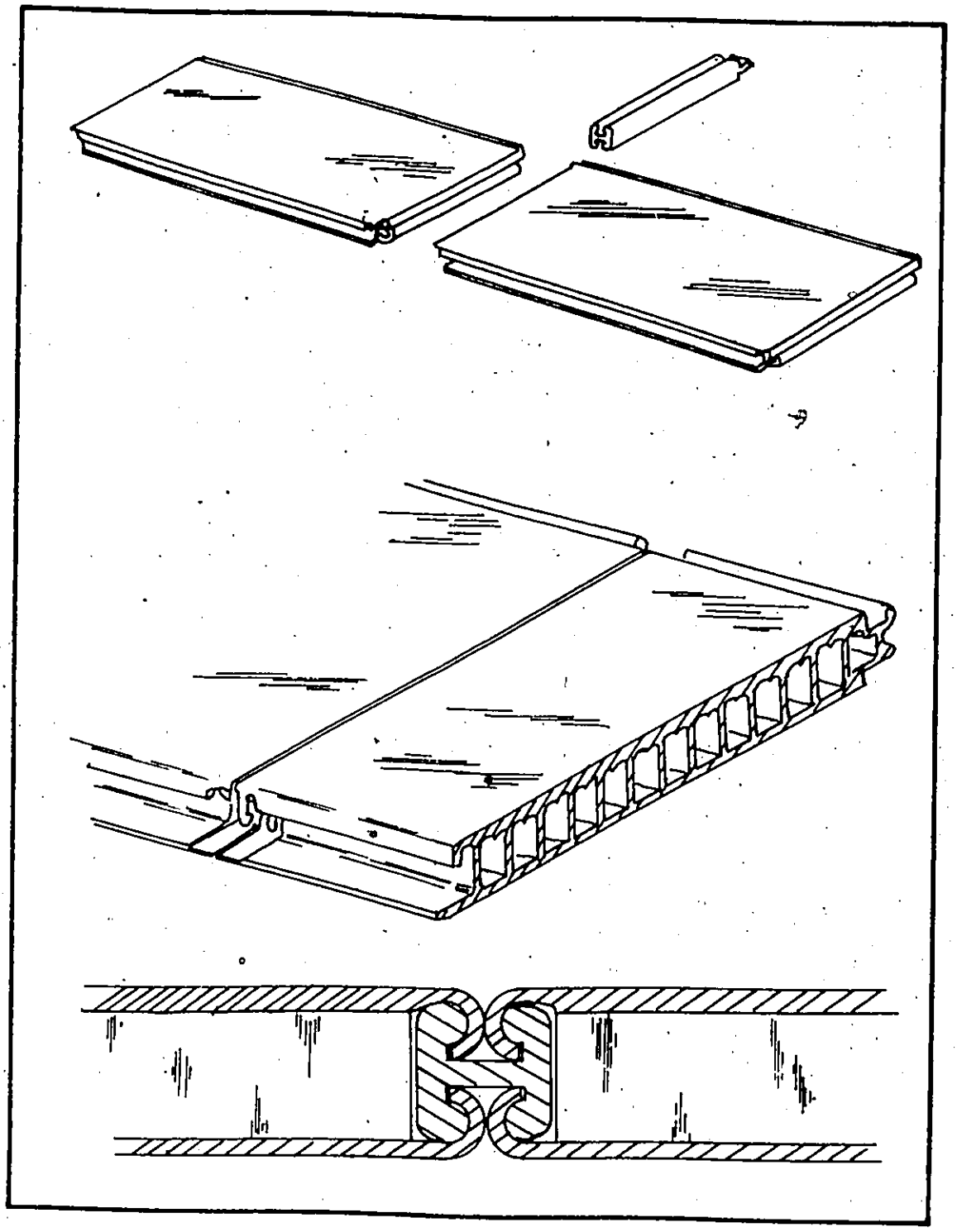

FIGURE 3.7 THE HARVEY COUPLING

(REPRODUCED FROM [13])

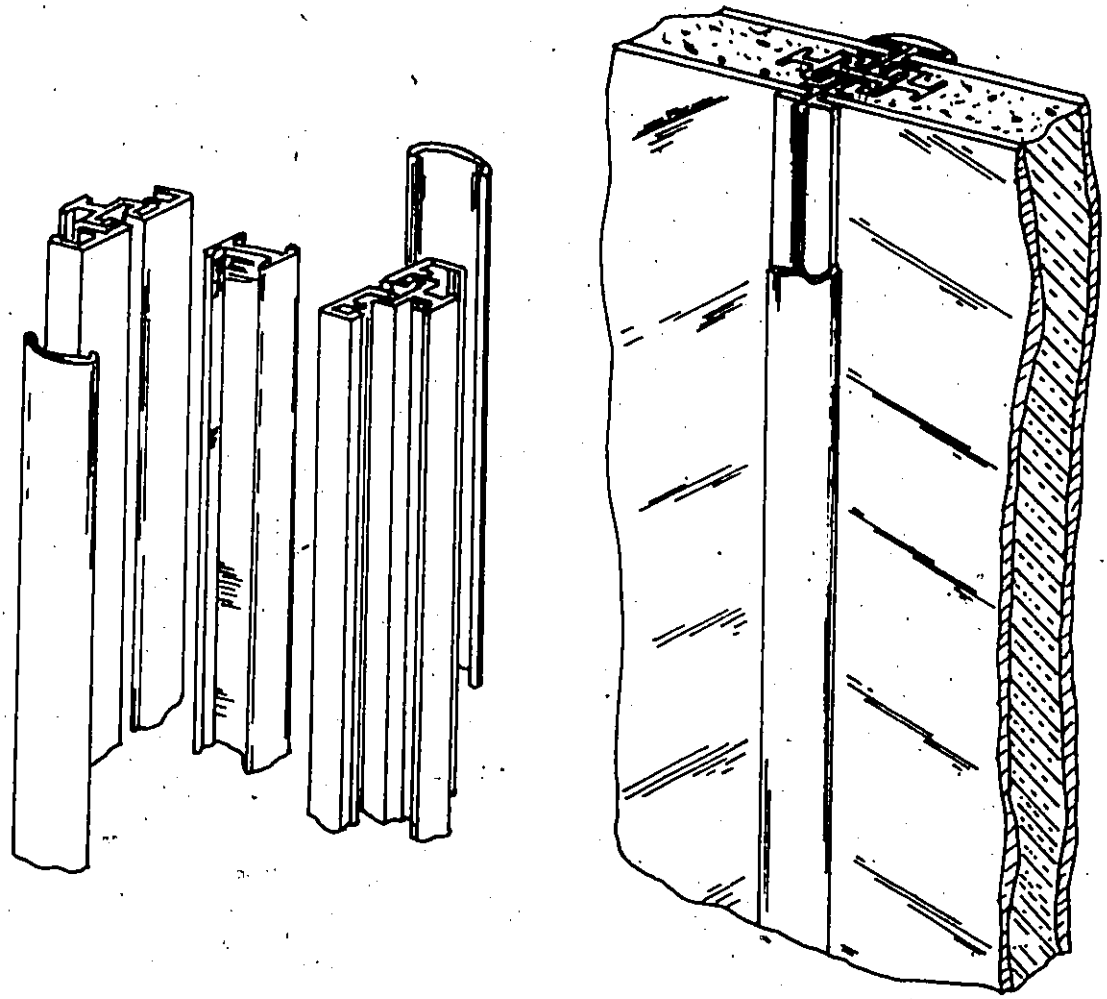

FIGURE 3.8 THE MORGAN CONNECTION

(REPRODUCED FROM [14])

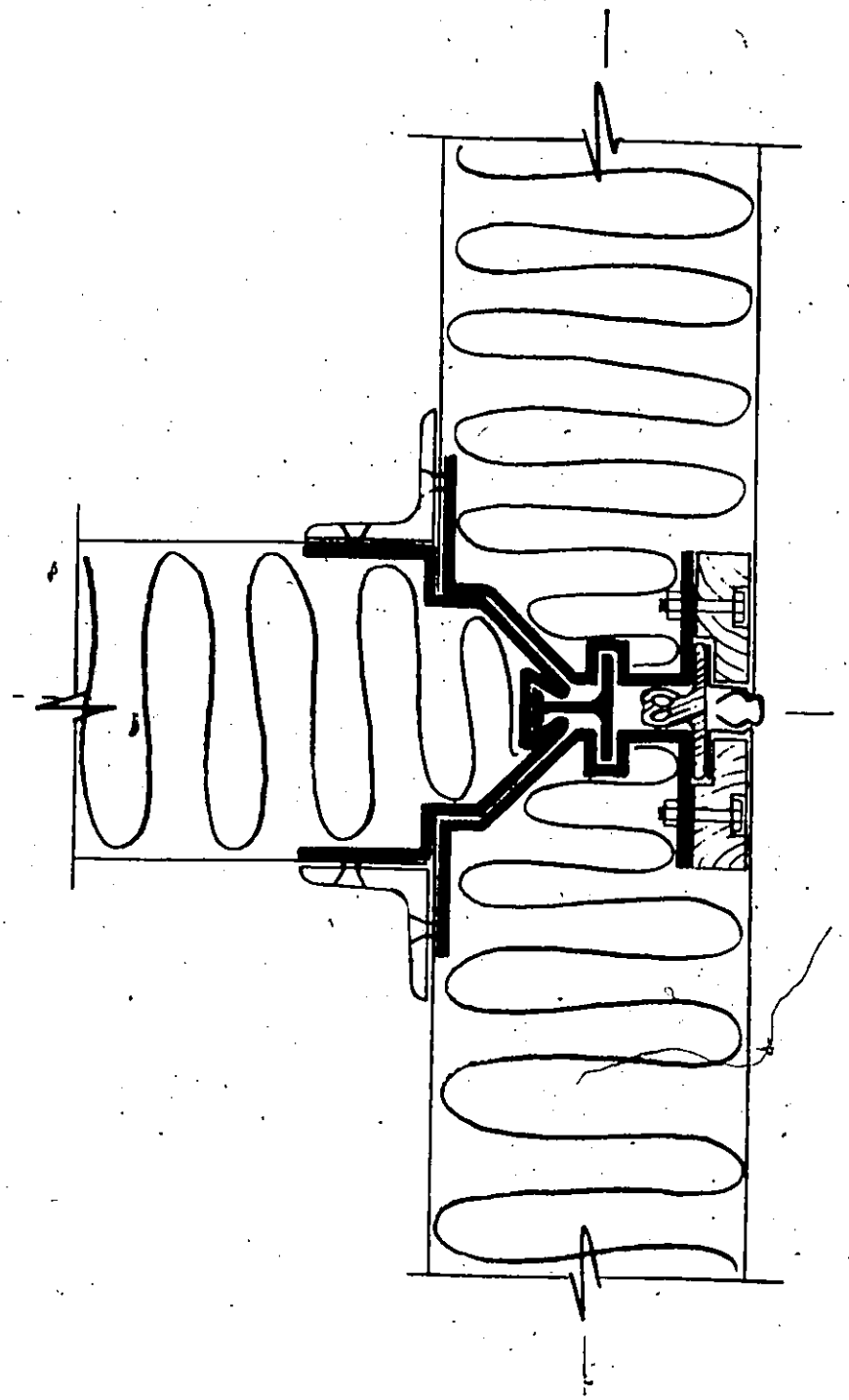

FIGURE 3.9 VERTICAL JOINT AT JUNCTION OF INTERNAL WALL PANEL WITH EXTERNAL WALL PANELS
(REPRODUCED FROM [15])

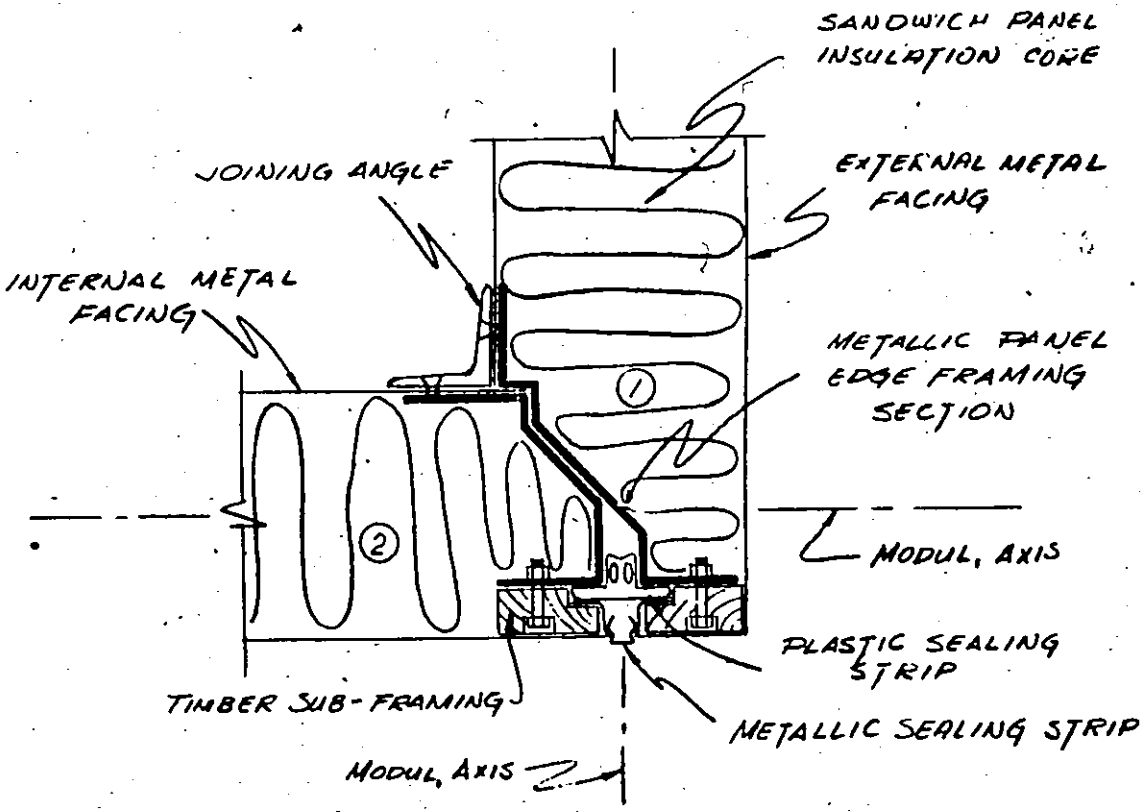

FIGURE 3.10 VERTICAL JOINT OF EXTERNAL WALL PANELS AT THE BUILDING CORNER
(REPRODUCED FROM [15])

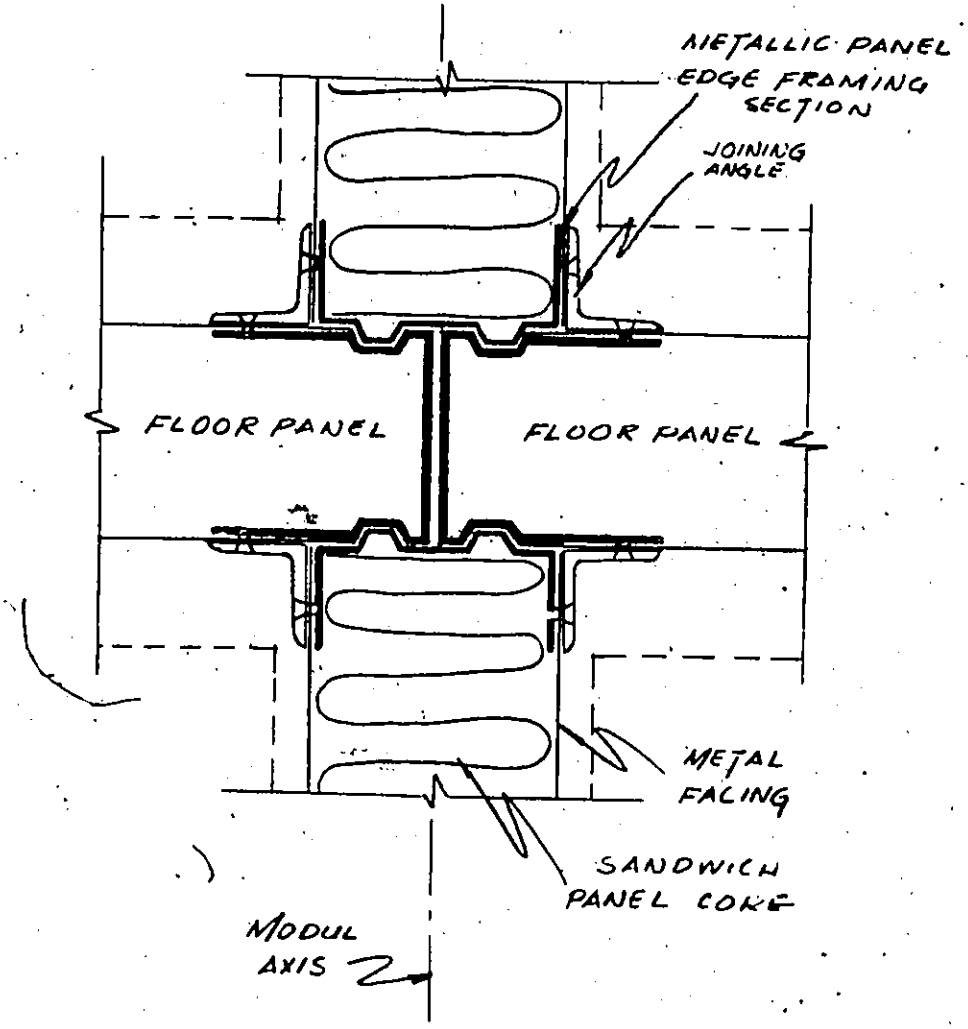

FIGURE 3.11 HORIZONTAL JOINT, INTERNAL WALL PANELS WITH FLOOR PANELS

(REPRODUCED FROM [15])

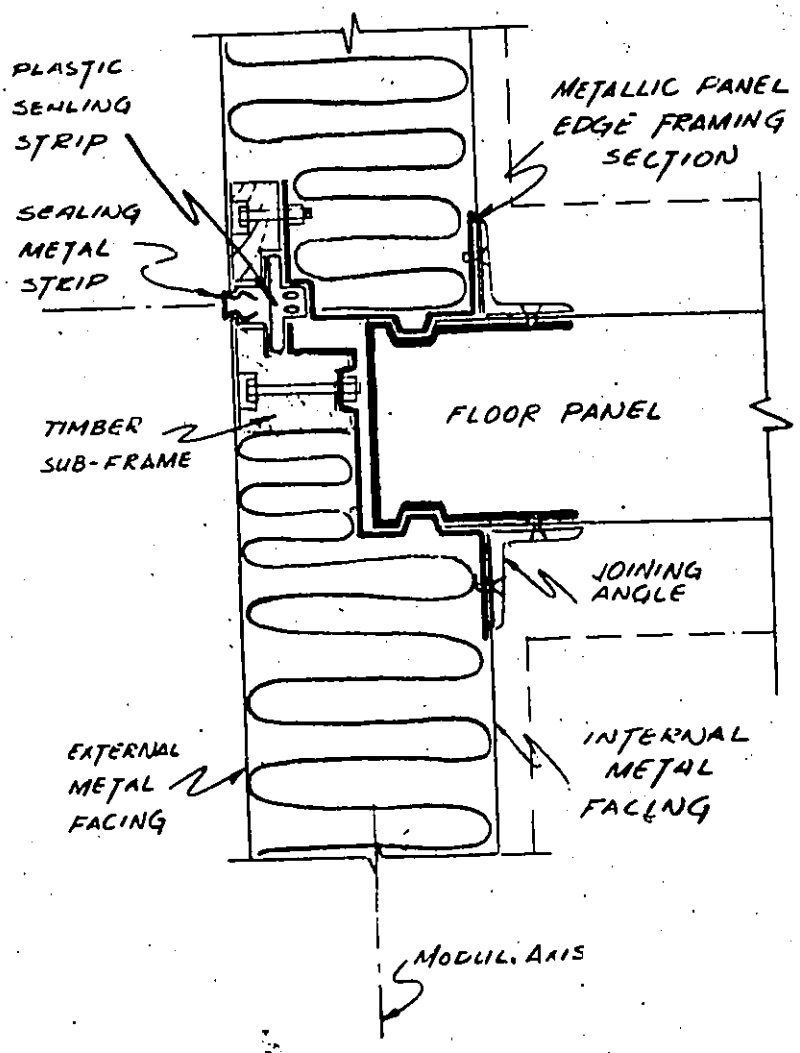

FIGURE 3.12 HORIZONTAL JOINT, EXTERNAL WALL PANELS WITH FLOOR PANELS

(REPRODUCED FROM [15])

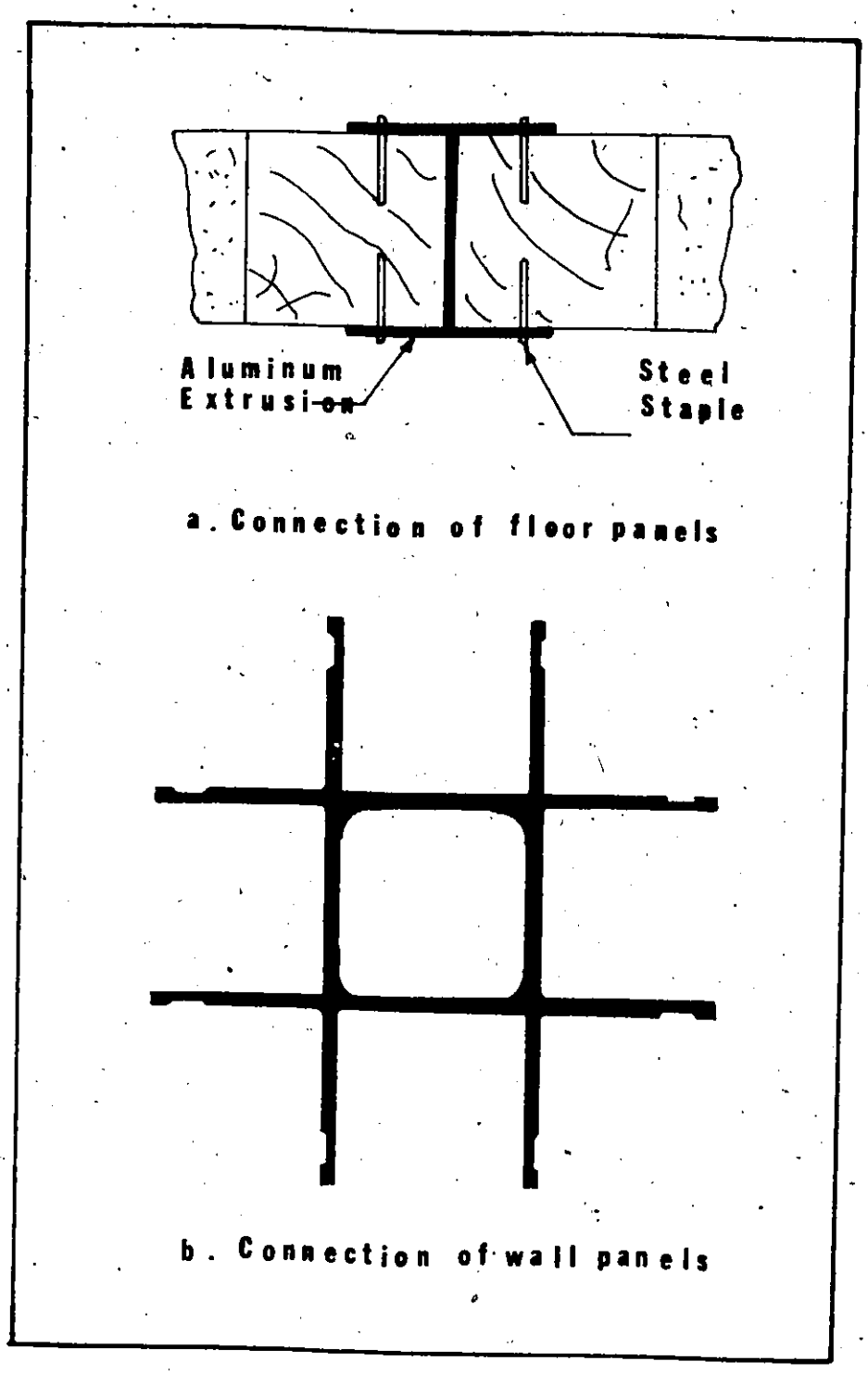

FIGURE 3.13 THE STAPLED CONNECTION
(REPRODUCED FROM [17])

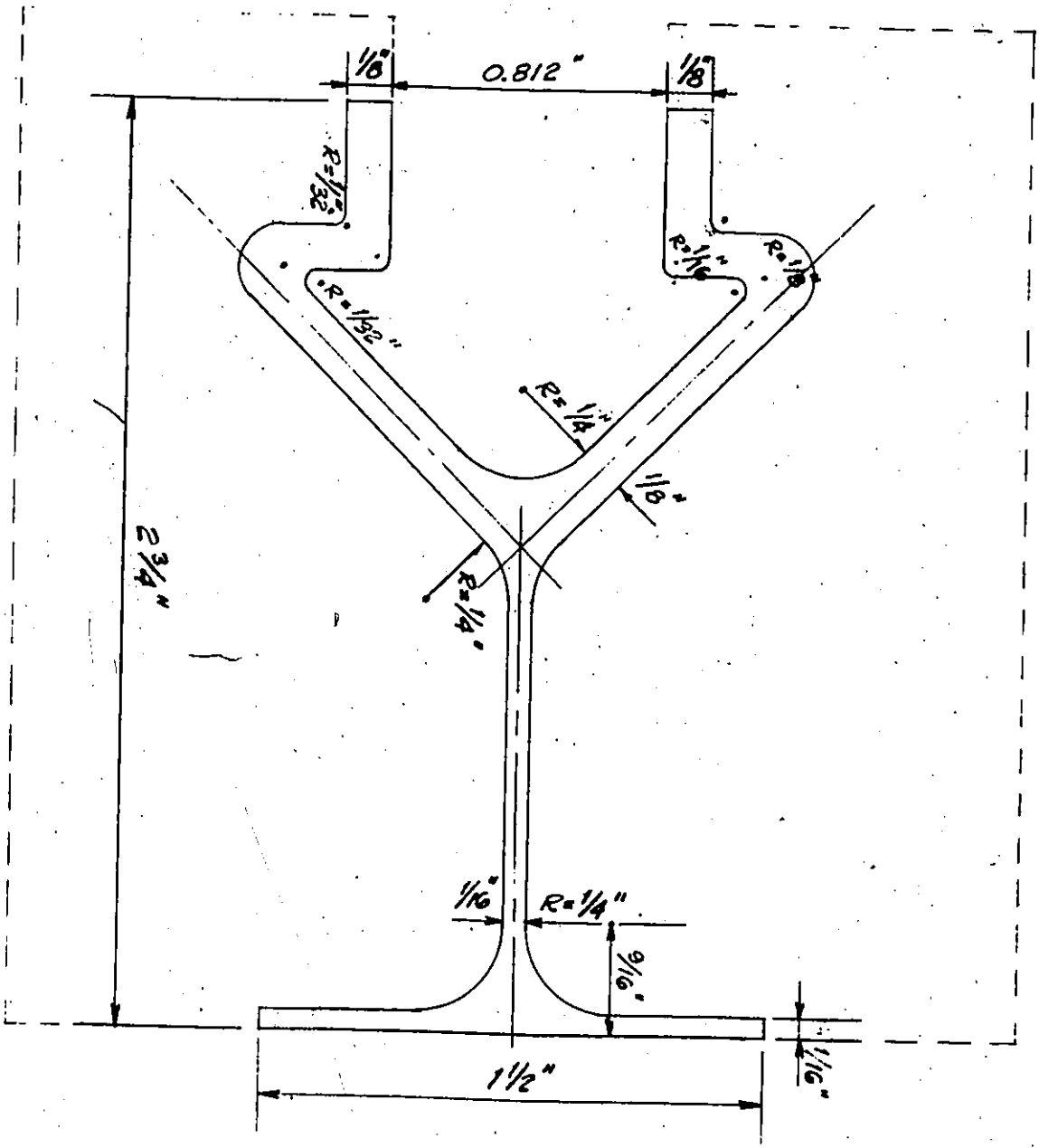

FIGURE 3.14 THE PANEL-TO-PANEL FEMALE EXTRUSION

(REPRODUCED FROM [1])

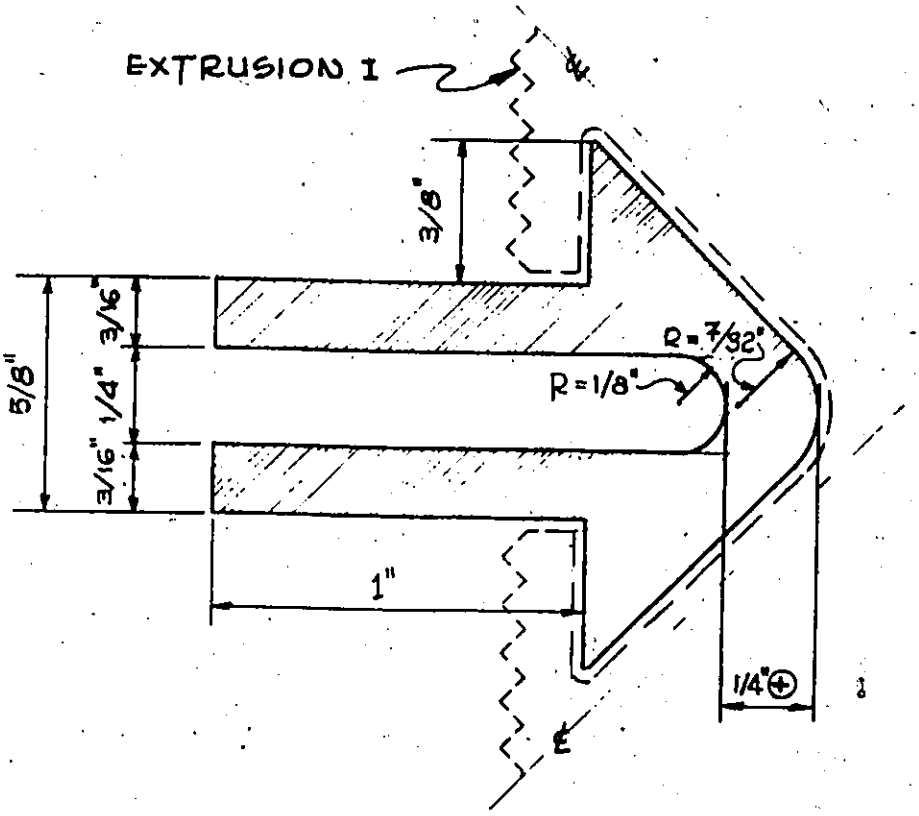

FIGURE 3.15 THE MALE EXTRUSION

(REPRODUCED FROM [1])

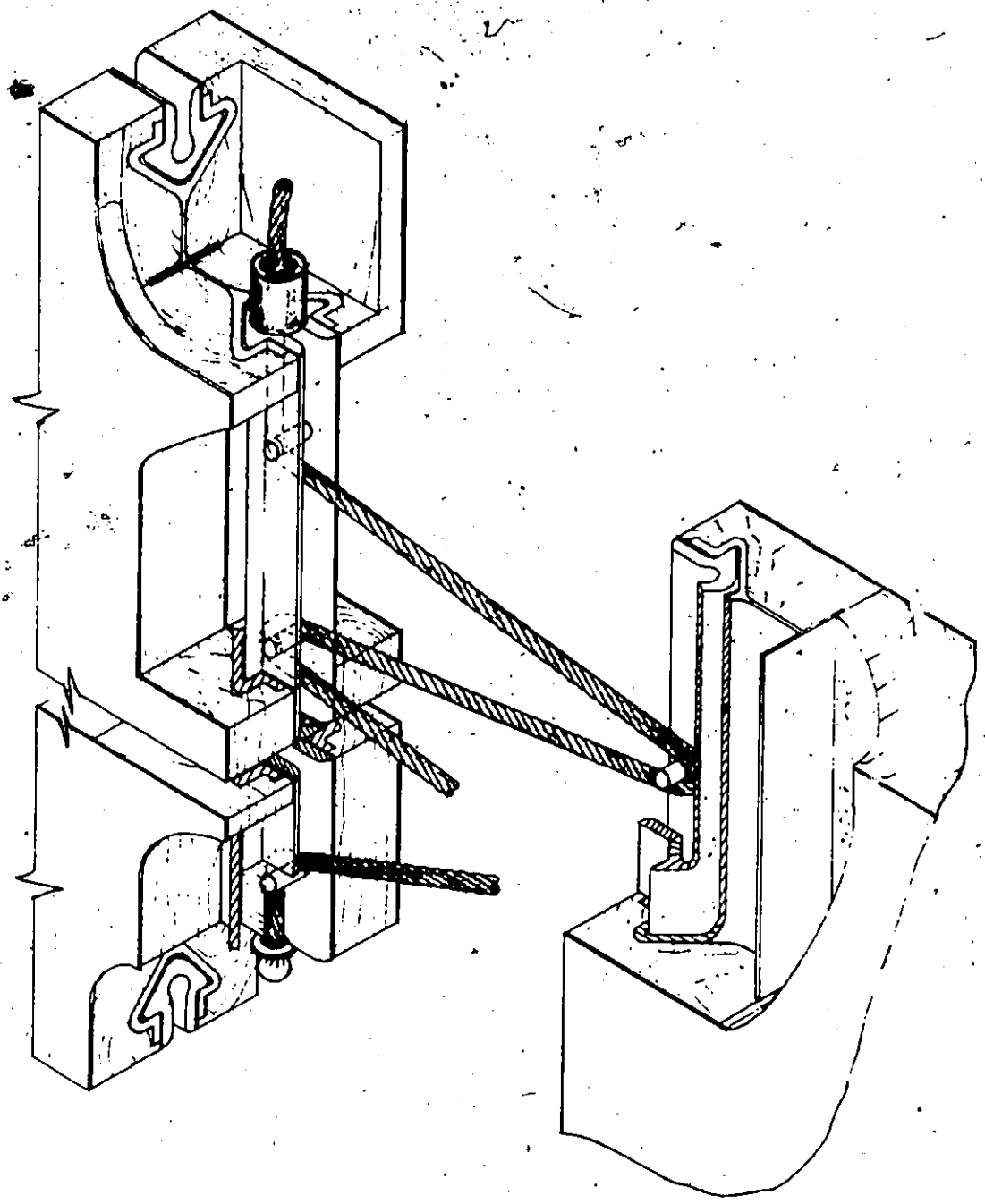

FIGURE 3.16 THE LACED CONNECTION SYSTEM

(REPRODUCED FROM [1])

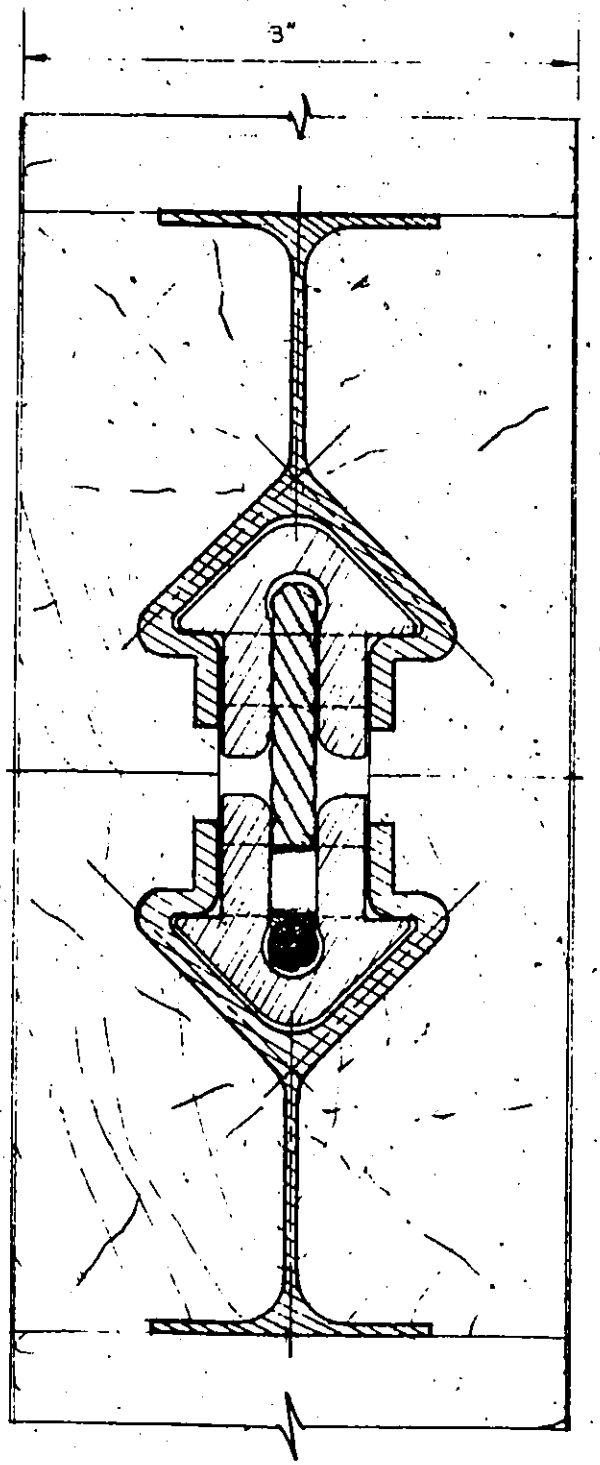

FIGURE 3.17 SECTION OF TWO PANELS SIDE BY SIDE JOINED WITH THE LACE
(REPRODUCED FROM [1])

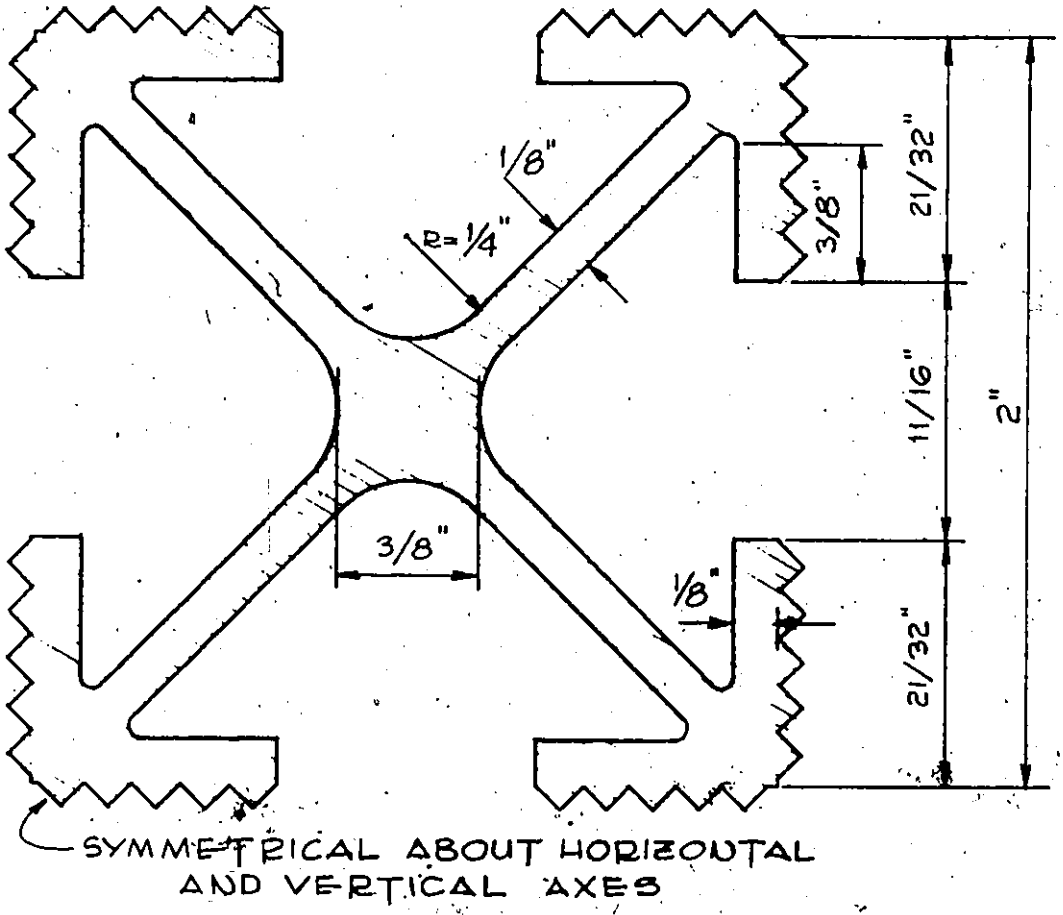

FIGURE 3.18 EXTRUSION USED TO JOIN FOUR PANELS
(REPRODUCED FROM [1])

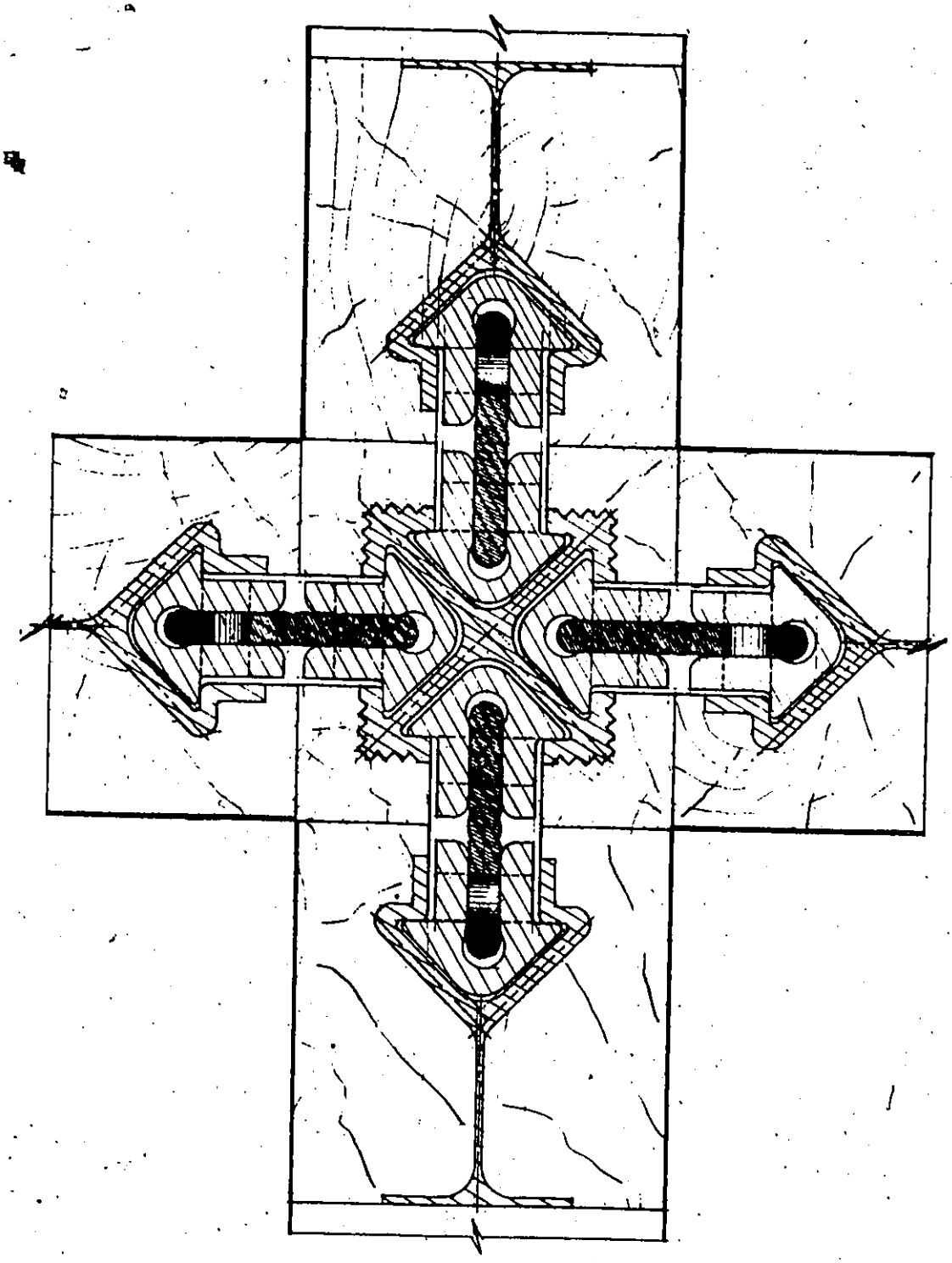

FIGURE 3.19 SECTION OF FOUR PANELS JOINED TOGETHER
(REPRODUCED FROM [1])

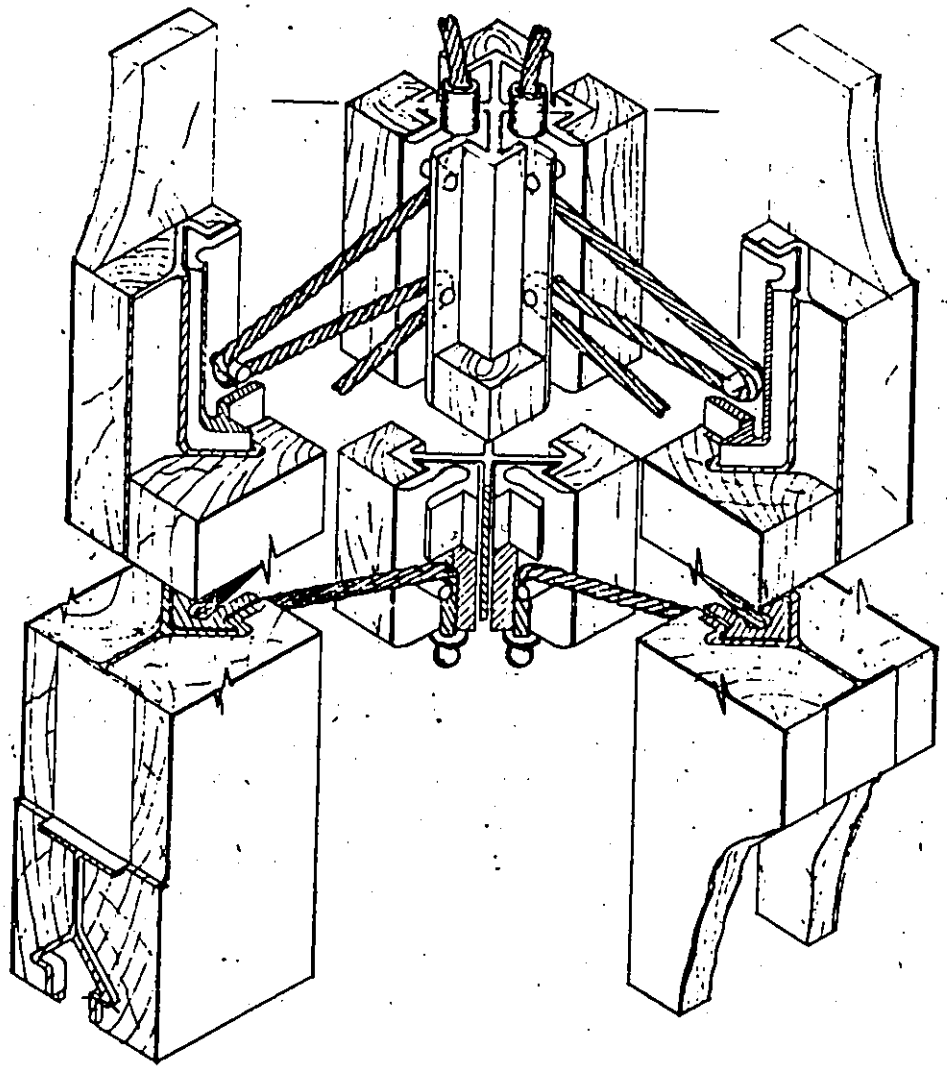

FIGURE 3.20 FORMING A CORNER (REPRODUCED FROM [1])

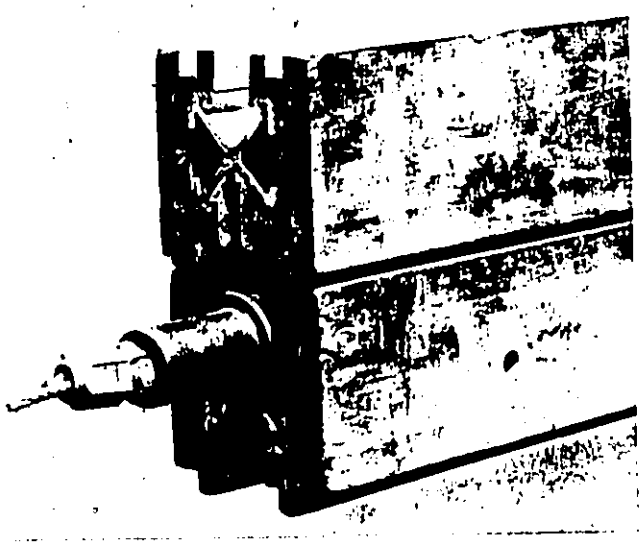

FIGURE 4.1 THE TONGUE AND GROOVE ARRANGEMENT AND FASTENING OF THE CABLE ENDS

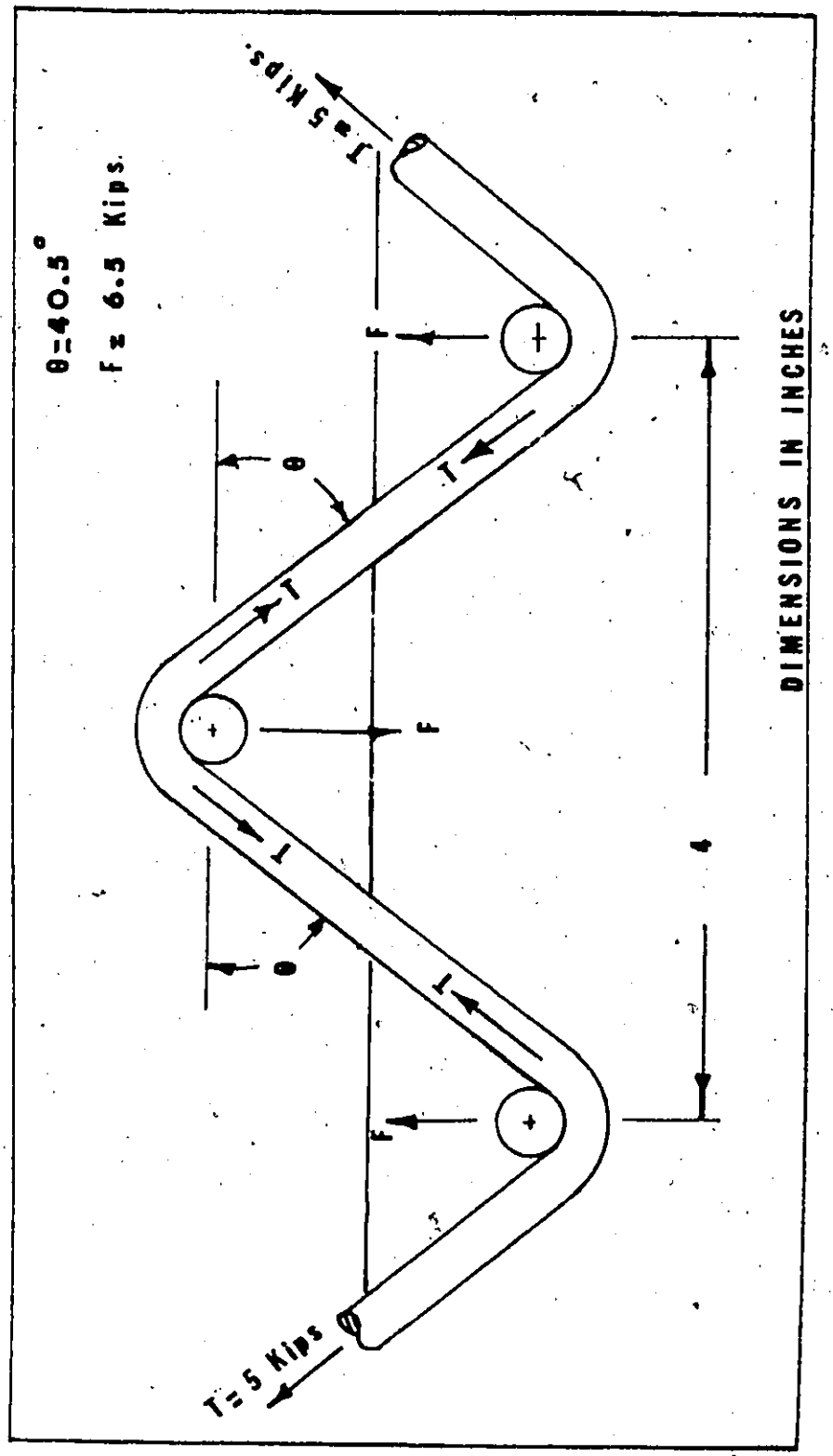

FIGURE 4.2 ORIGINAL CONFIGURATION AND EXPECTED LOADS

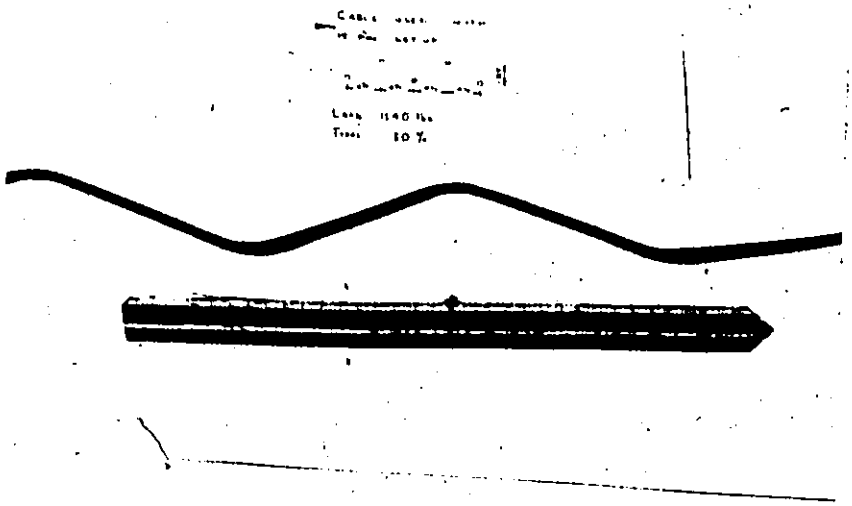

FIGURE 4.3 STEEL CABLE AFTER INITIAL TEST

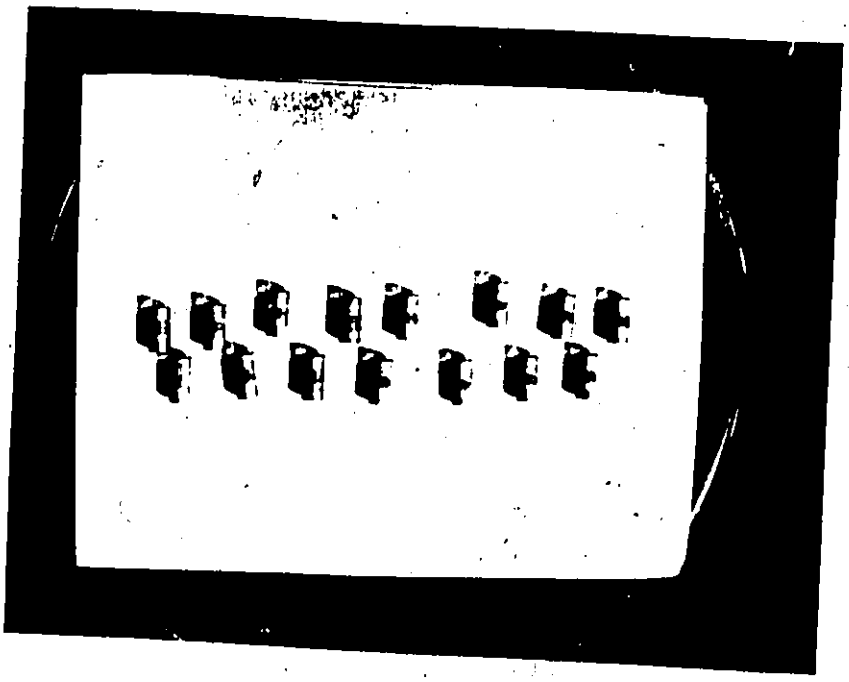

FIGURE 4.4 ALUMINUM PINS AFTER INITIAL TEST

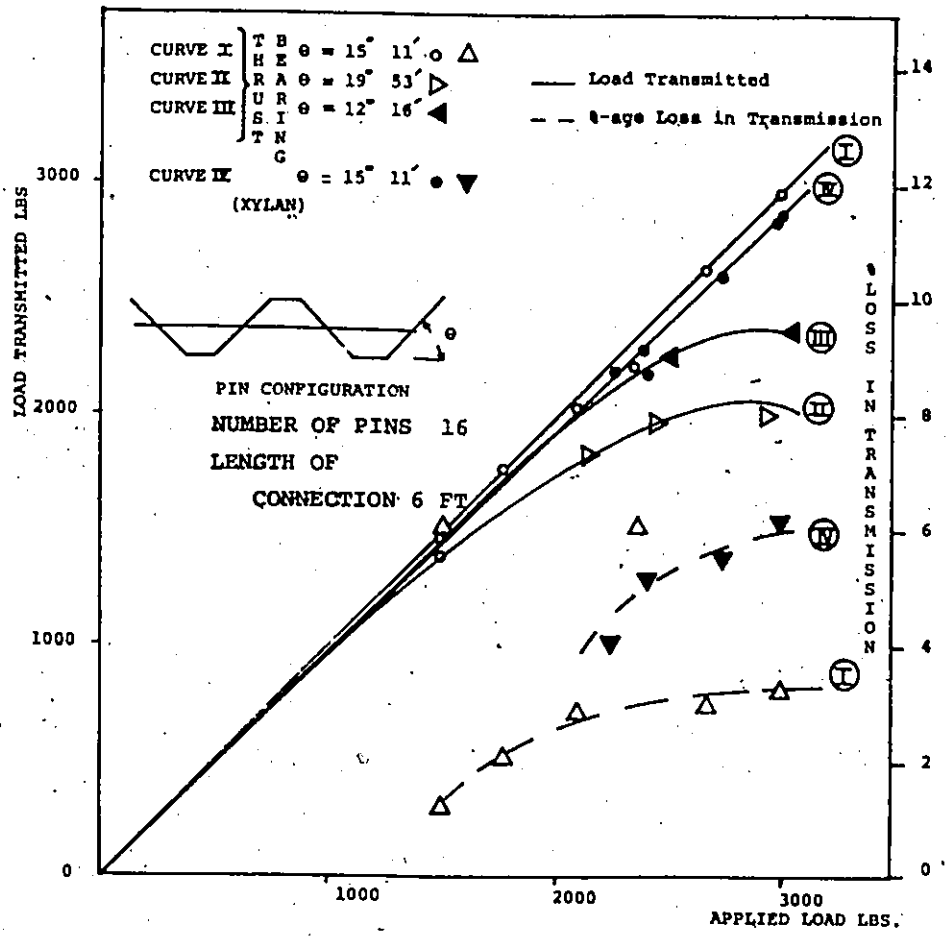

FIGURE 4.5 THRUST BEARINGS AND XYLAN COATED BUSHINGS

FIGURE 4.6 SET-UP FOR TENSION TEST

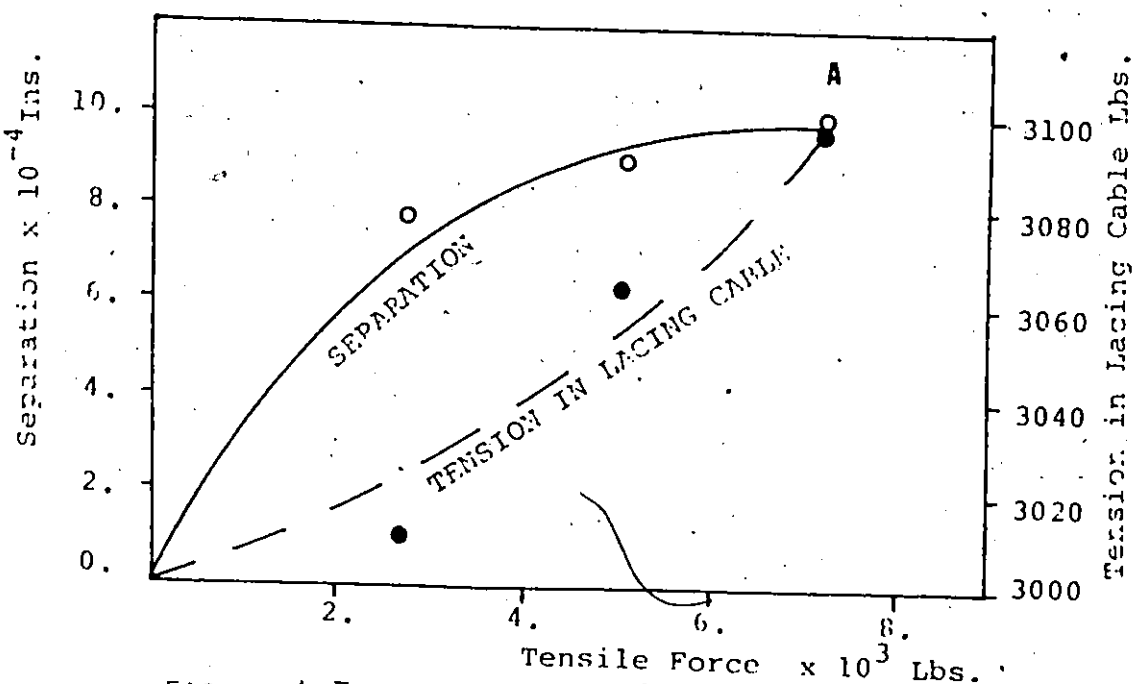

FIGURE 4.7 RESULTS FROM TENSION TESTS

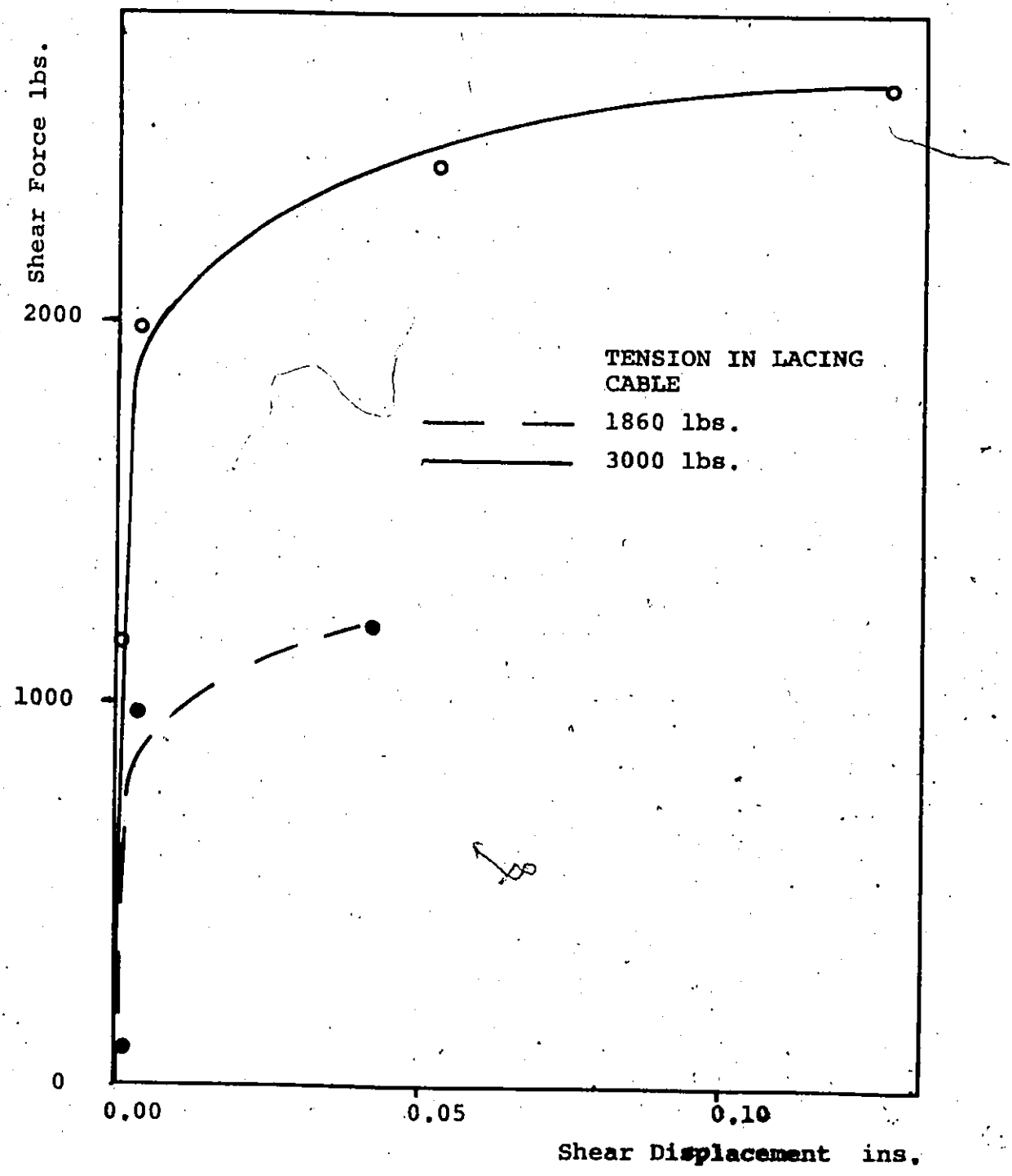

FIGURE 4.8 EFFECT OF SINGLE SHEAR FORCE ON DISPLACEMENT

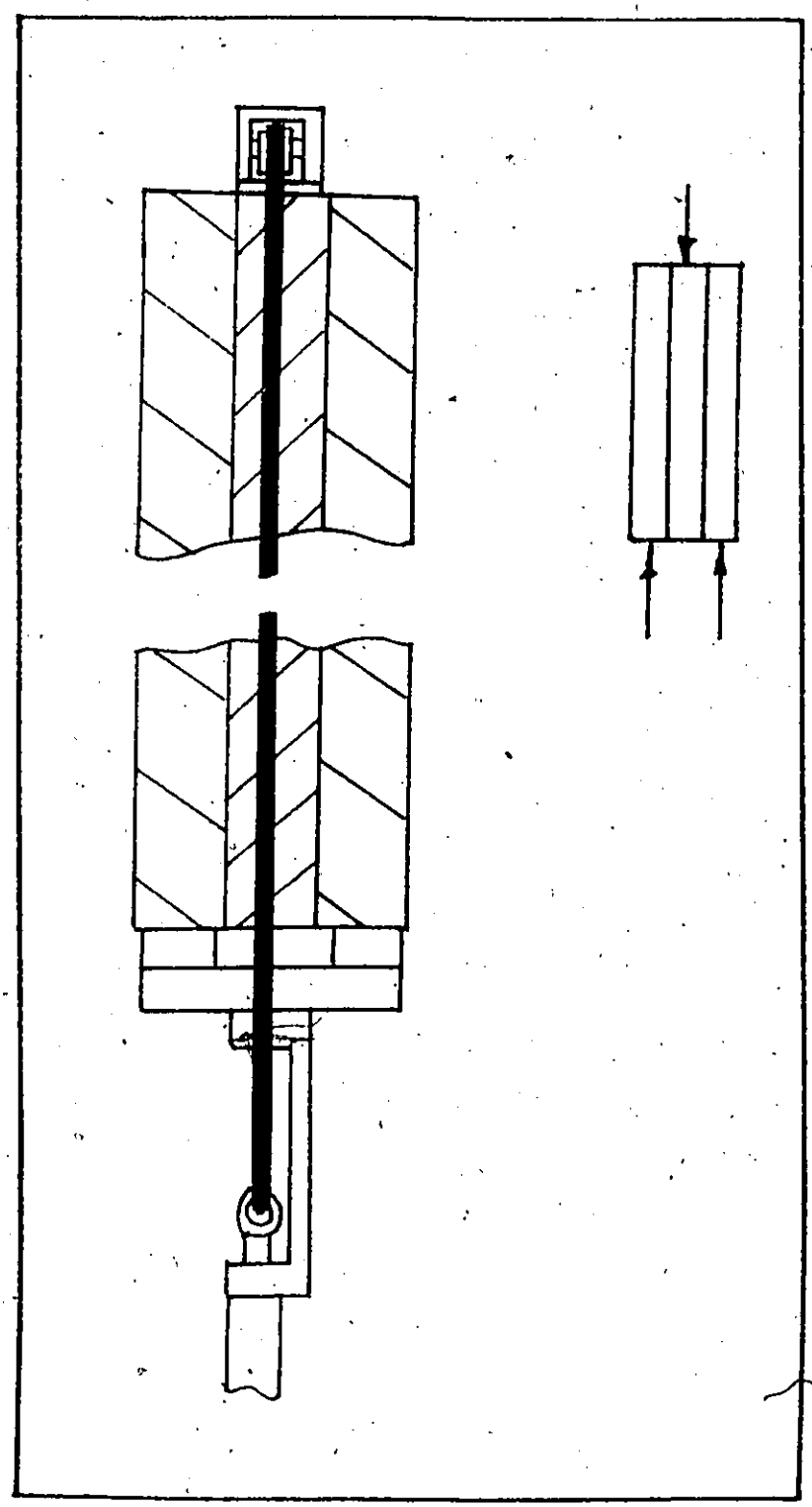

FIGURE 4.9 SCHEMATIC DIAGRAM FOR DOUBLE SHEAR TEST ARRANGEMENT

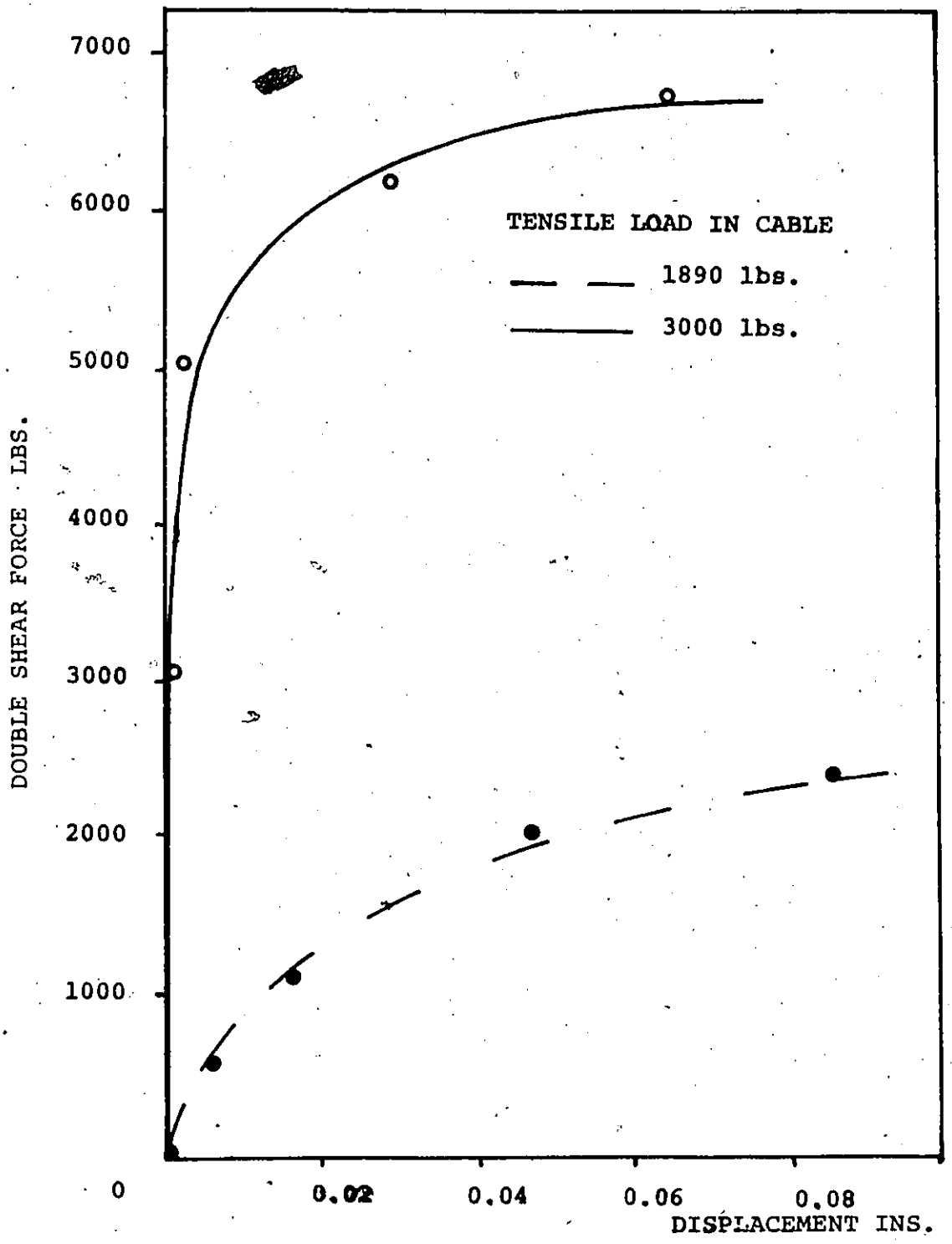

FIGURE 4.10 RESULTS FROM DOUBLE SHEAR TESTS

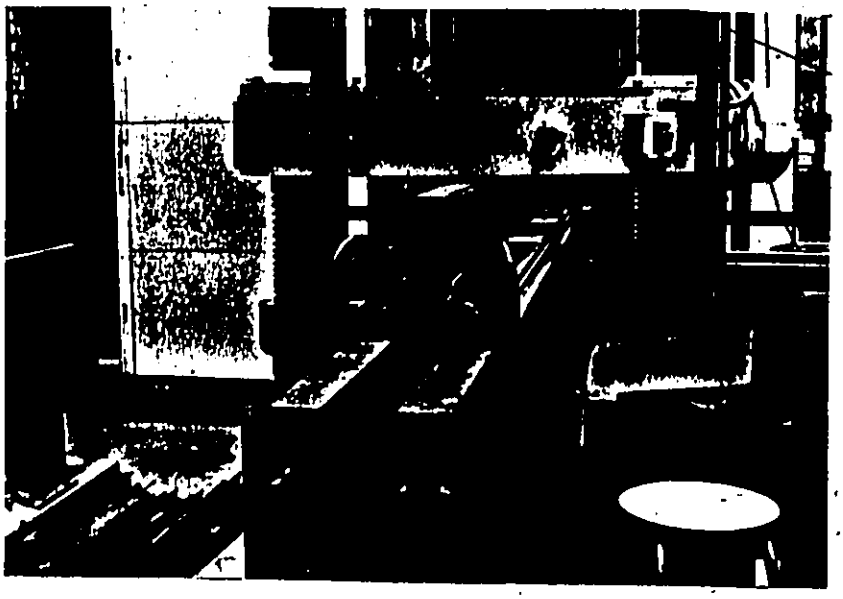

FIGURE 4.11 ARRANGEMENT FOR TRANSVERSE SHEAR TESTS

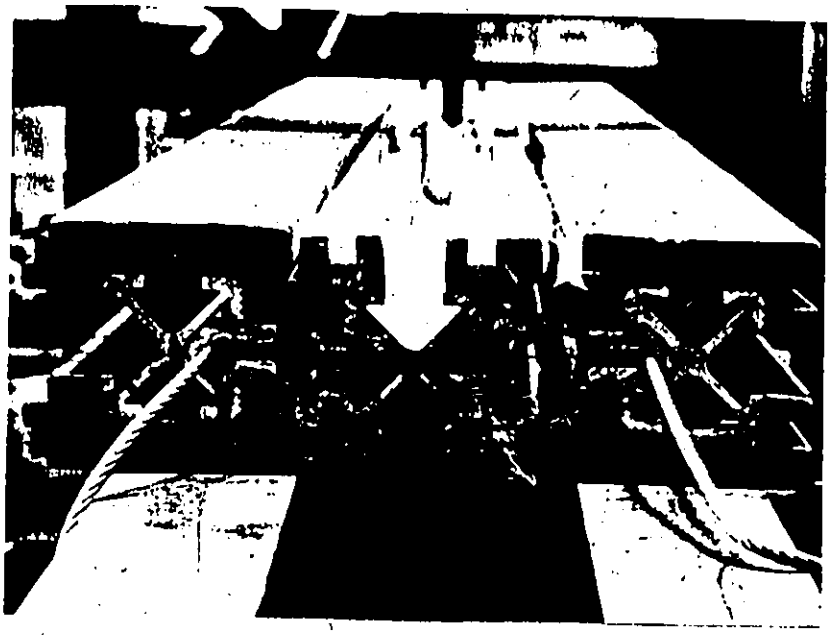

FIGURE 4.12 CONNECTION AFTER FAILURE IN TRANSVERSE SHEAR TEST

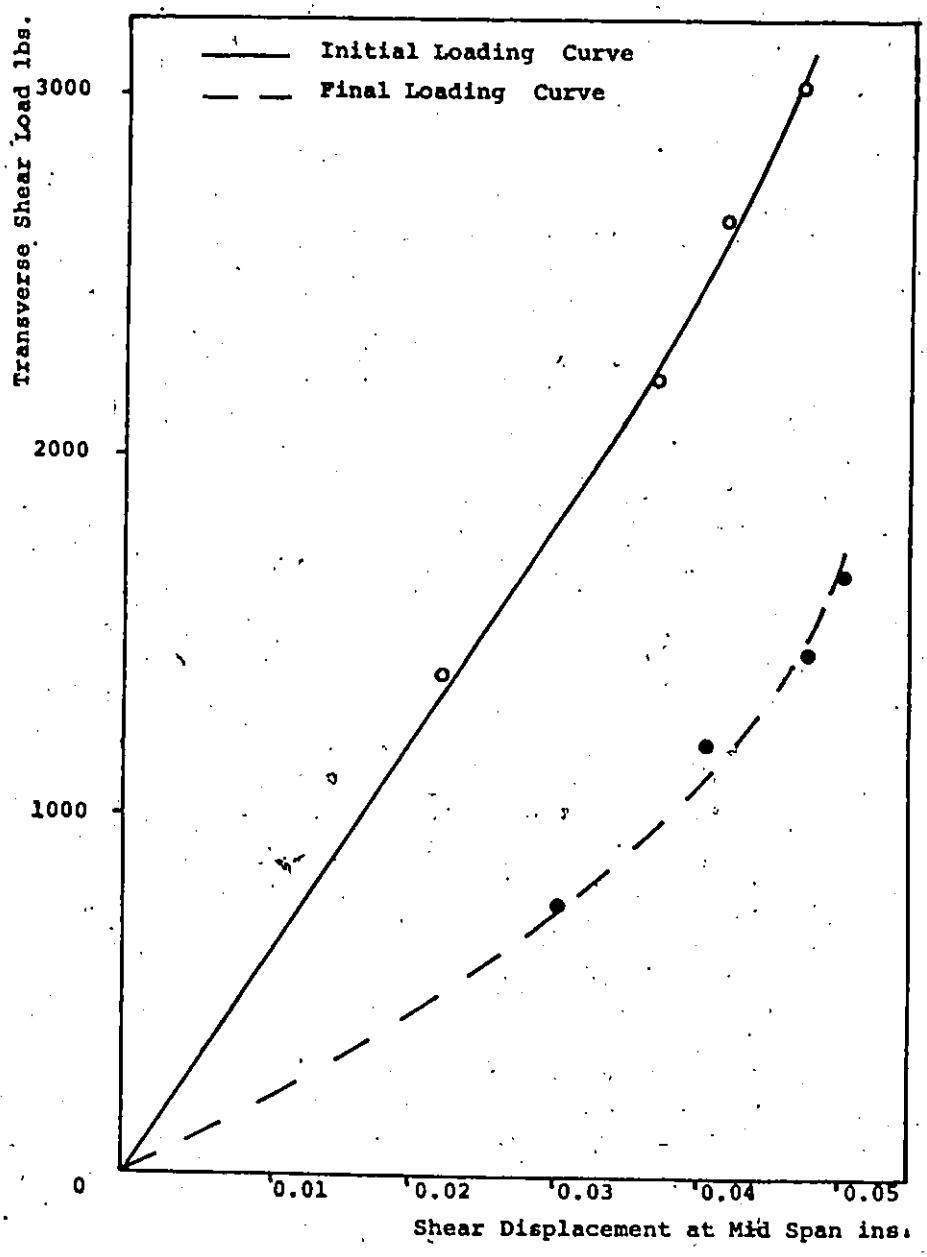

FIGURE 4.13 RESULTS FROM TRANSVERSE SHEAR TESTS

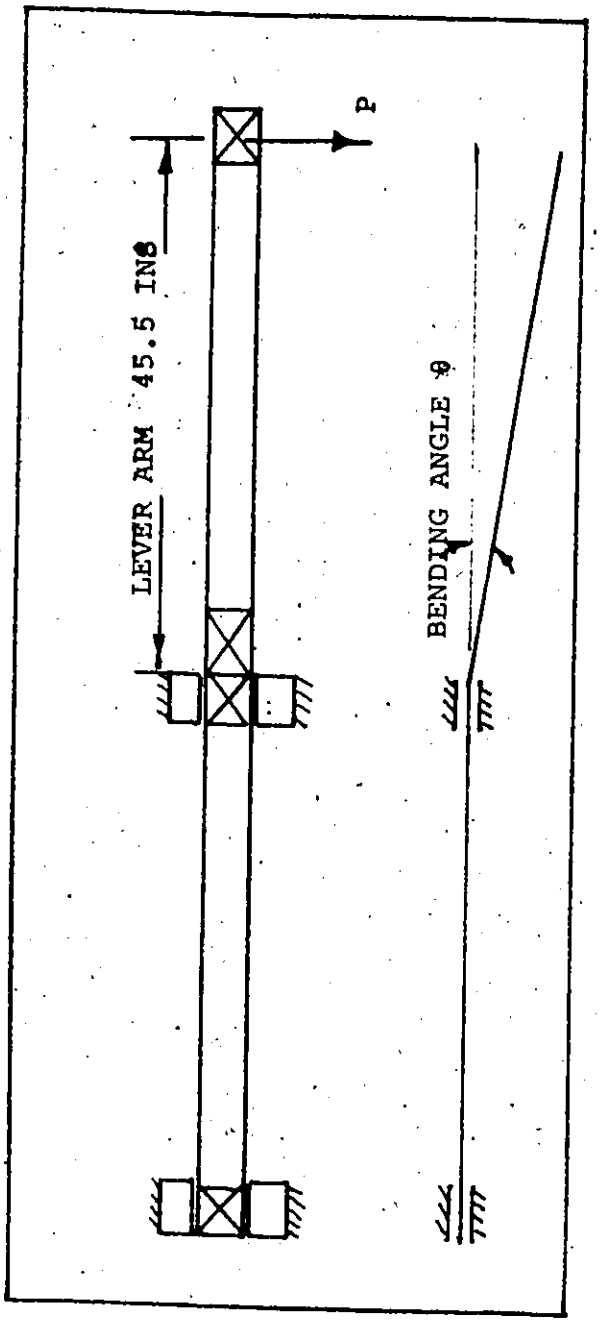

FIGURE 4.14 SCHEMATIC DIAGRAM FOR BENDING TESTS

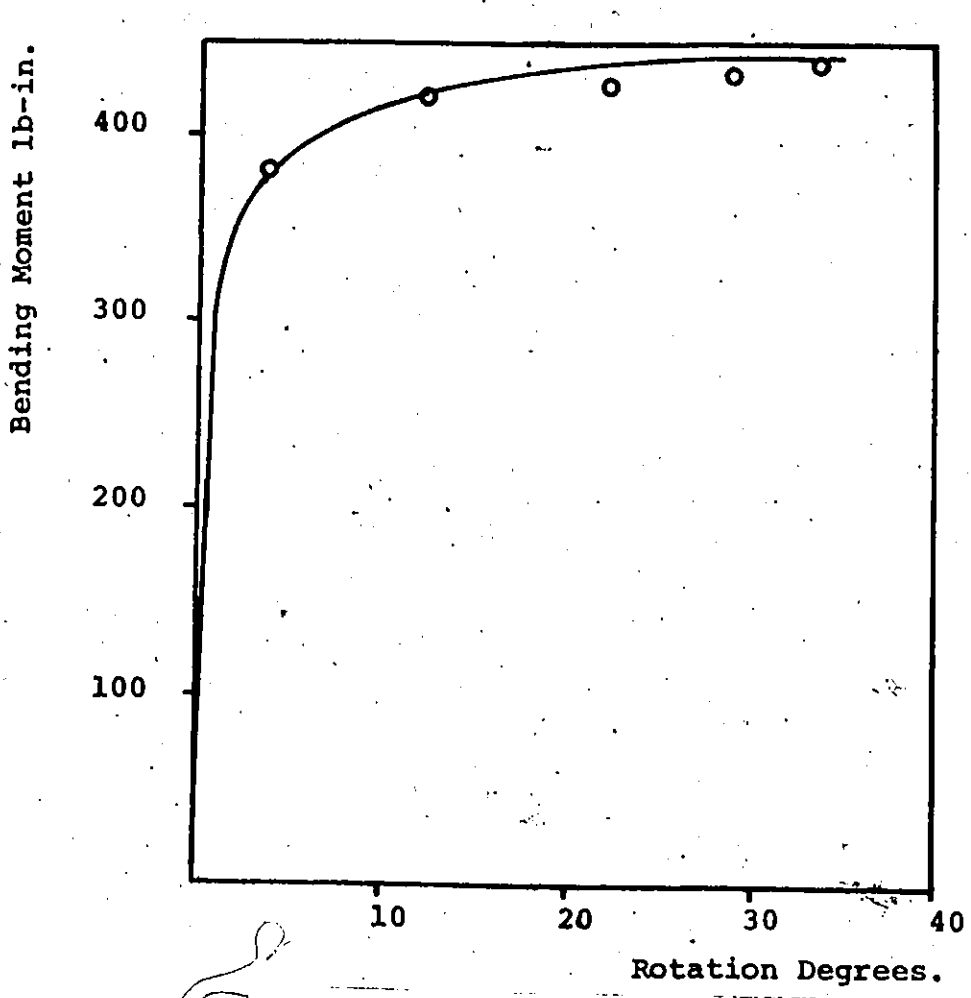

FIGURE 4.15 RESULTS FROM BENDING TESTS

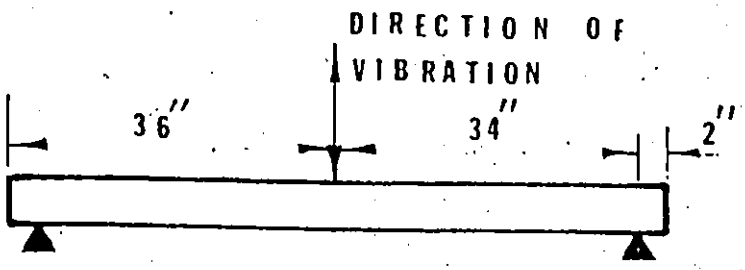

FIGURE 4.16 SCHEMATIC DIAGRAM FOR ARRANGEMENT USED IN THE VIBRATION TESTS

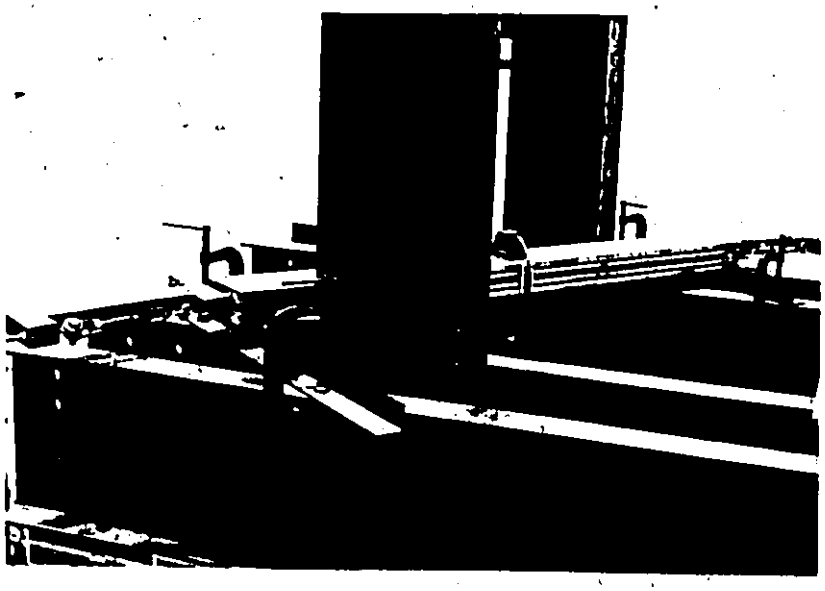

FIGURE 4.17 CONNECTION SYSTEM SUBJECTED TO VIBRATIONS

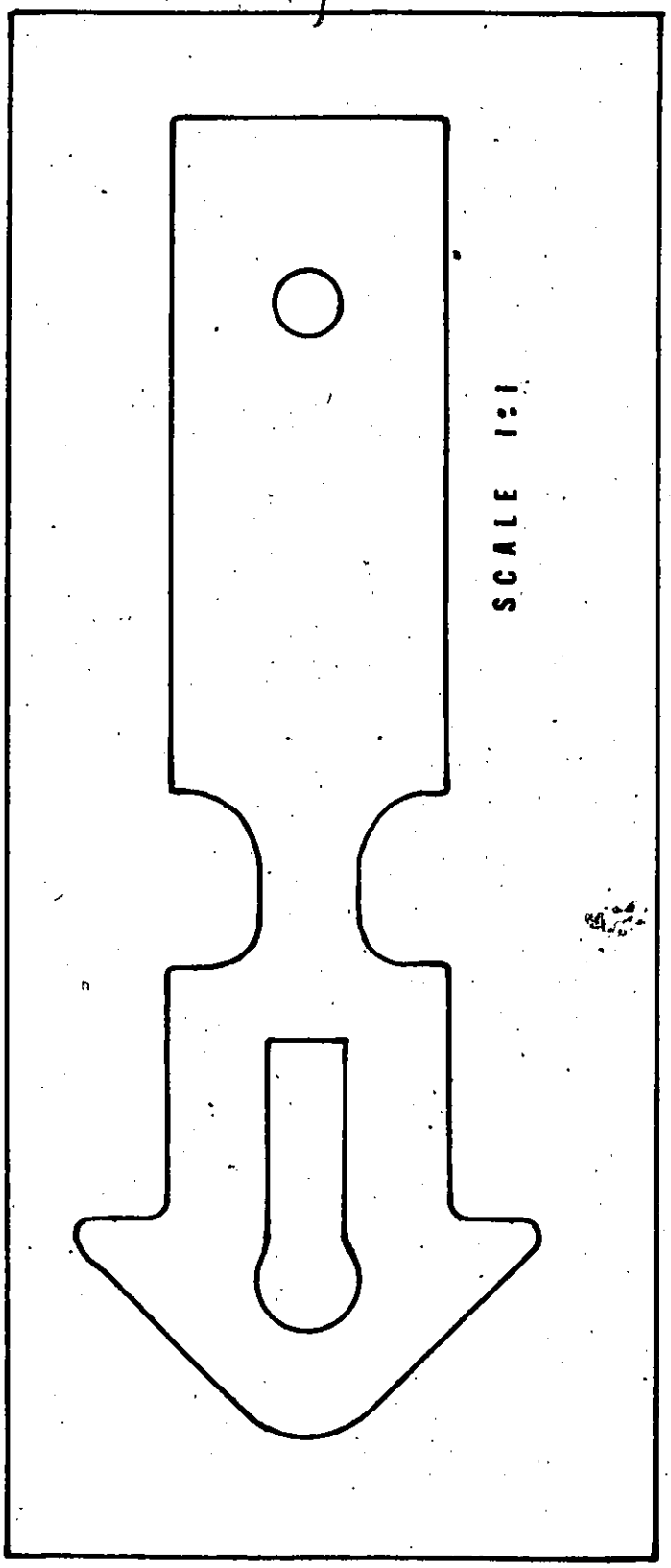

FIGURE 4.18 MODEL OF ORIGINAL DESIGN OF MALE EXTRUSION

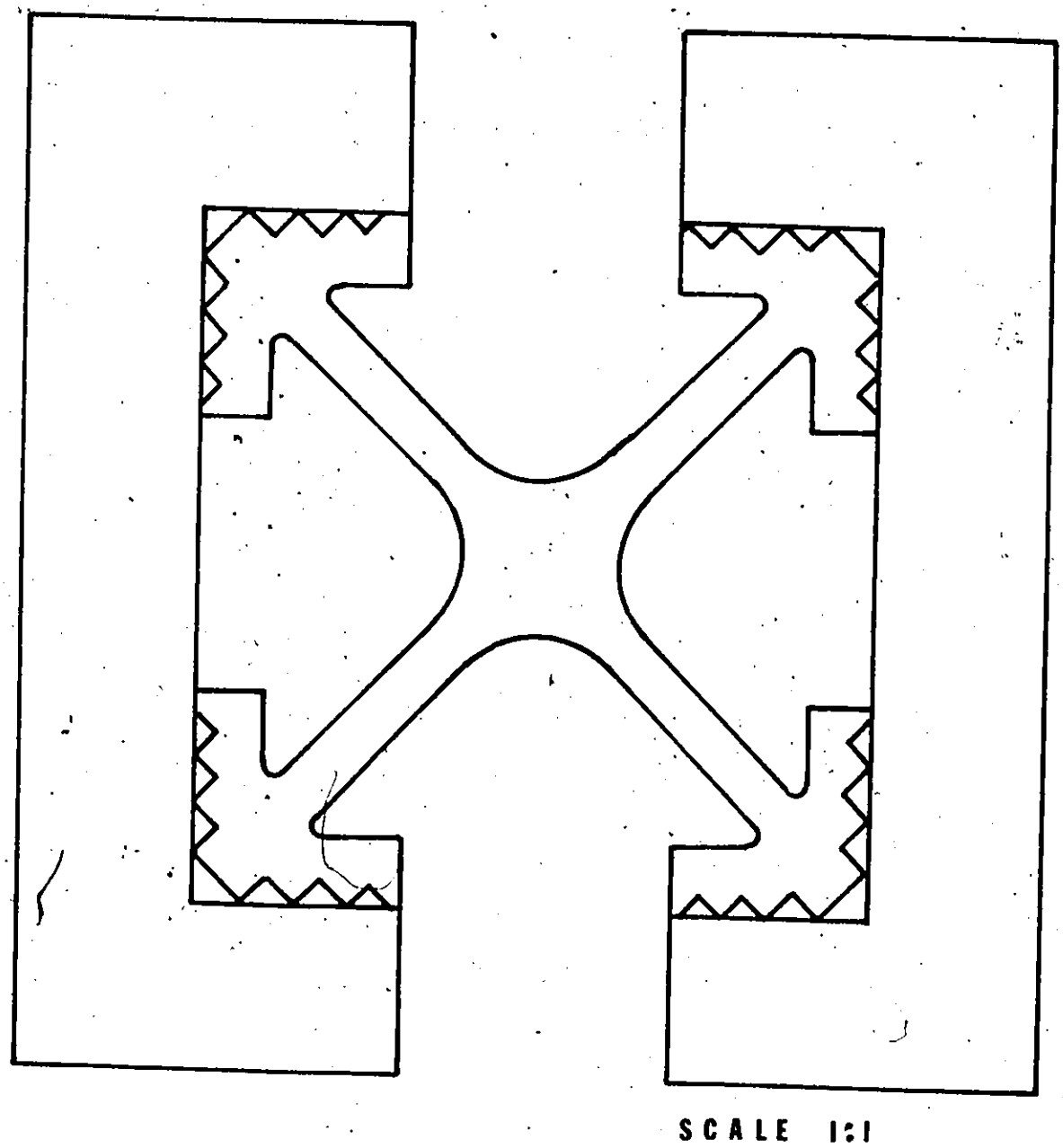

FIGURE 4.19 MODEL OF ORIGINAL DESIGN OF FOUR-WAY FEMALE EXTRUSION

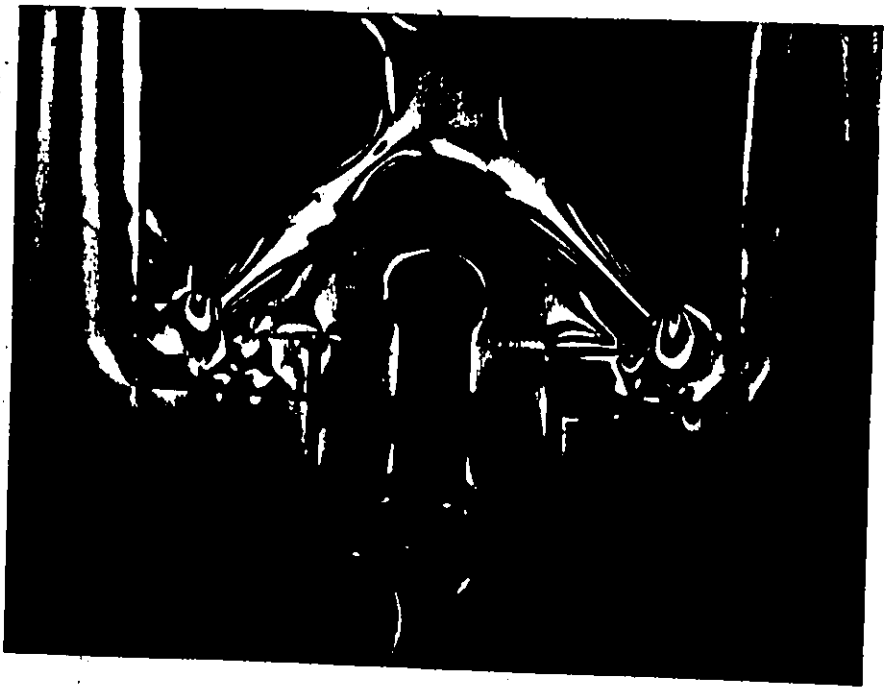

FIGURE 4.20 PHOTOGRAPH OF ORIGINAL MODEL UNDER LOAD IN A POLARISCOPE

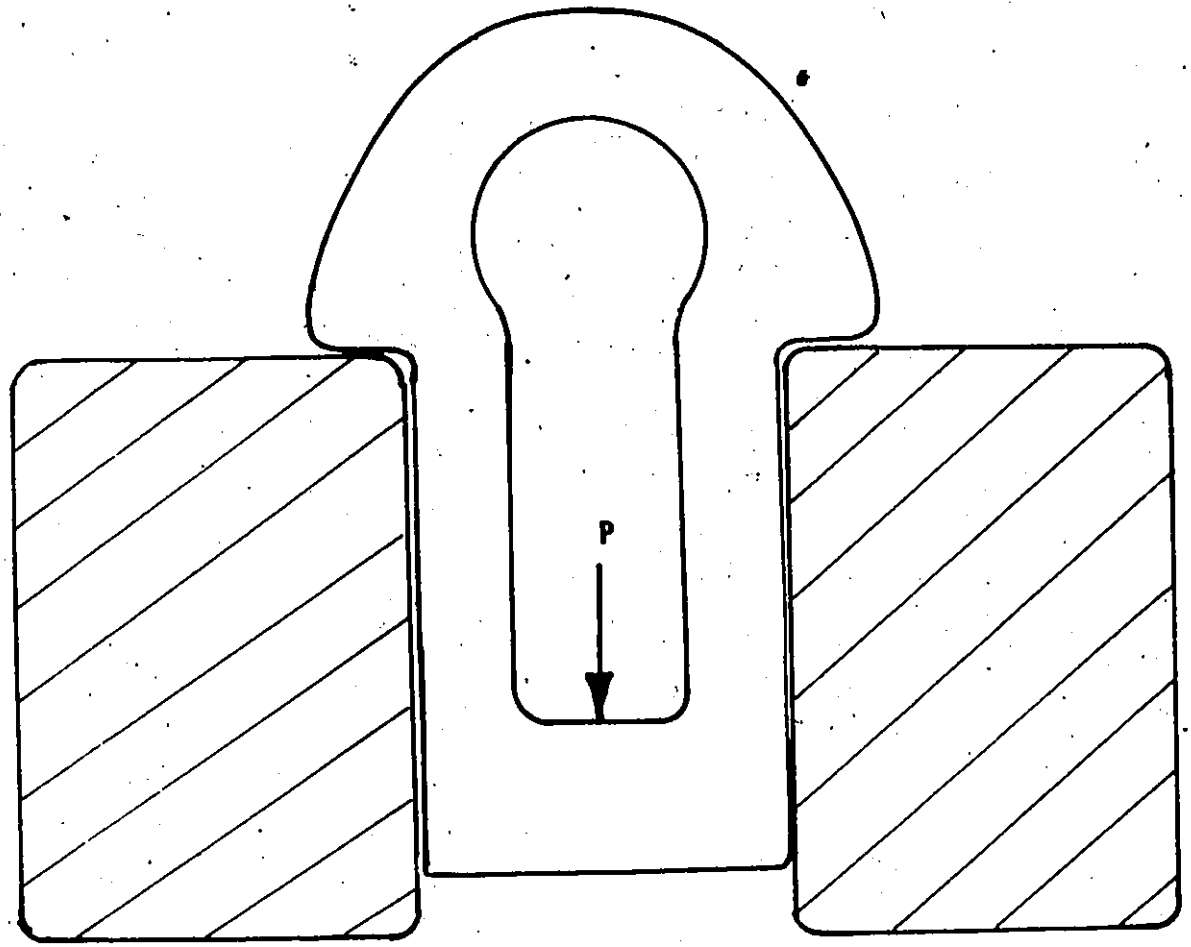

FIGURE 4.21 OPTIMIZED SHAPE OF THE MALE EXTRUSION UNDER LOAD

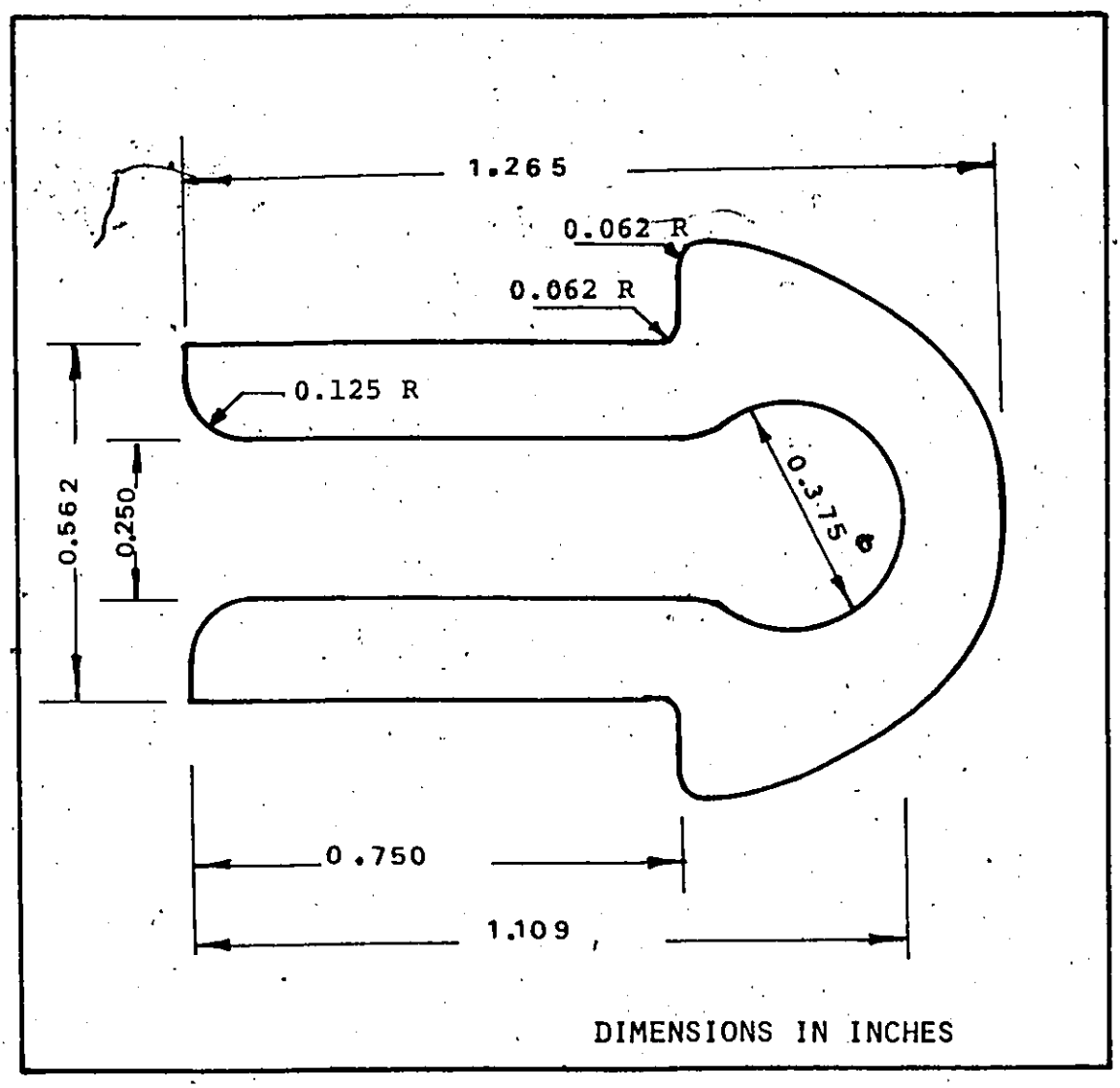

FIGURE 4.22 DIMENSIONS OF OPTIMIZED MALE EXTRUSION

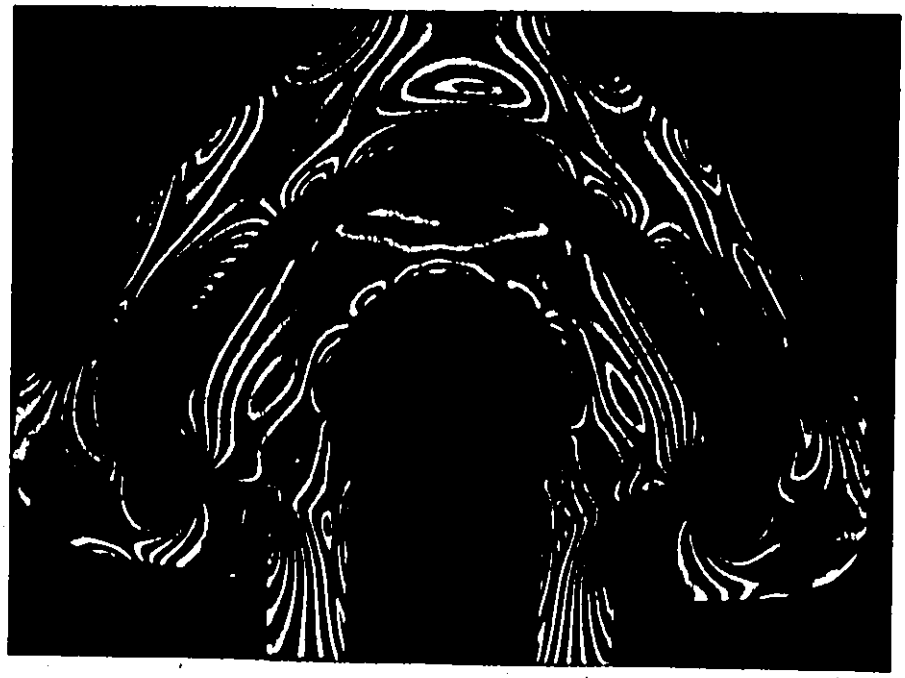

FIGURE 4.23 SHEAR STRESSES IN MODEL OF CONNECTION SYSTEM

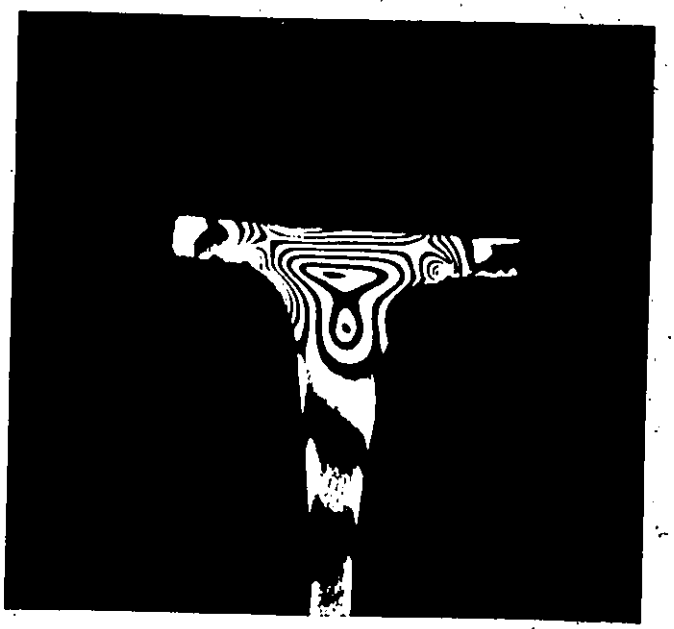

FIGURE 4.24 STRESSES IN SUPPORTING END OF A PANEL-TO-PANEL EXTRUSION

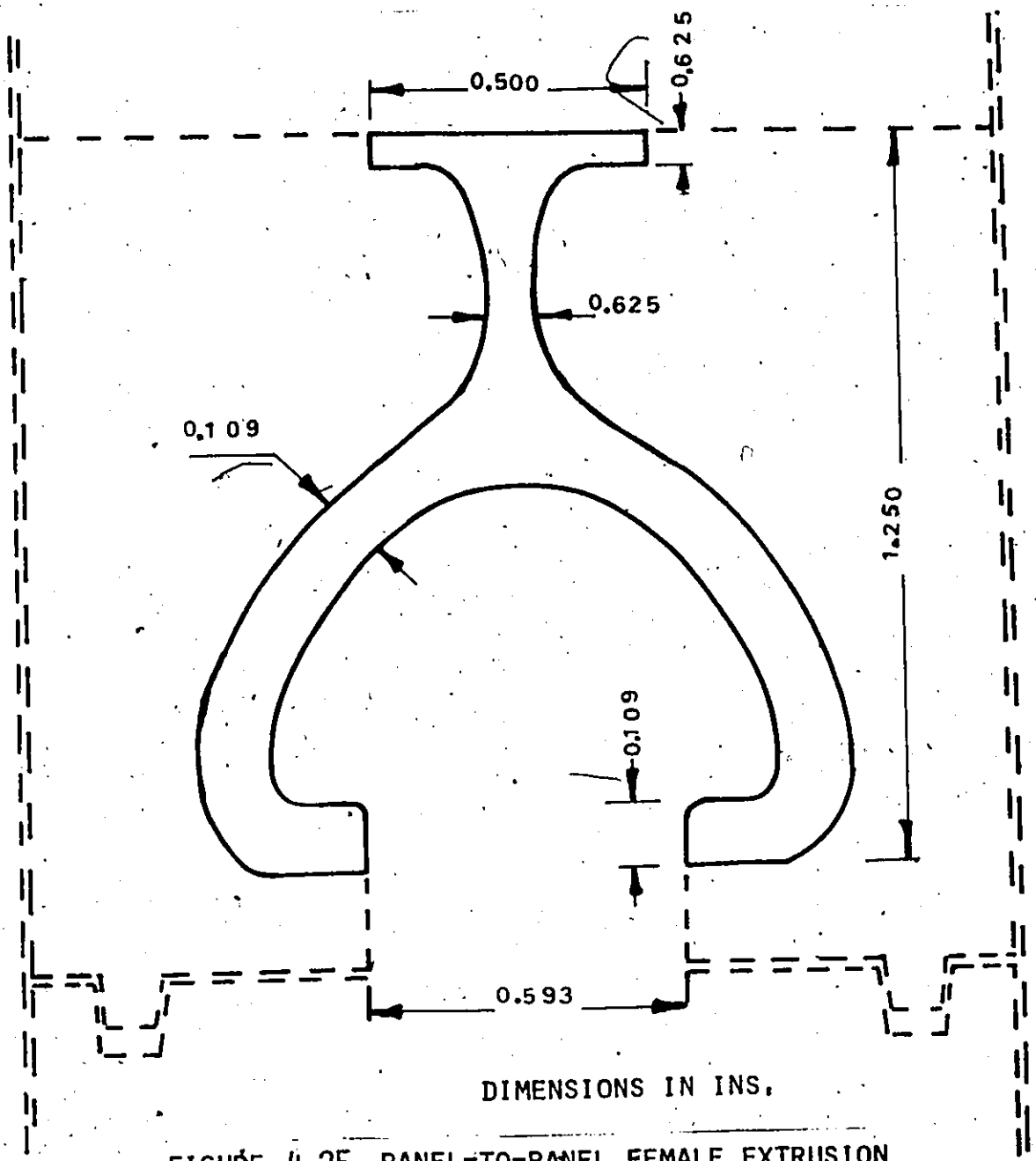

FIGURE 4.25 PANEL-TO-PANEL FEMALE EXTRUSION

FIGURE 4.26 STRESSES IN ONE DESIGN OF THE FOUR-WAY EXTRUSION LOADED IN FOUR DIRECTIONS

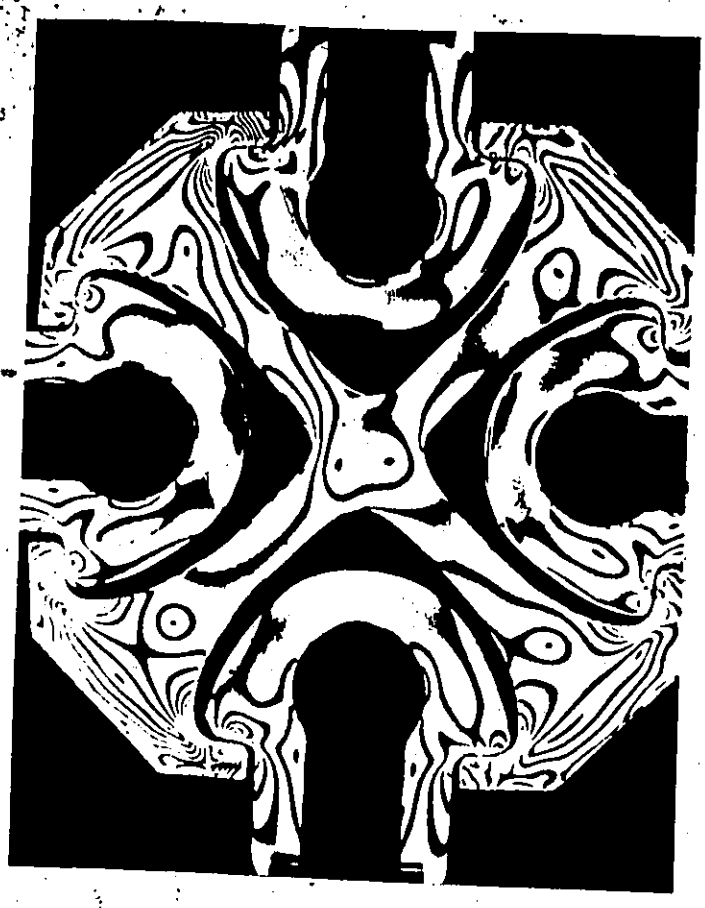

FIGURE 4.27 STRESSES IN FOUR-WAY FEMALE EXTRUSION LOADED IN FOUR DIRECTIONS

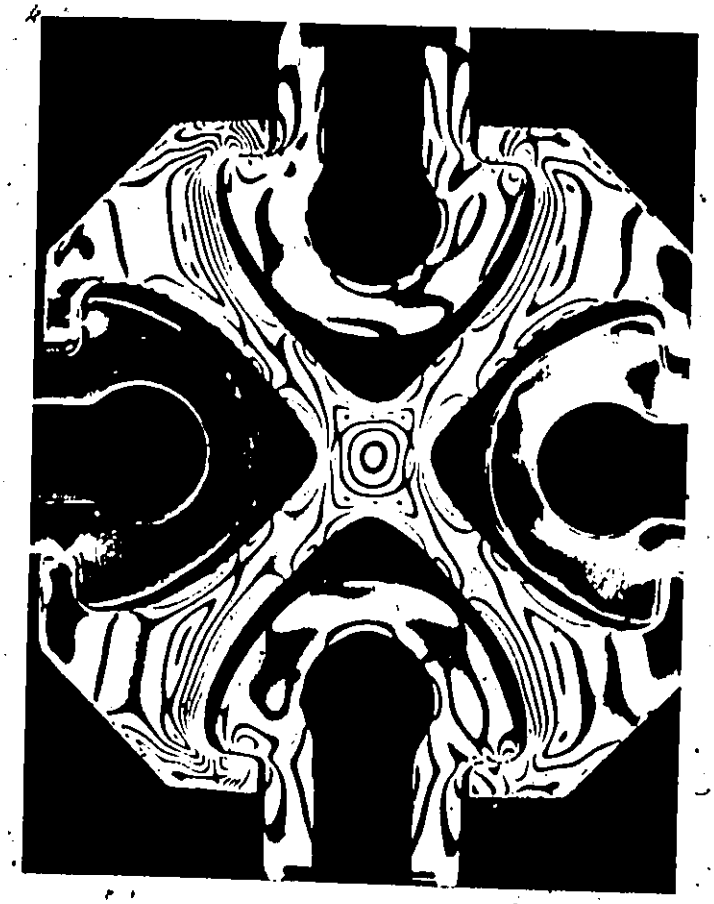

FIGURE 4.28 STRESSES IN FOUR-WAY FEMALE EXTRUSION LOADED IN TWO DIRECTIONS

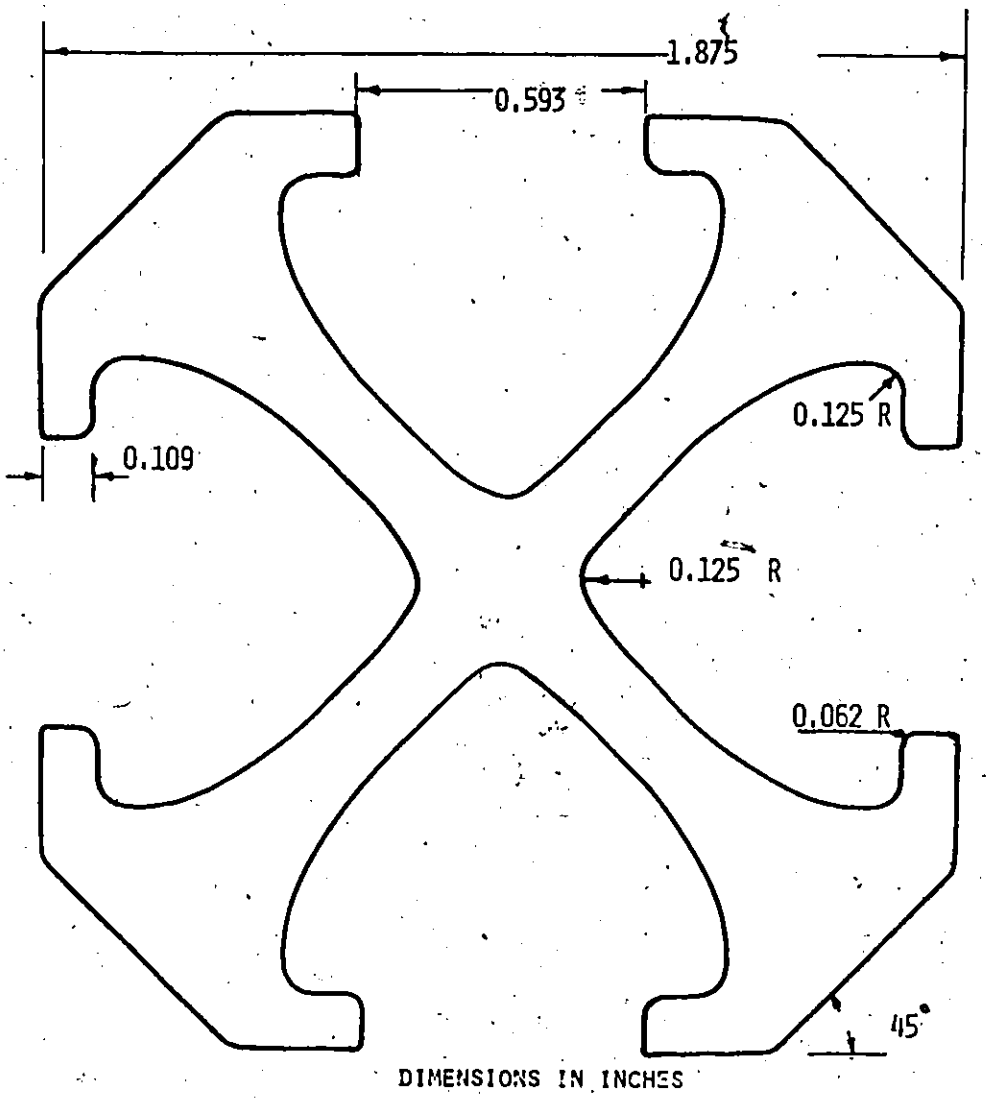

FIGURE 4.29 DIMENSIONS OF FINAL DESIGN OF OPTIMIZED FOUR-WAY FEMALE EXTRUSION

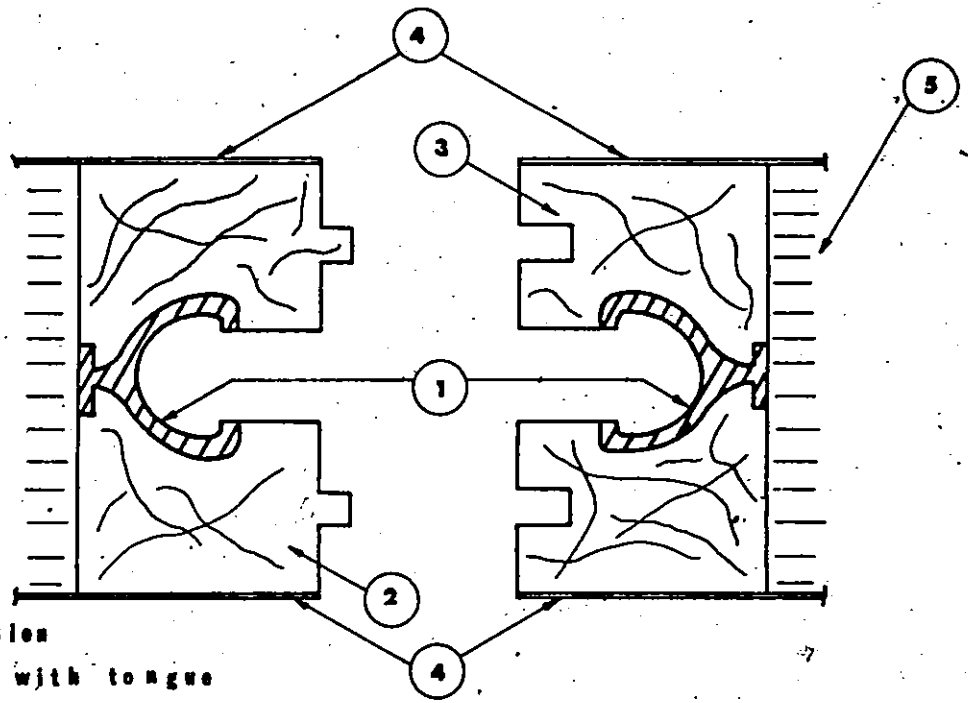

1. Female extrusion
2. Wooden frame with tongue
3. Wooden frame with groove
4. Skin, high density material
5. Insulater, low density material

FIGURE 4.30 THE TONGUE AND GROOVE ASSEMBLY IN PANELS

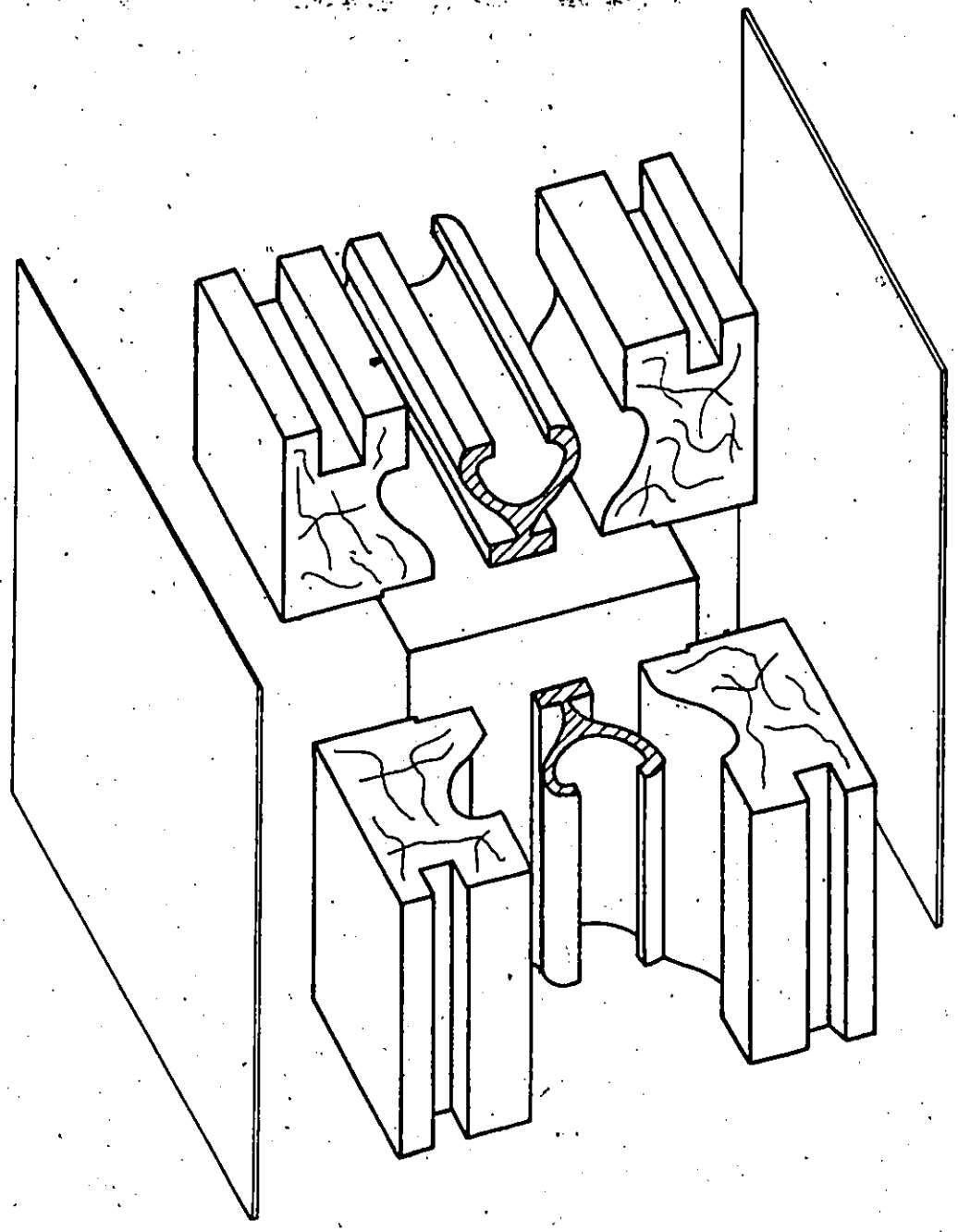

FIGURE 4.31 EXPLODED VIEW OF THE FEMALE EXTRUSION AS WOULD BE INCORPORATED IN A SANDWICH PANEL

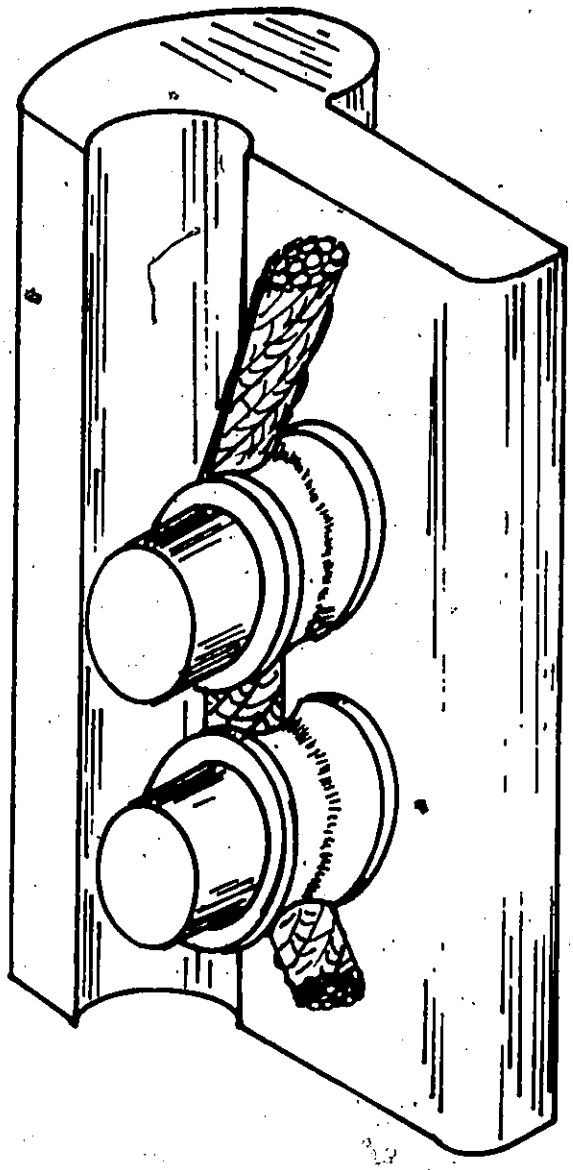

FIGURE 4.32 THE LACE PASSING OVER TWO PINS AND BUSHINGS IN THE MALE EXTRUSION

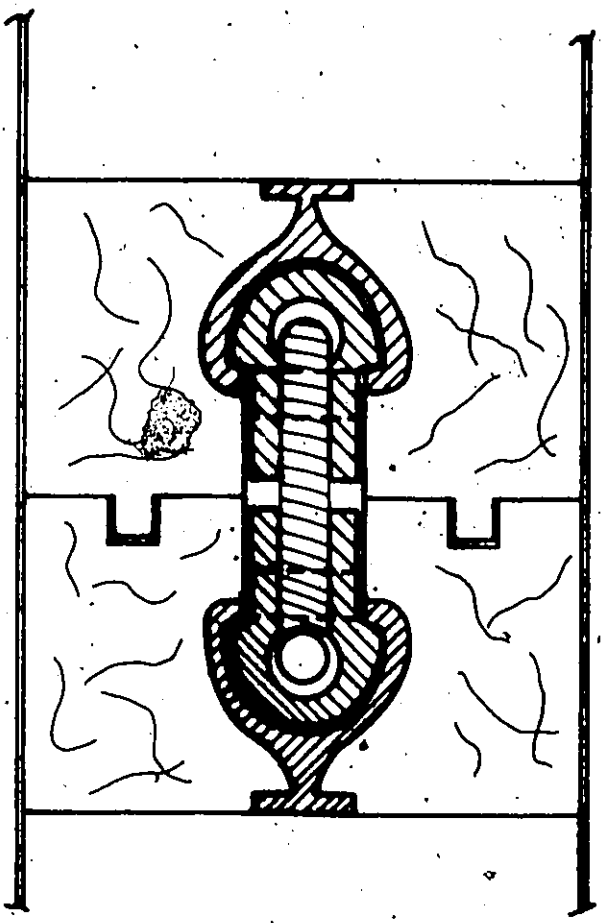

FIGURE 4.33 PANEL-TO-PANEL CONNECTION

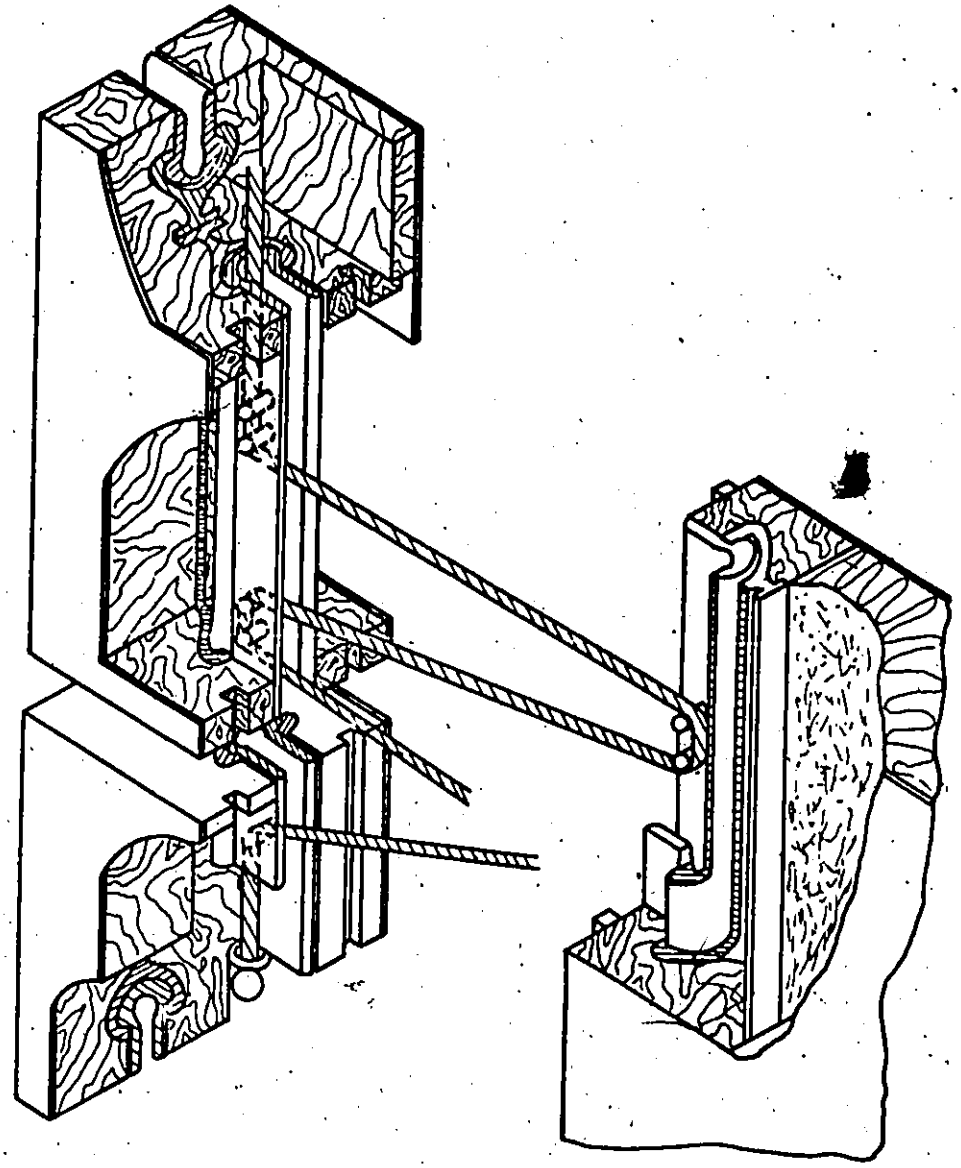

FIGURE 4.34 TWO PANELS BEING ASSEMBLED

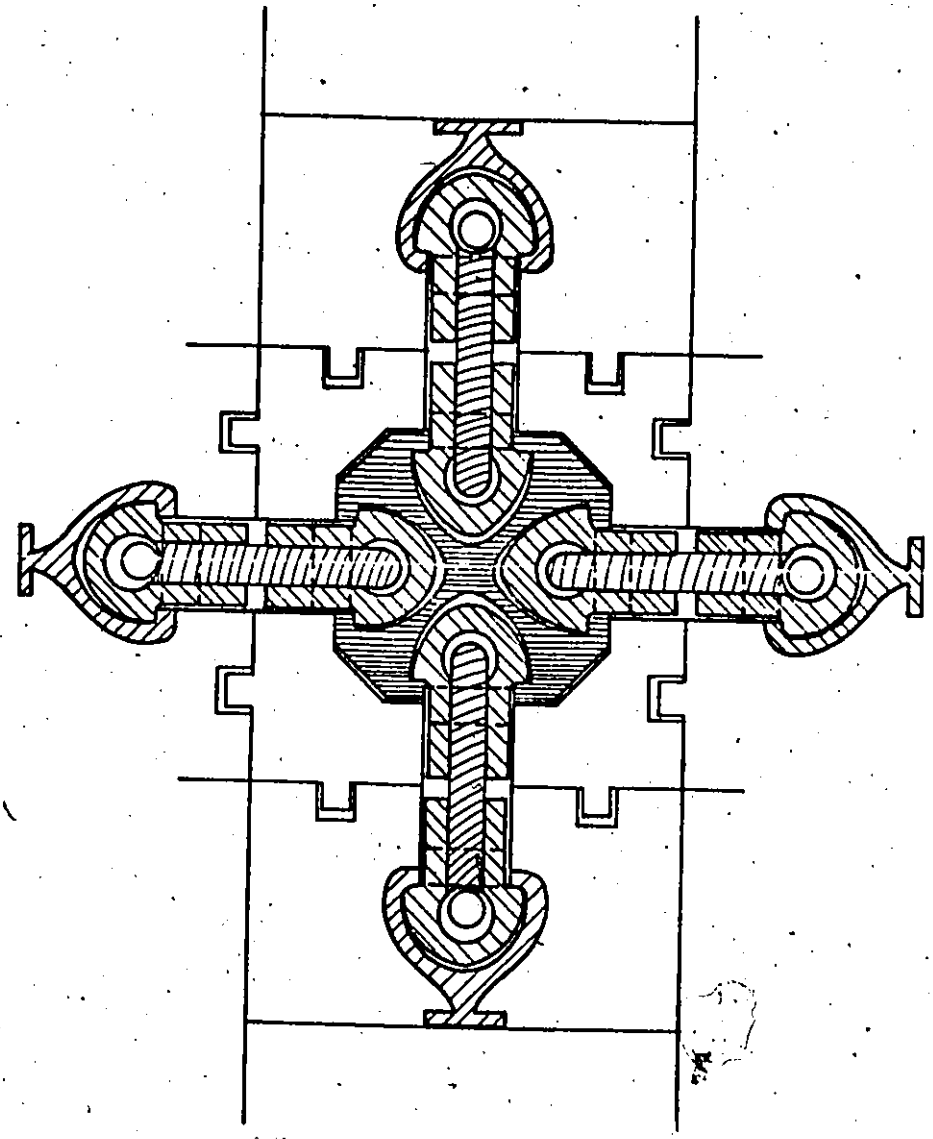

FIGURE 4.35 FOUR PANELS JOINED TOGETHER BY THE FOUR-WAY MEMBER

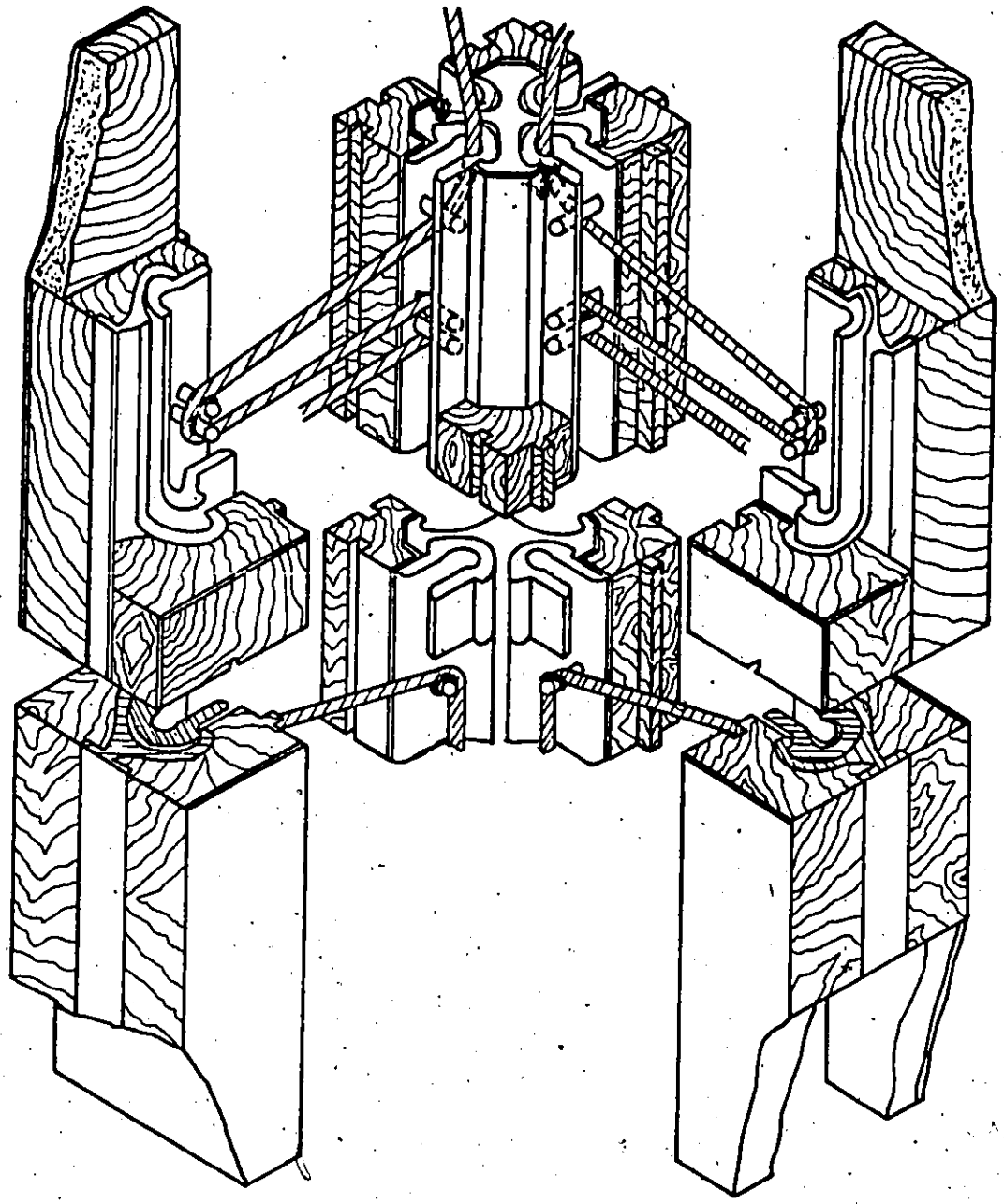

FIGURE 4.36 JOINING TWO PANELS TO FORM A CORNER

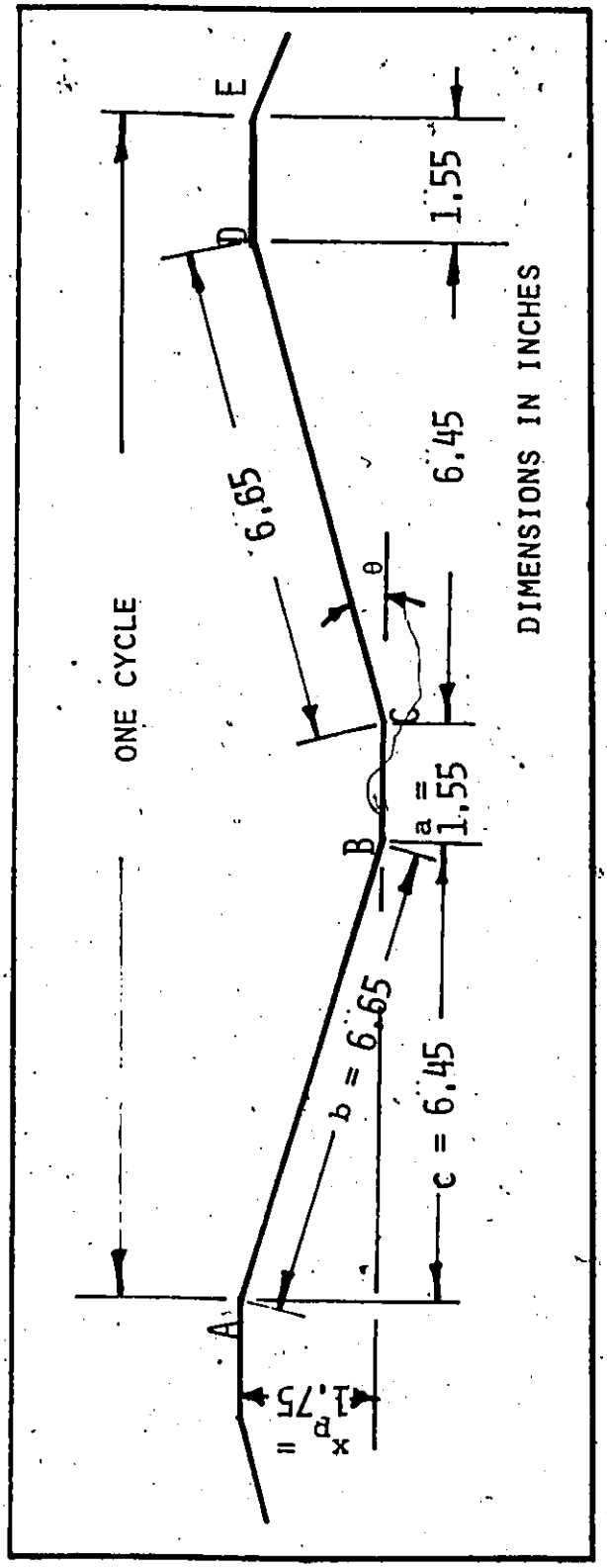

FIGURE 4.37 ARRANGEMENT OF ONE CYCLE OF CABLE IN THE LACED CONNECTION SYSTEM

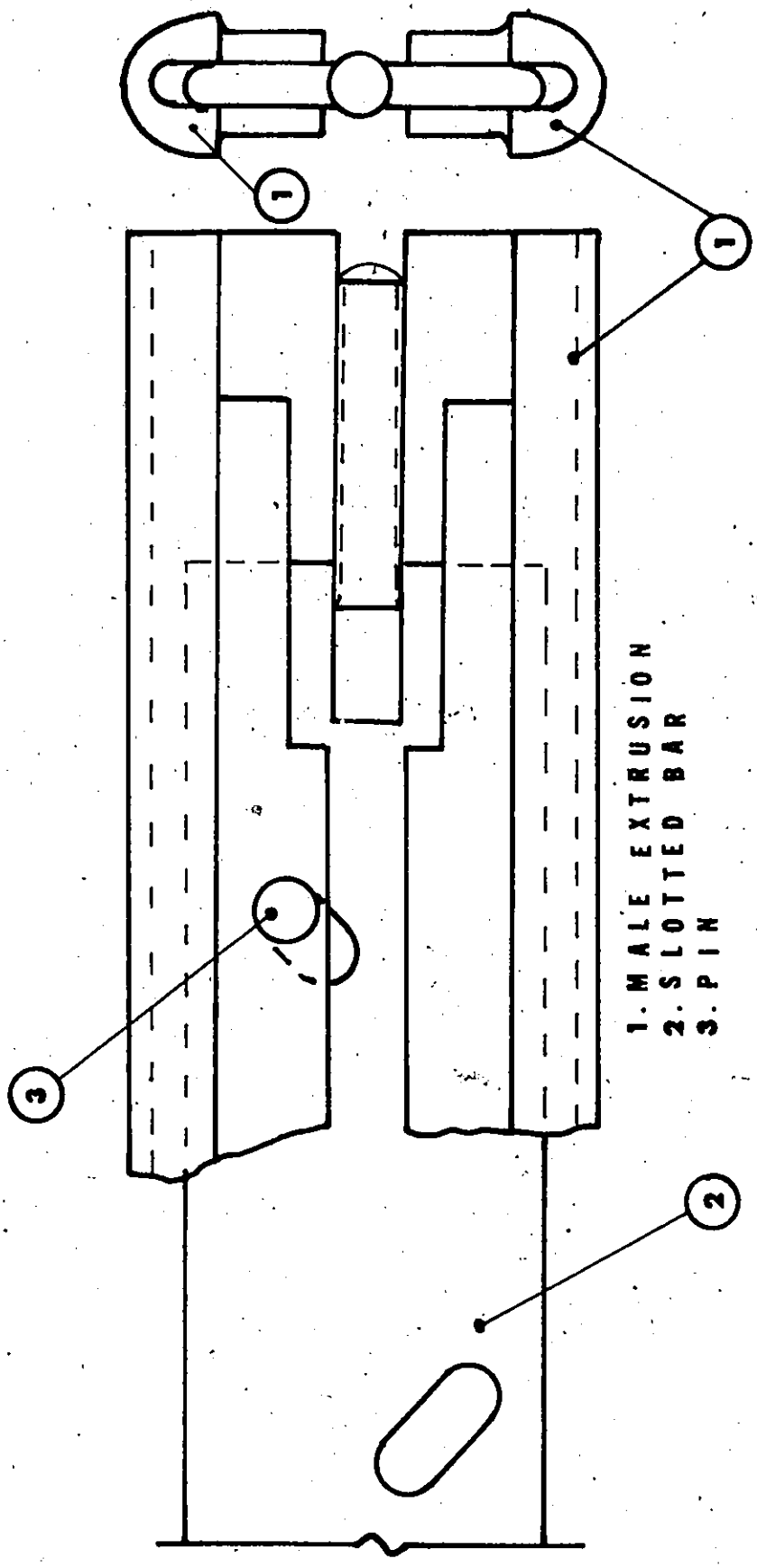

FIGURE 5.1 THE SLOTTED BAR ASSEMBLY

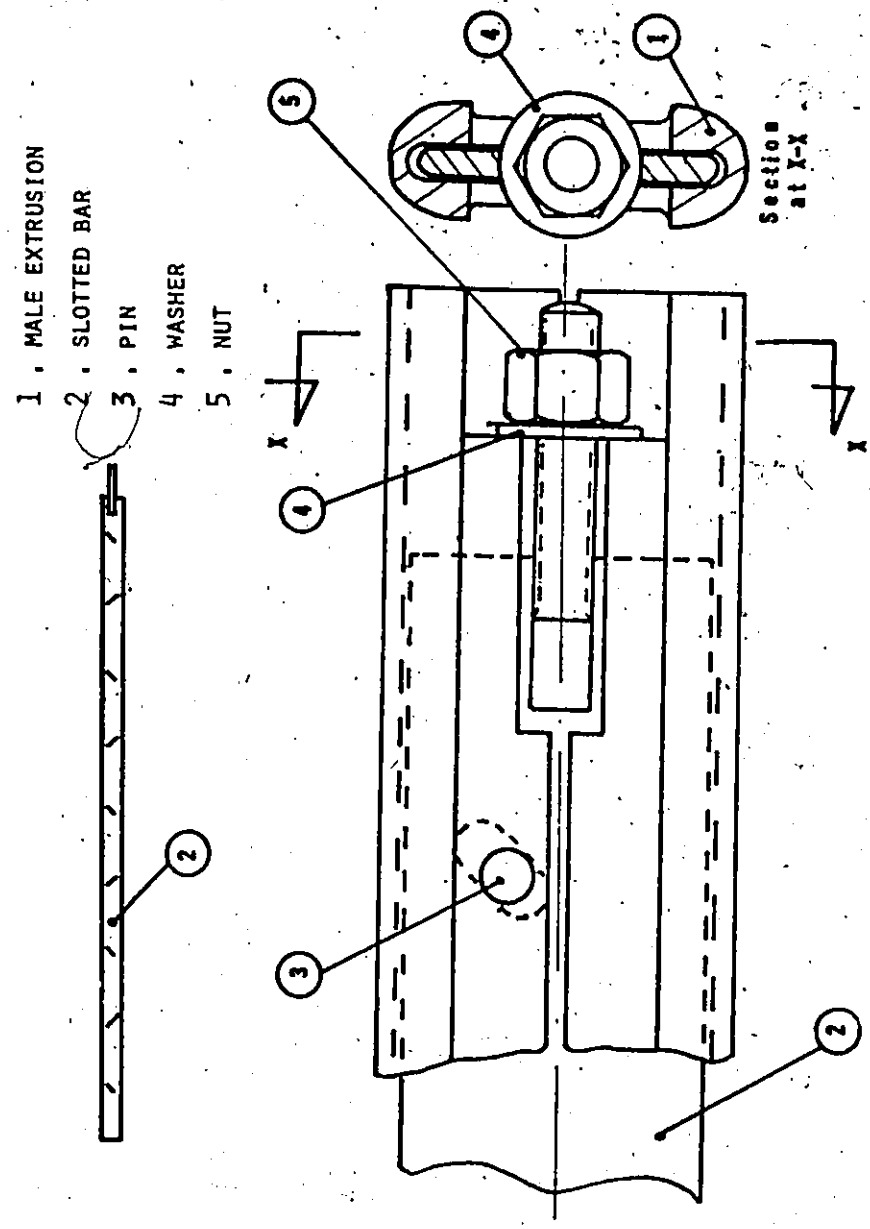

FIGURE 5.2 TIGHTENED NUT ON SLOTTED BAR ASSEMBLY

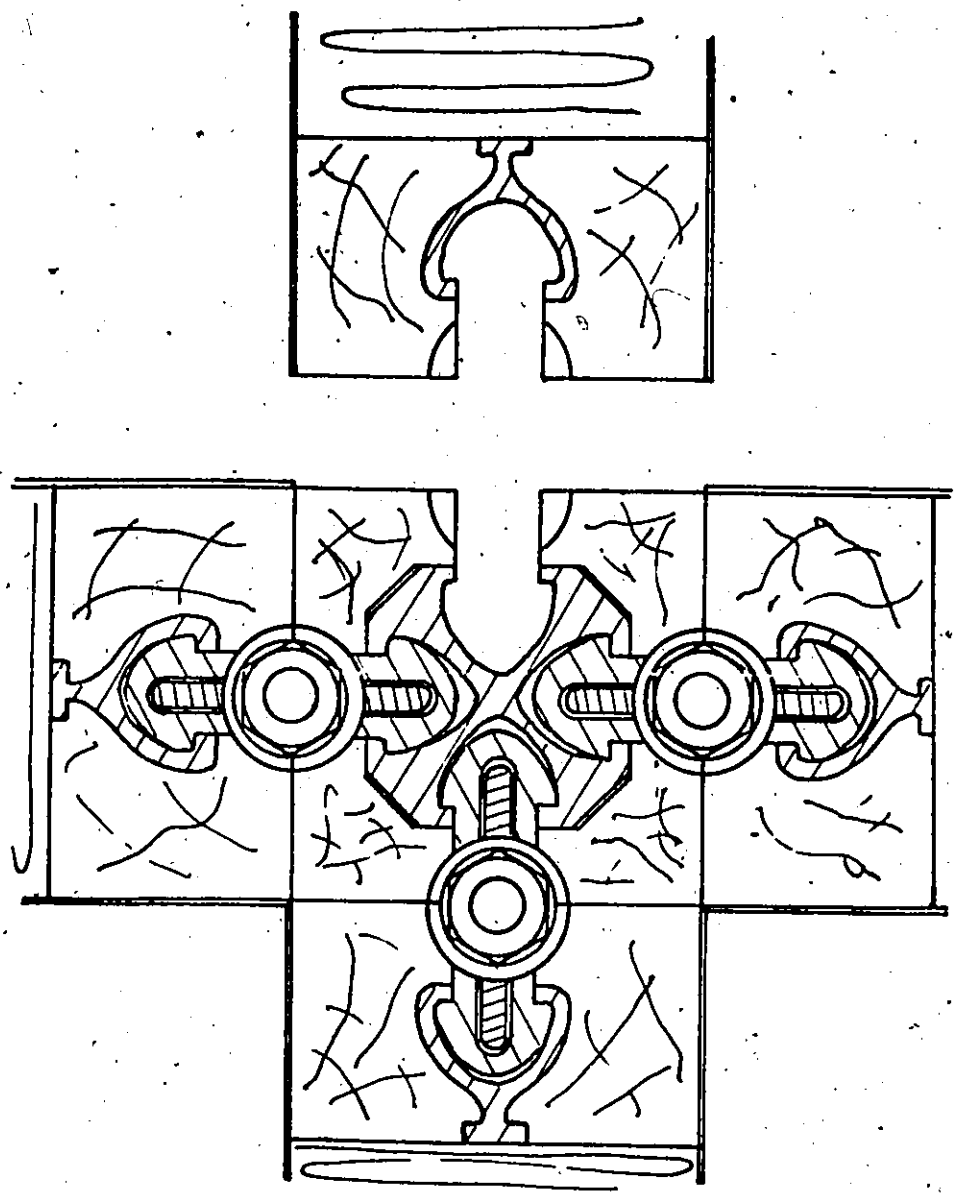

FIGURE 5.3 CONNECTING FOUR PANELS TOGETHER

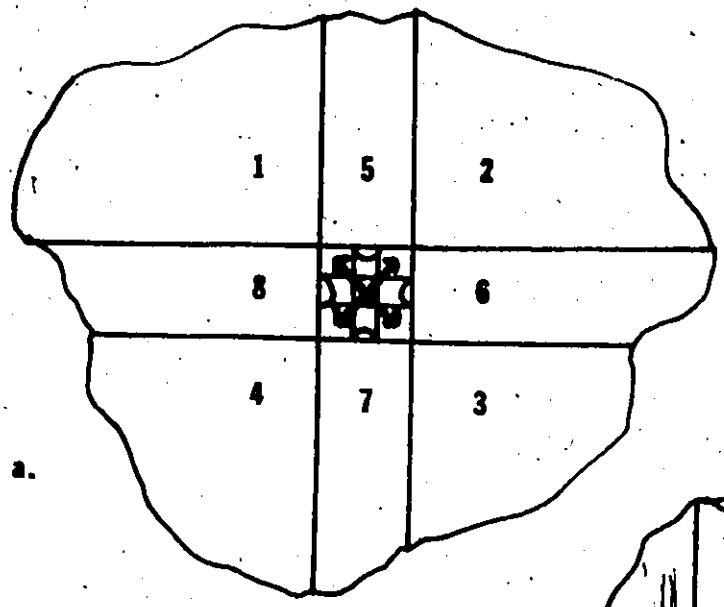

a.

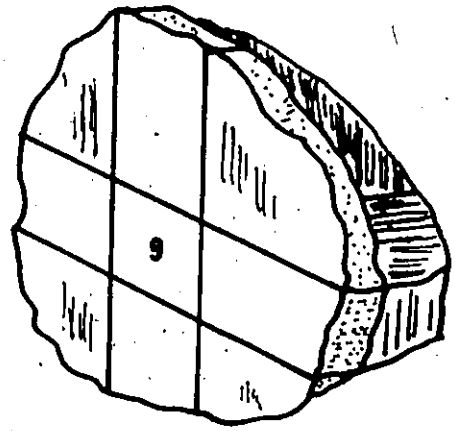

b.

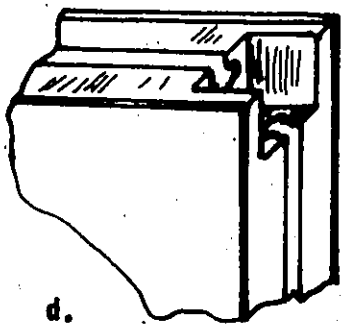

d.

Typical panel corner

c.

Typical intermediate member for the outside

FIGURE 5.4 CONNECTION OF FOUR PANELS IN AN EXTERNAL WALL

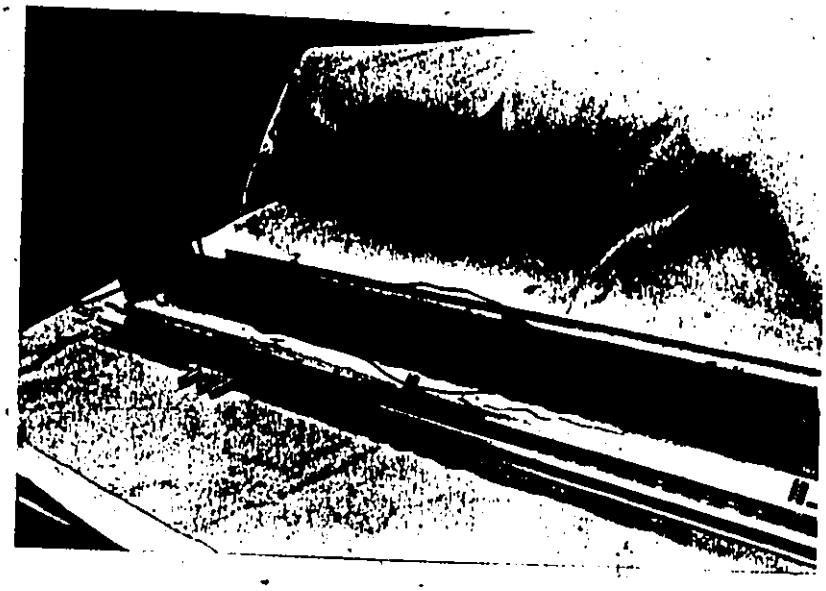

FIGURE 5.5 DISMANTLED SLOTTED BAR CONNECTION

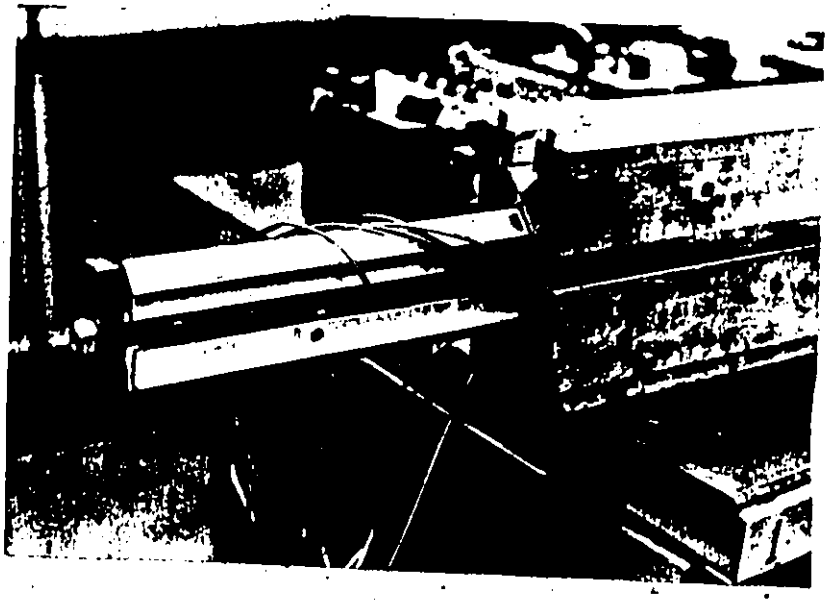

FIGURE 5.6 ASSEMBLED SLOTTED BAR CONNECTION

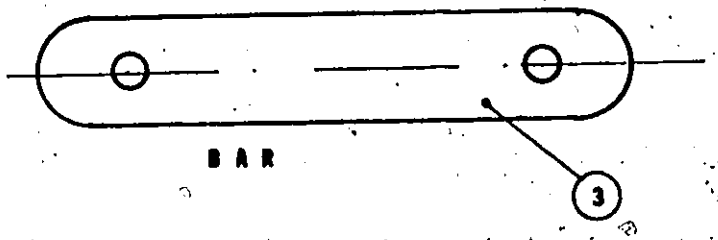

1 . FEMALE EXTRUSION
2 . PIN
3 . BAR

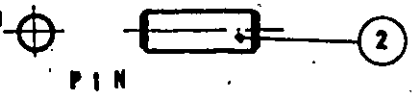

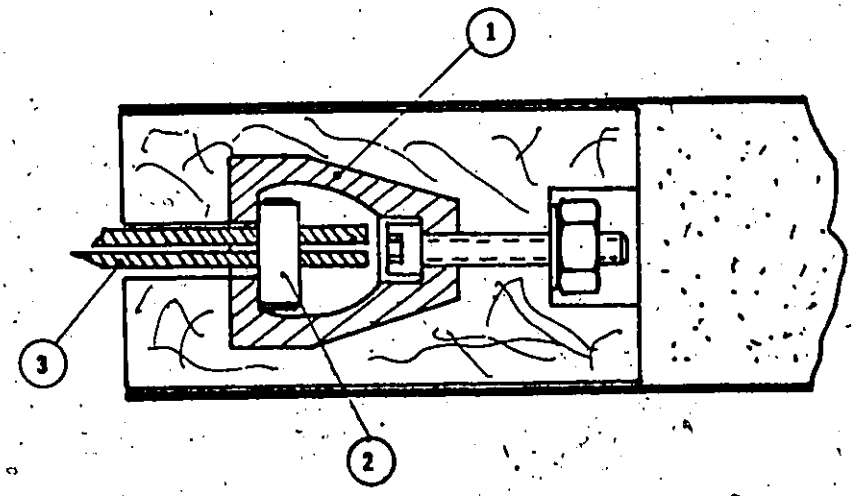

FIGURE 5.7 THE ZIG-ZAG BAR CONNECTION

4 . RETAINING PLATE
5 . PULLING ACCESSORY
6 . NUT

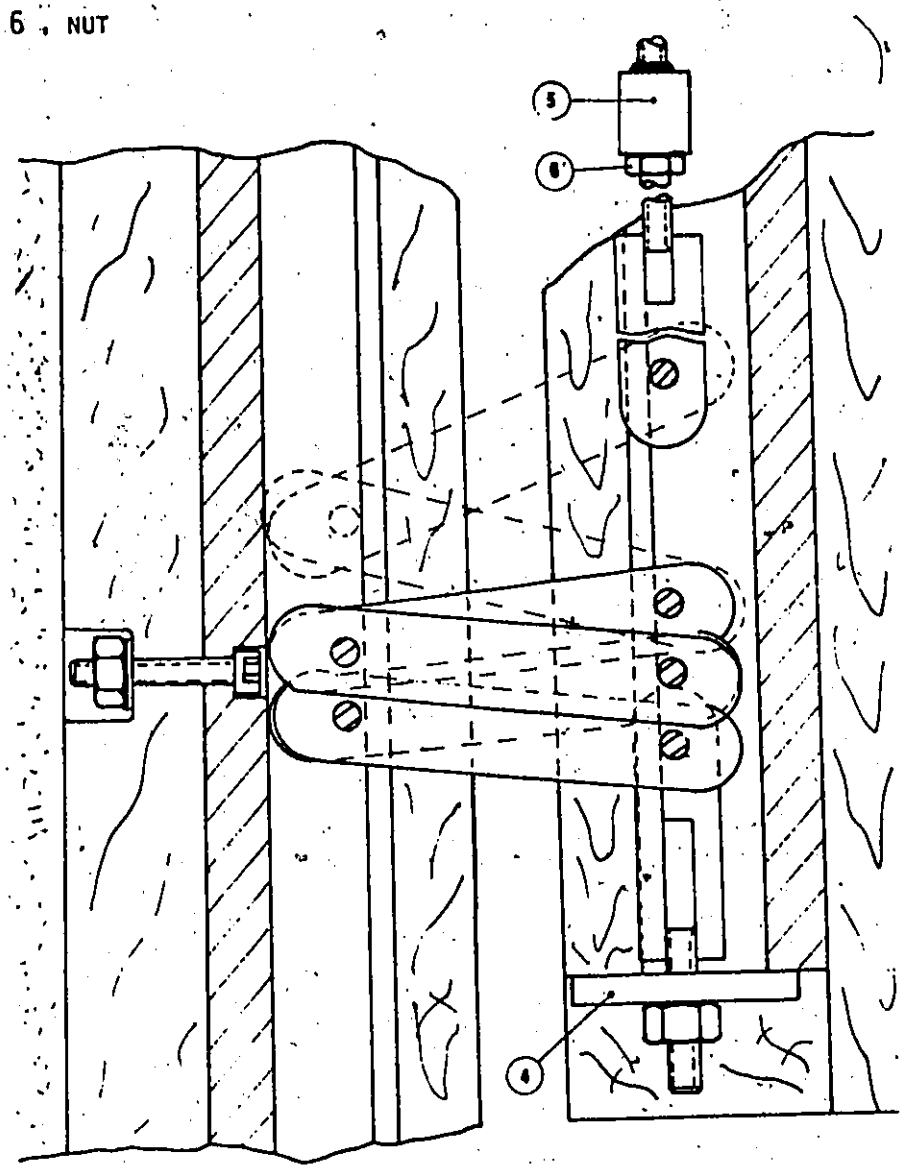

FIGURE 5,8 TWO PANELS JOINED BY THE ZIG-ZAG BAR CONNECTION

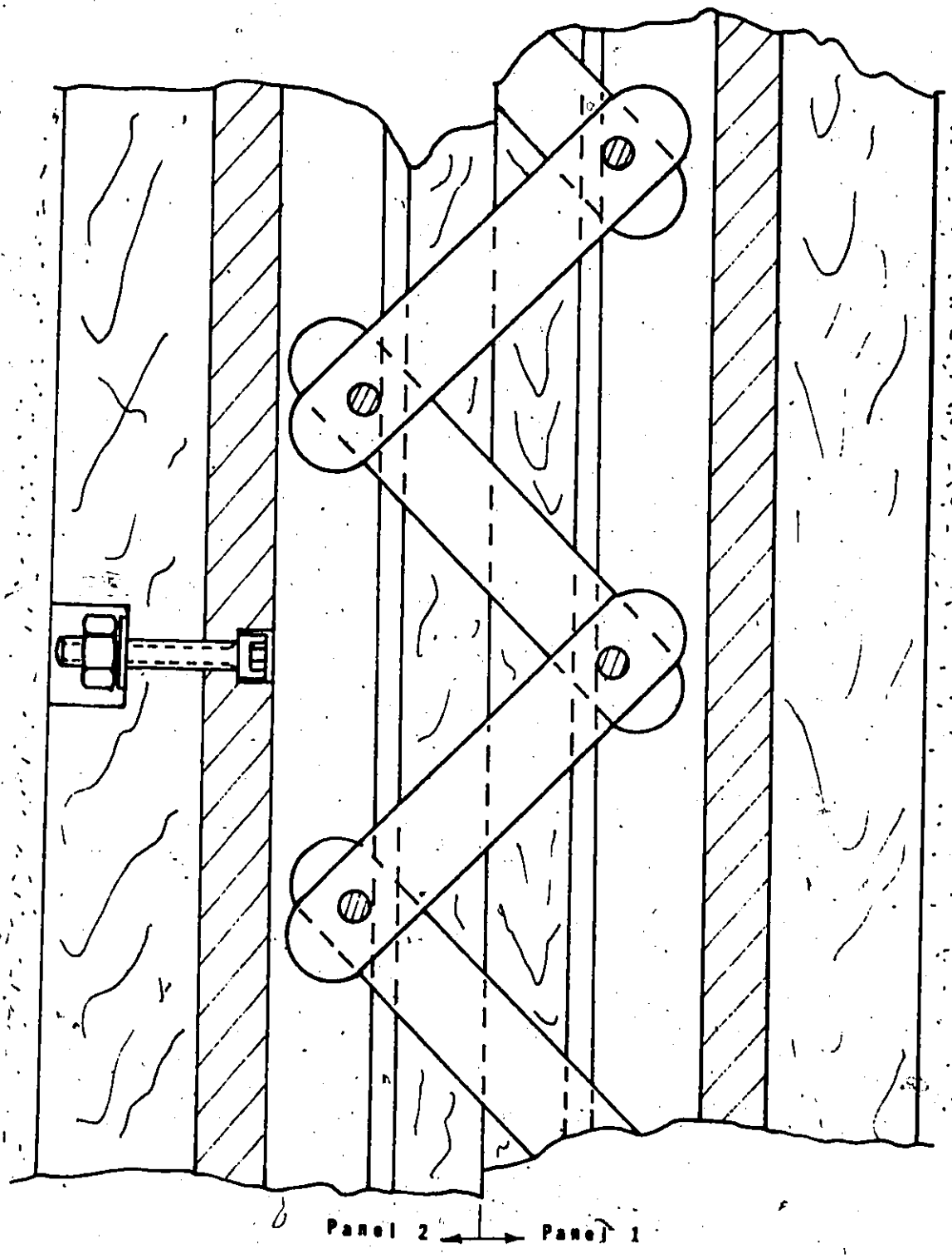

FIGURE 5.9 PANELS WITH TAUT CONNECTION

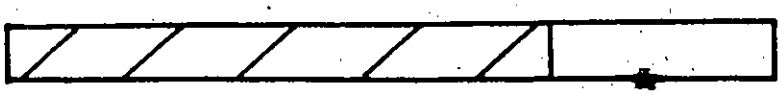

PART 7

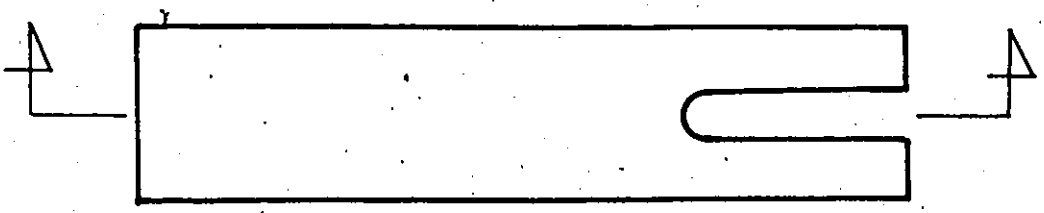

FIGURE 5.10 THE RETAINING PLATE

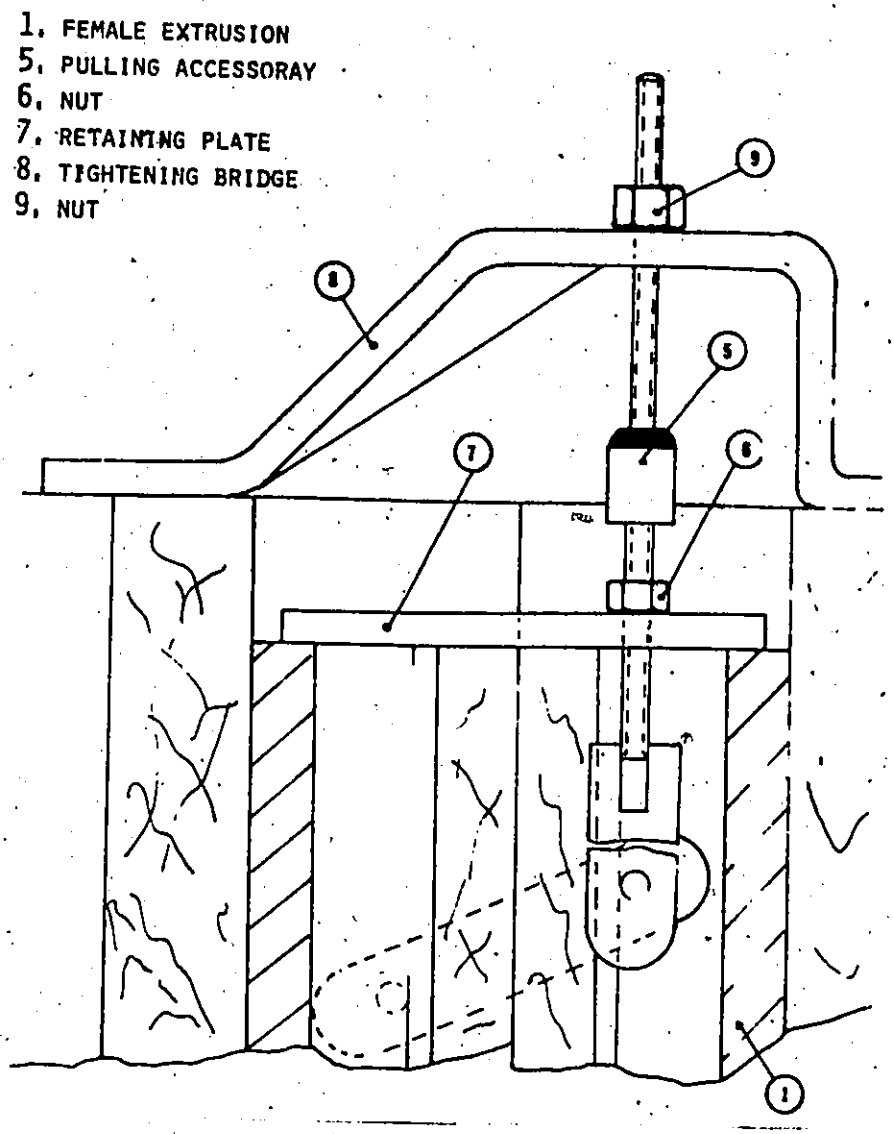

FIGURE 5.11 THE LOADING MECHANISM

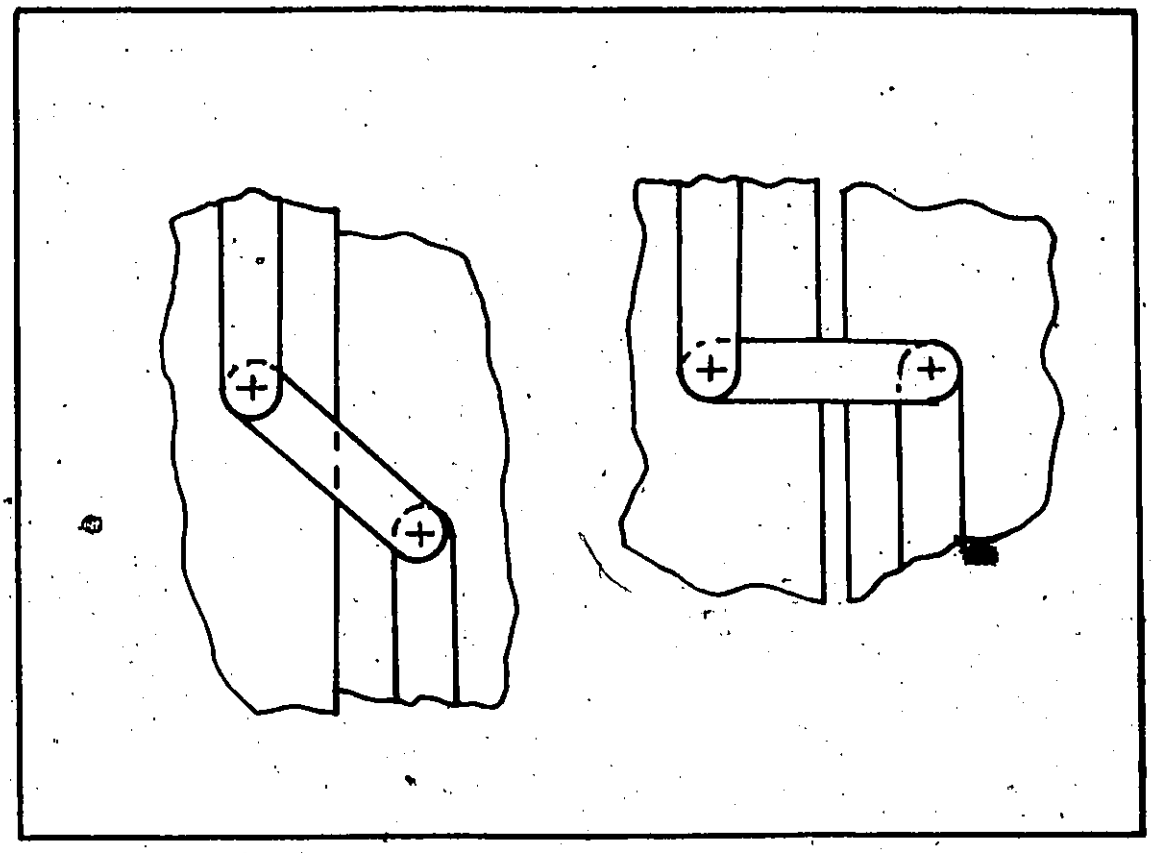

FIGURE 5.12 OTHER ARRANGEMENT OF
ZIG-ZAG BAR CONNECTION

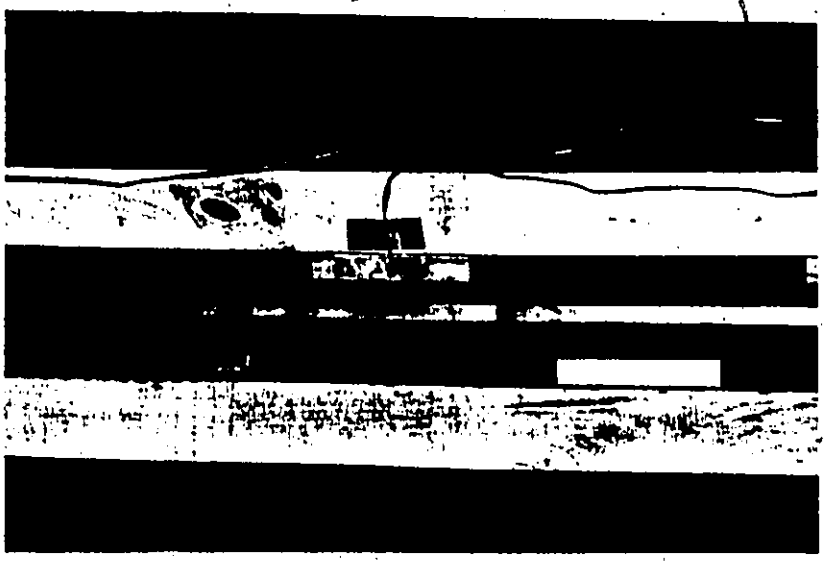

1 . BOX SECTION
2 . WOODEN MEMBER
3 . SQUARE ROD

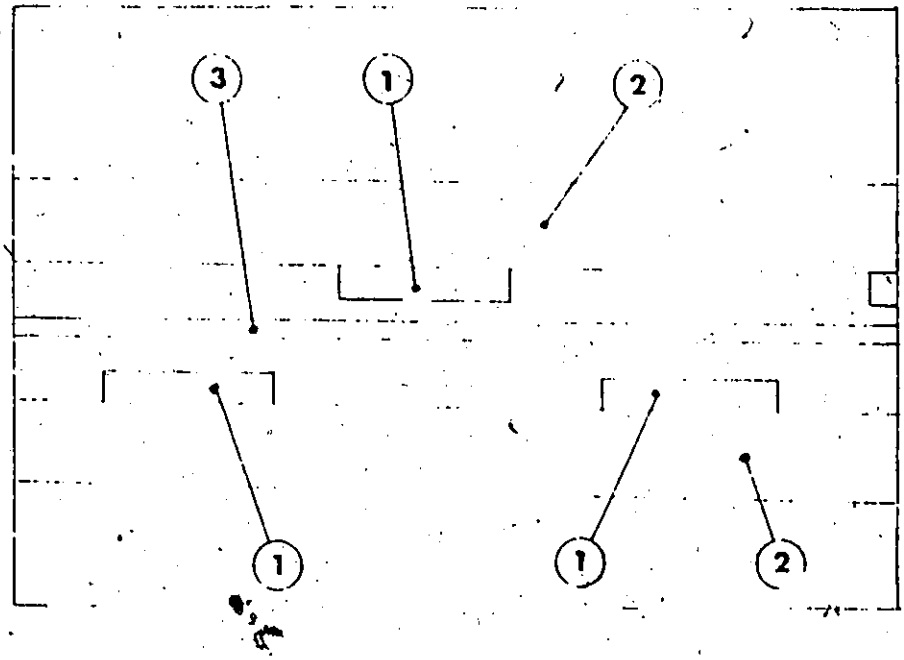

FIGURE 5.13 DISMANTLED ROD CONNECTION SYSTEM

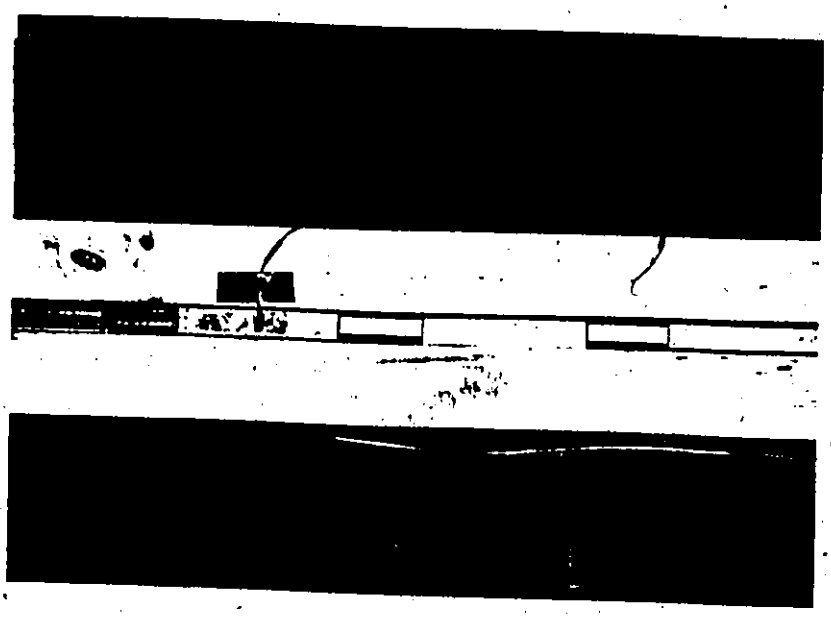

FIGURE 5.14 THE SQUARE ROD INTRODUCED INTO BOX SECTIONS

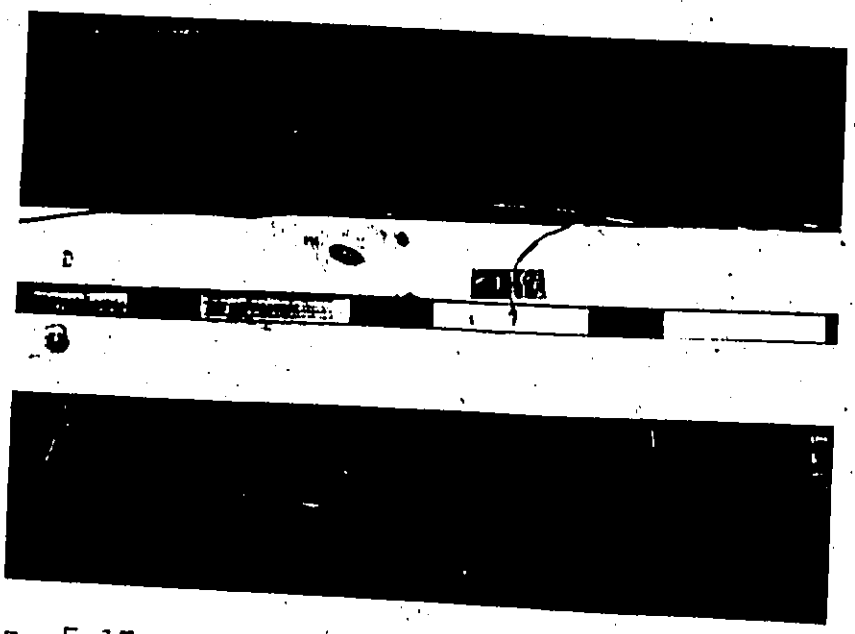

FIGURE 5.15 THE CONNECTION IS FORMED BY TWISTING THE ROD

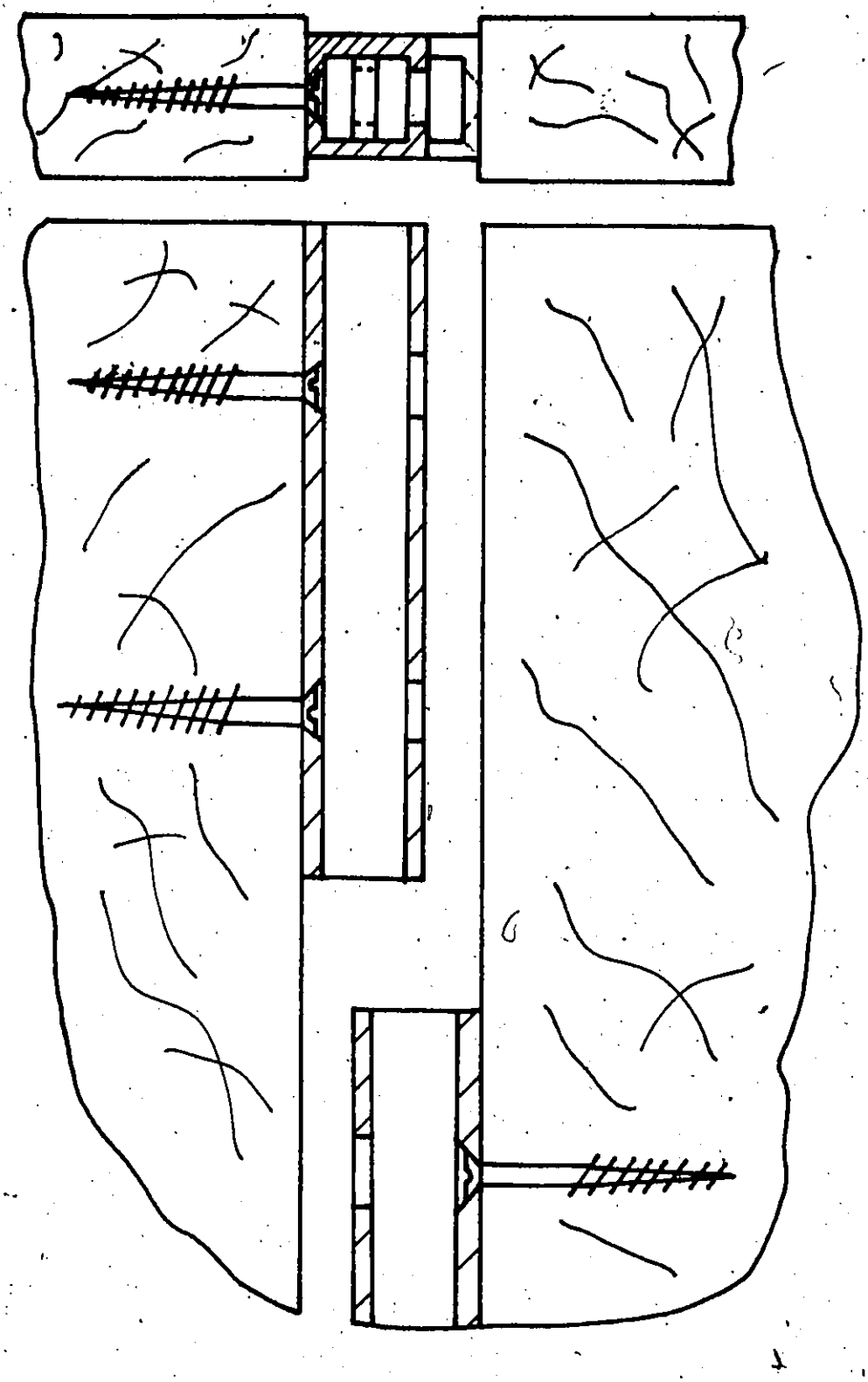

FIGURE 5.16 PANELS READY FOR THE INTRODUCTION OF THE ROD

1. BOX SECTION
2. PANEL
3. SQUARE ROD
4. CIRCULAR ROD

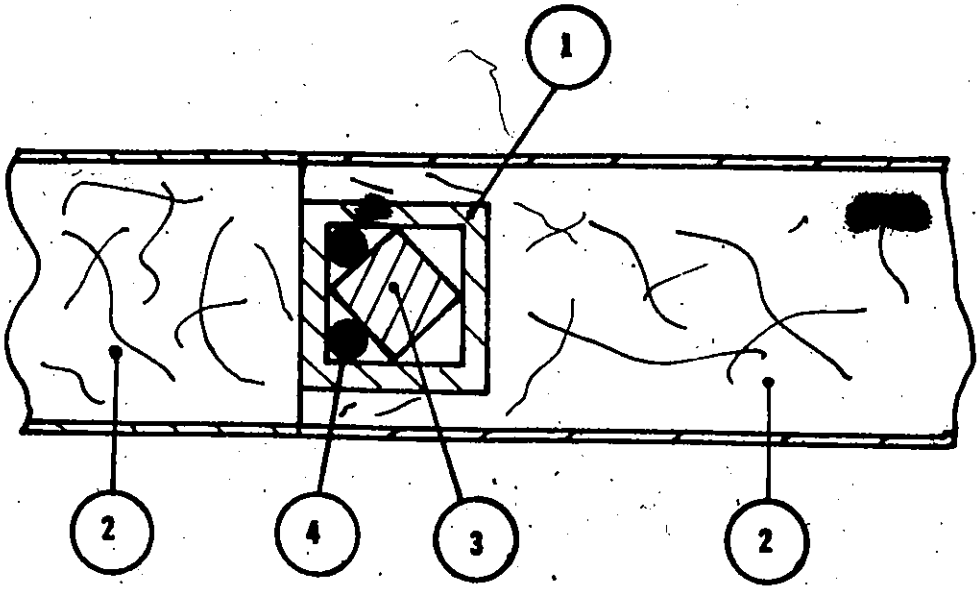

FIGURE 5.17 LOCKING THE ROD CONNECTION

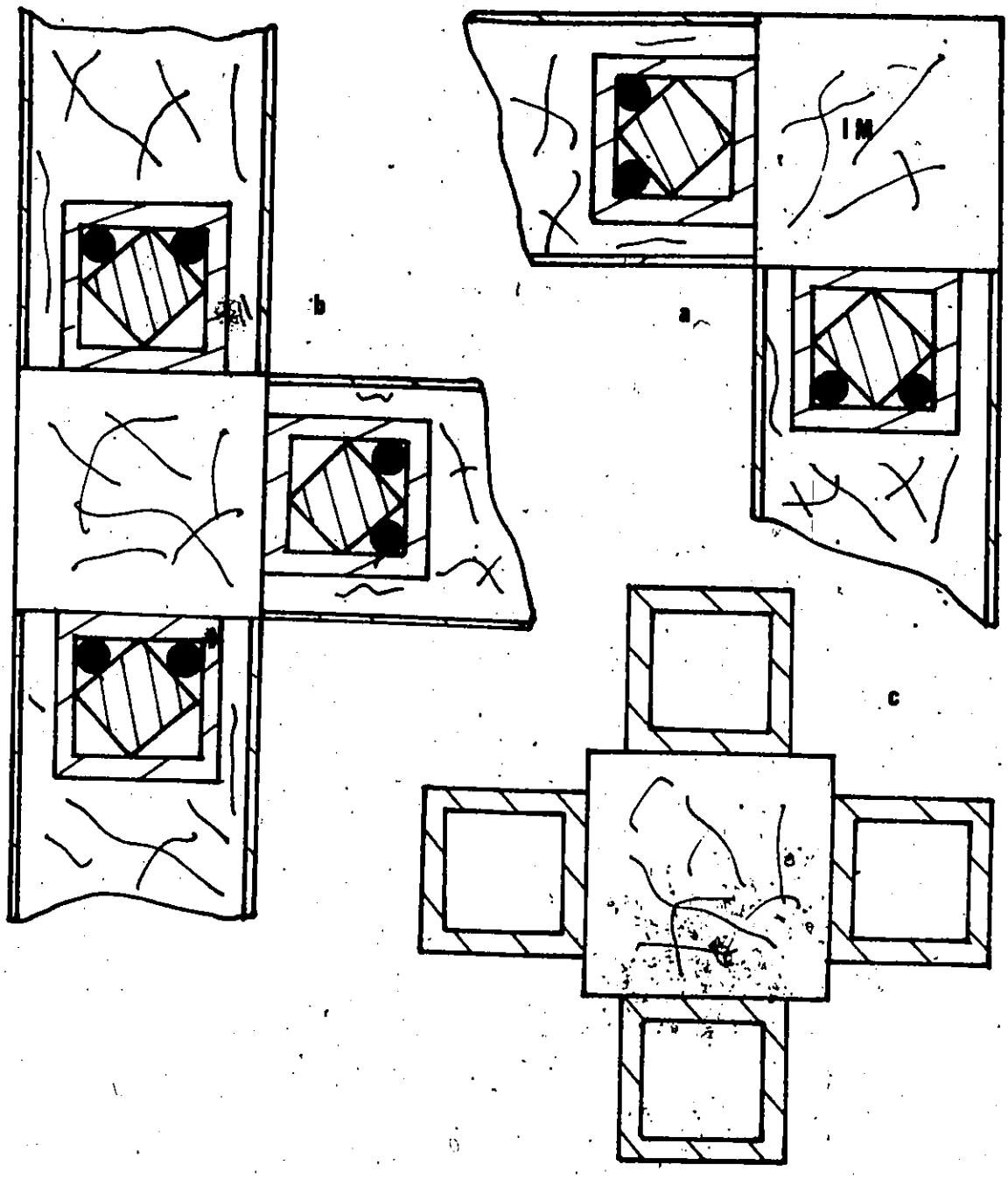

FIGURE 5.18 CORNER, WALL TO FLOOR AND INTERMEDIATE CONNECTIONS

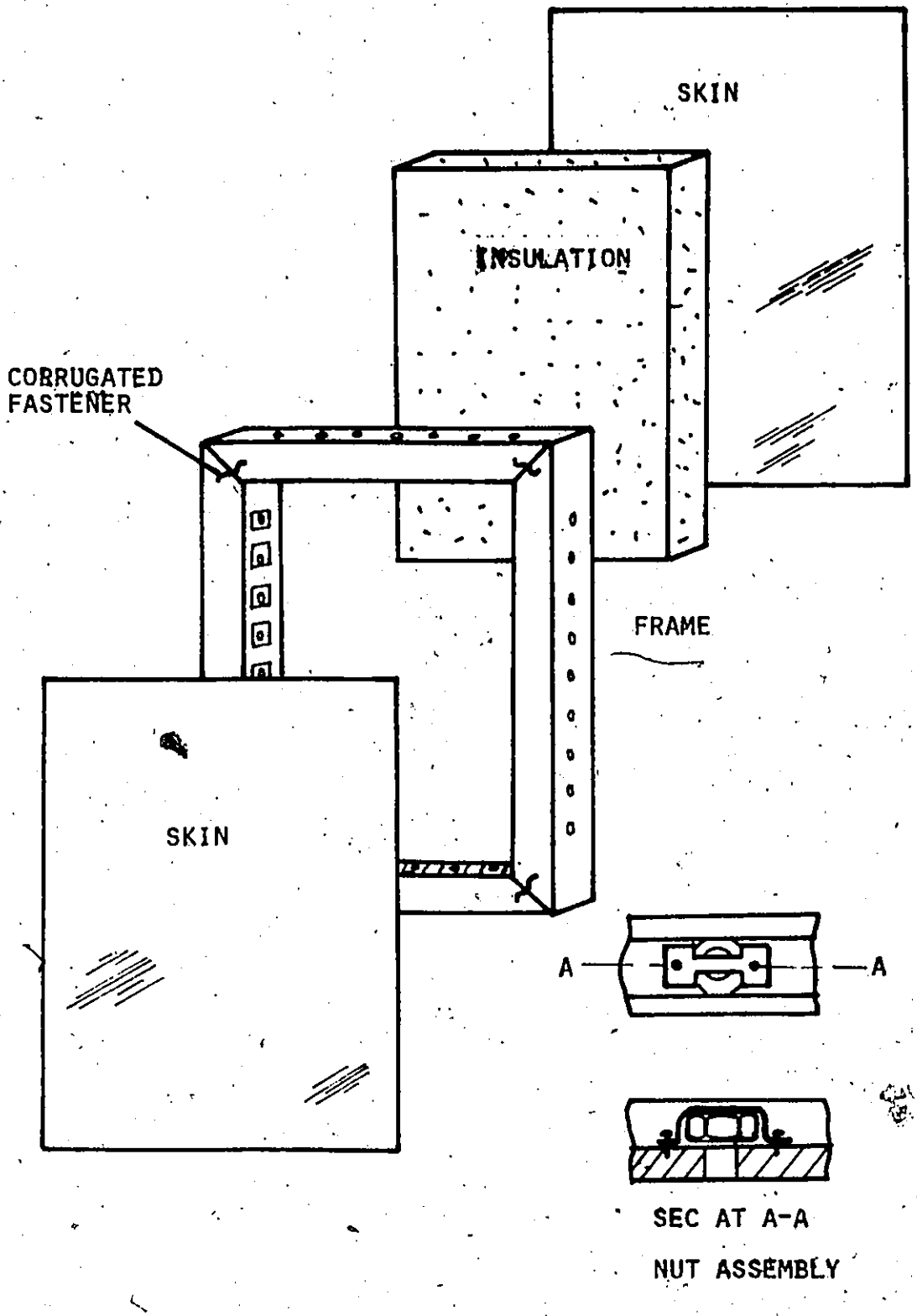

FIGURE 5.19 EXPLODED VIEW OF THE BASIC PANEL

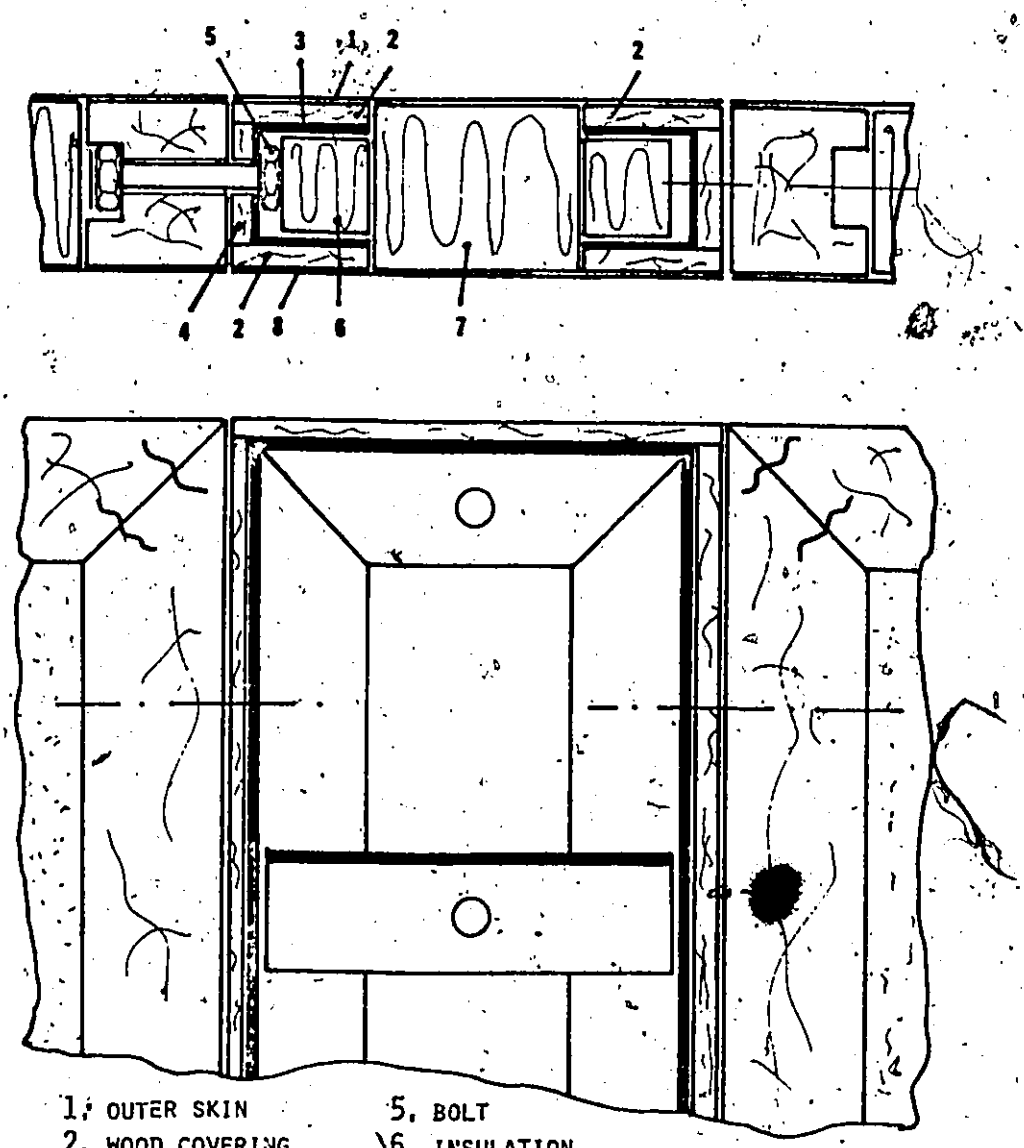

FIGURE 5.20 A JOINING PANEL PLACED IN A STRUCTURE ASSEMBLY

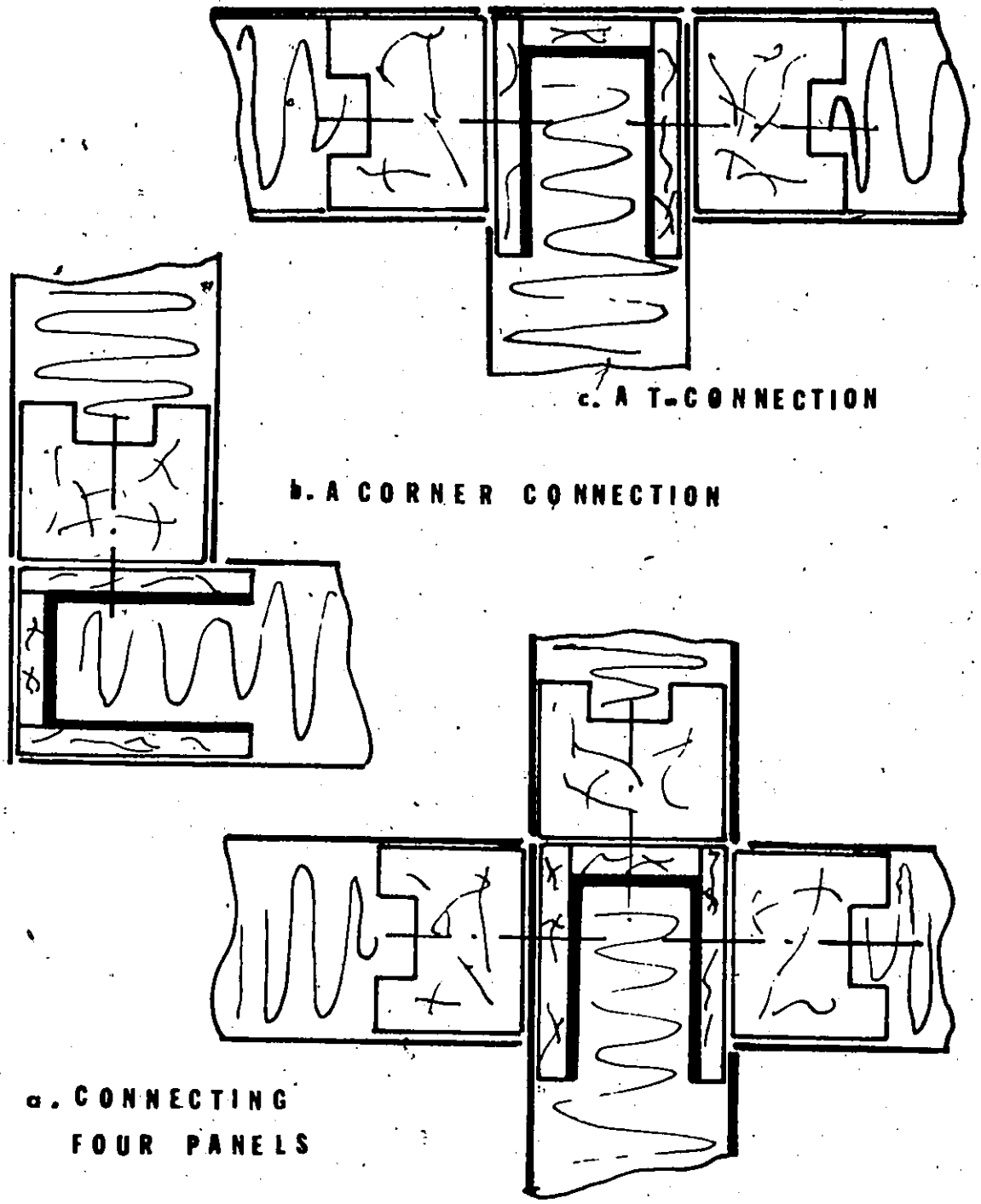

FIGURE 5.21 SOLUTIONS TO THE DIFFERENT JUNCTIONS IN A BUILDING SYSTEM

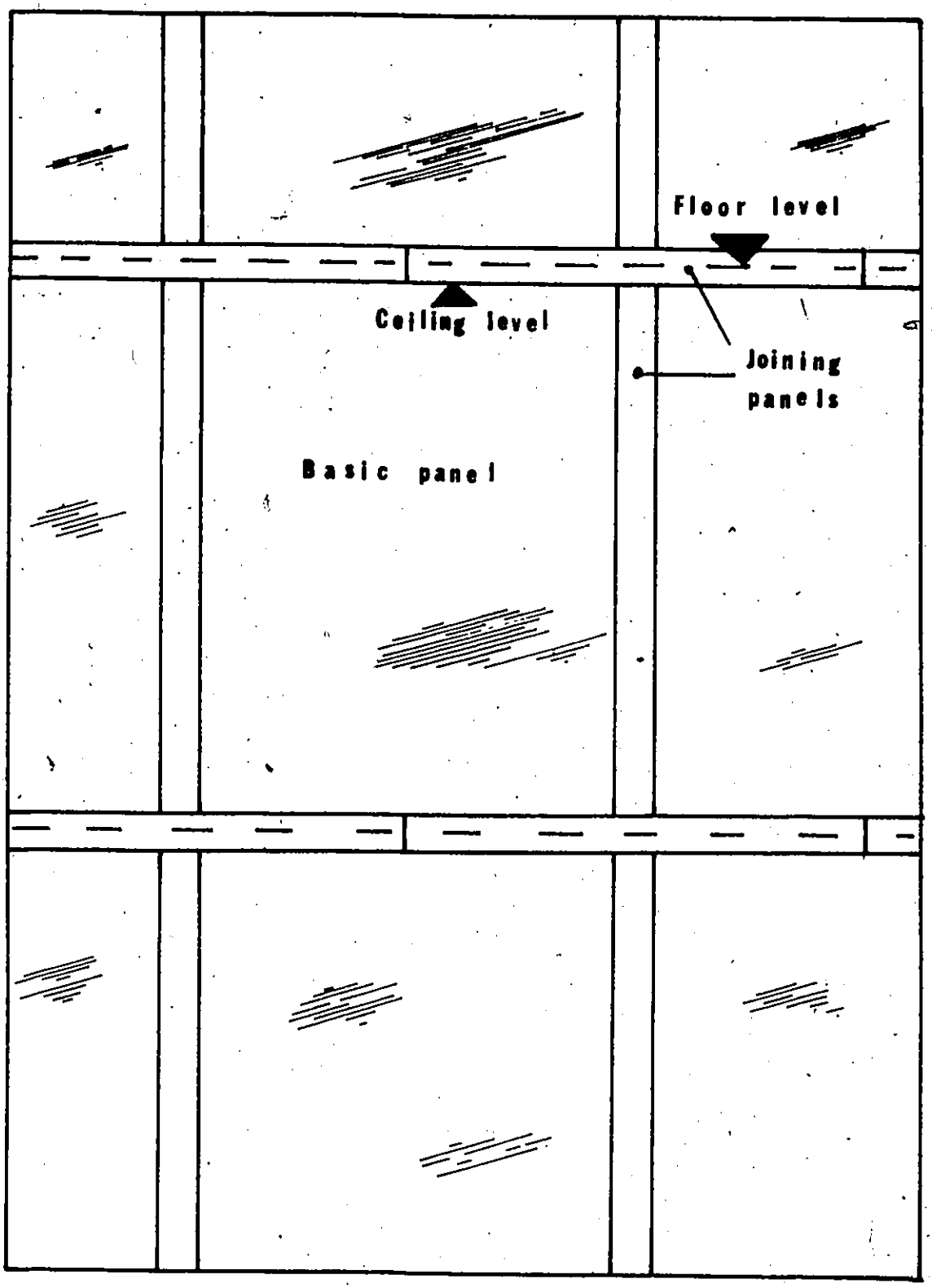

FIGURE 5.22 A WALL ASSEMBLY

FIGURE A.1 THE STEEL LOADING FRAME

FIGURE A.2 2-TON HYDRAULIC RAM

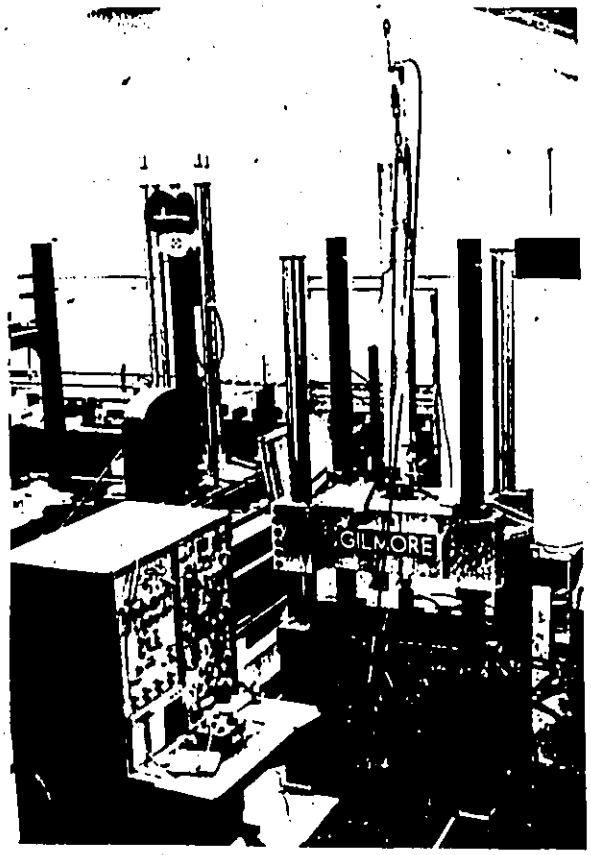

FIGURE A.3 UNIVERSAL GILMORE MACHINE WITH 3-KIP ACTUATOR

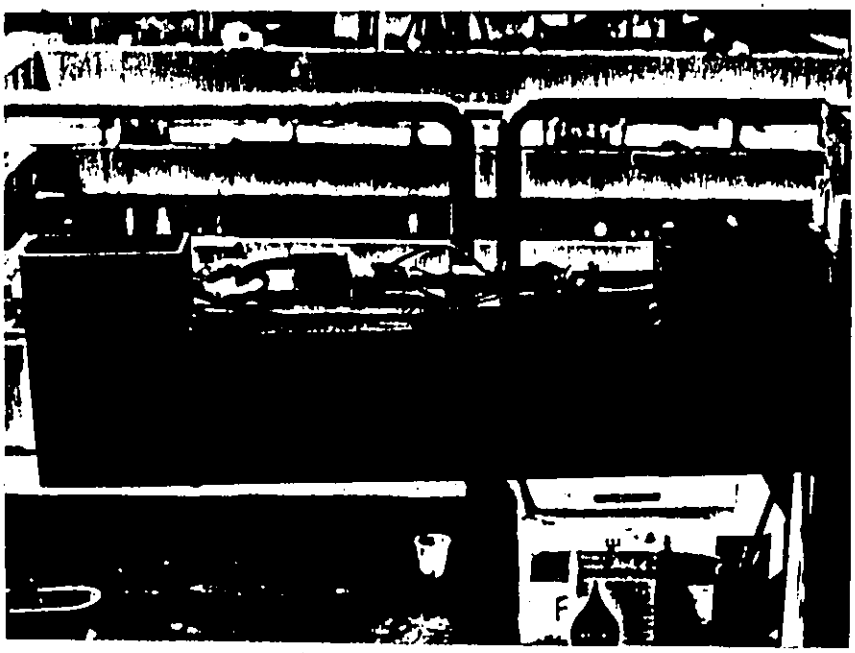

FIGURE A.4 C-SHAPED END PIECE

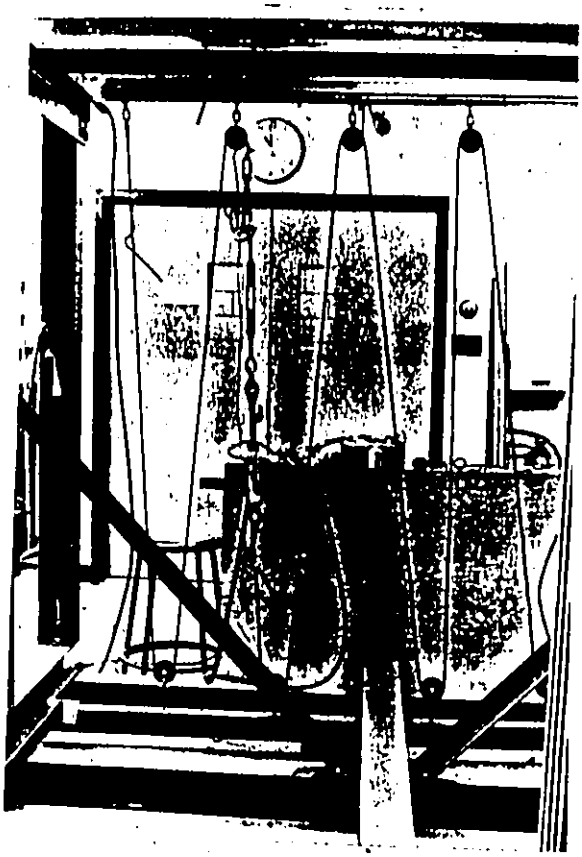

FIGURE A.5 APPLICATION OF DISTRIBUTED LOAD

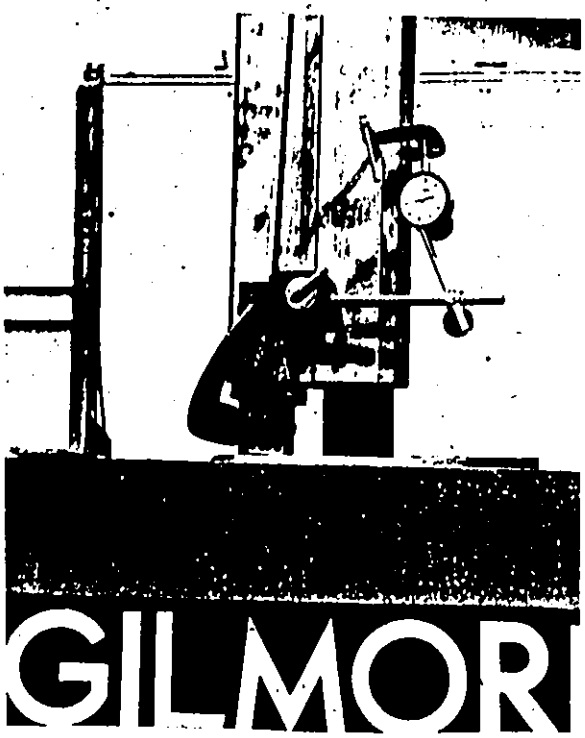

FIGURE A.6 DIAL GAGE ATTACHMENT USED IN CONJUNCTION WITH SHEAR TEST

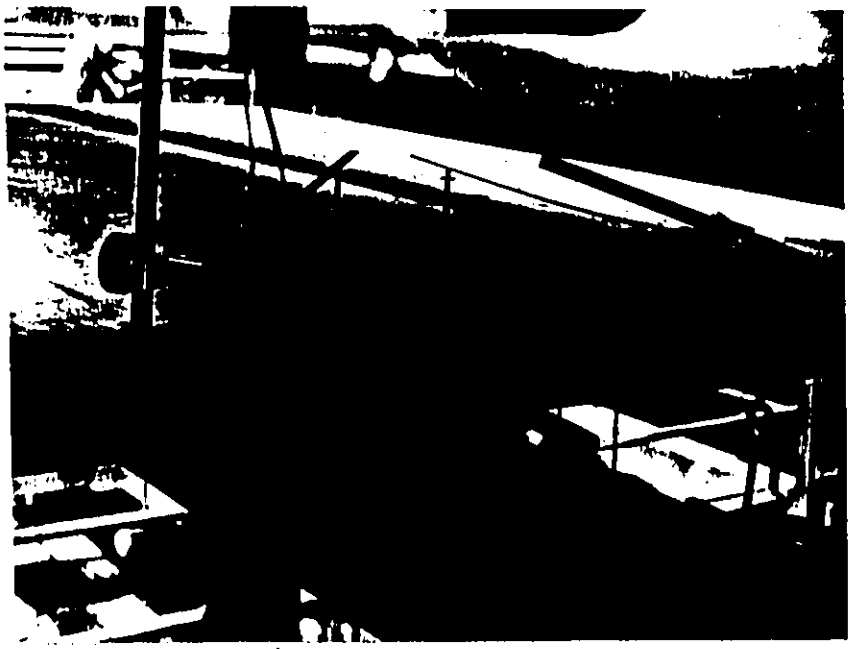

FIGURE A.7 DISPLACEMENT TRANSDUCERS

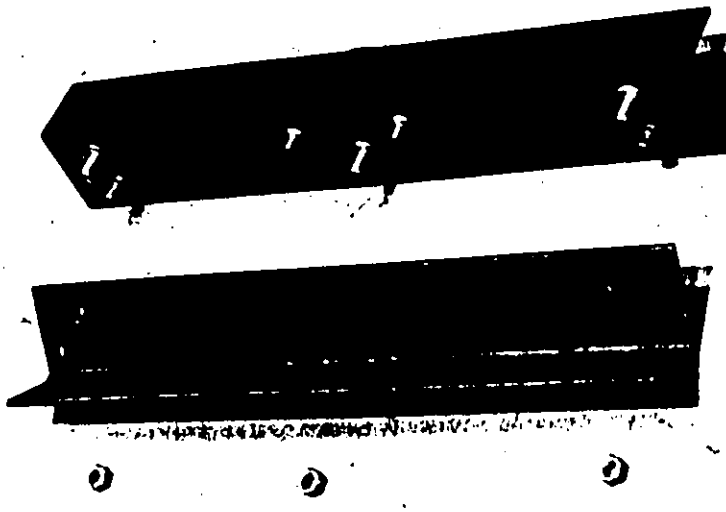

FIGURE A.8 TWO ANGLE SECTION CONNECTION DISASSEMBLED

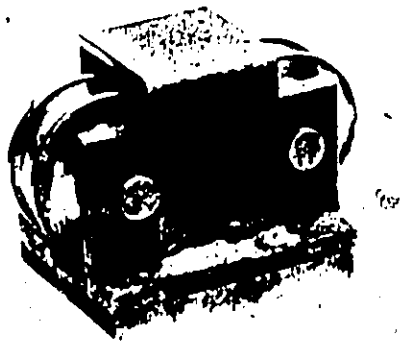

FIGURE A.9 THE PULLEY CONNECTION

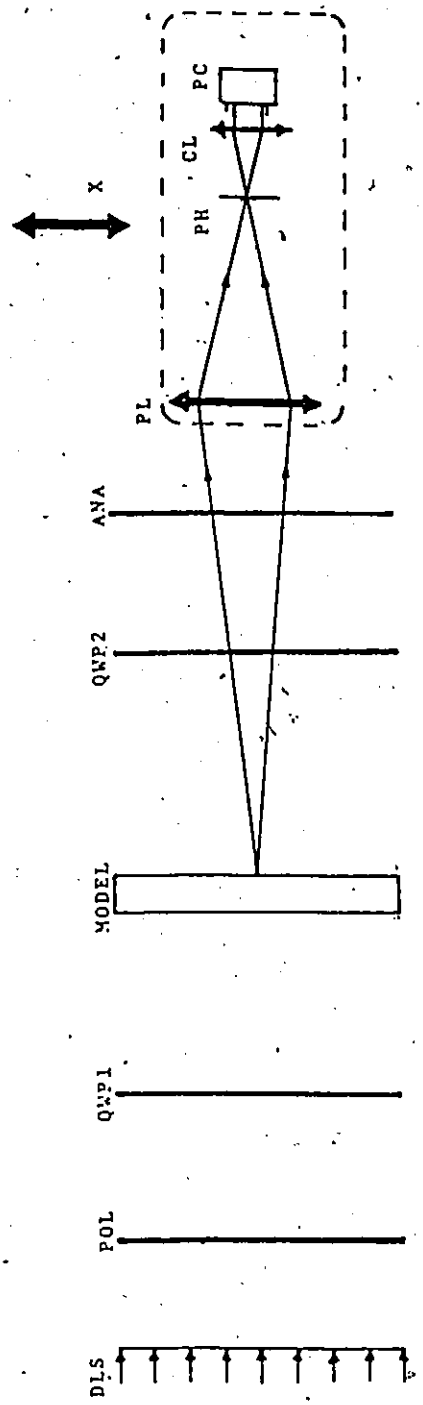

FIGURE A.10 SET-UP FOR MOVING PROJECTING LENS AND SCANNING DEVICE

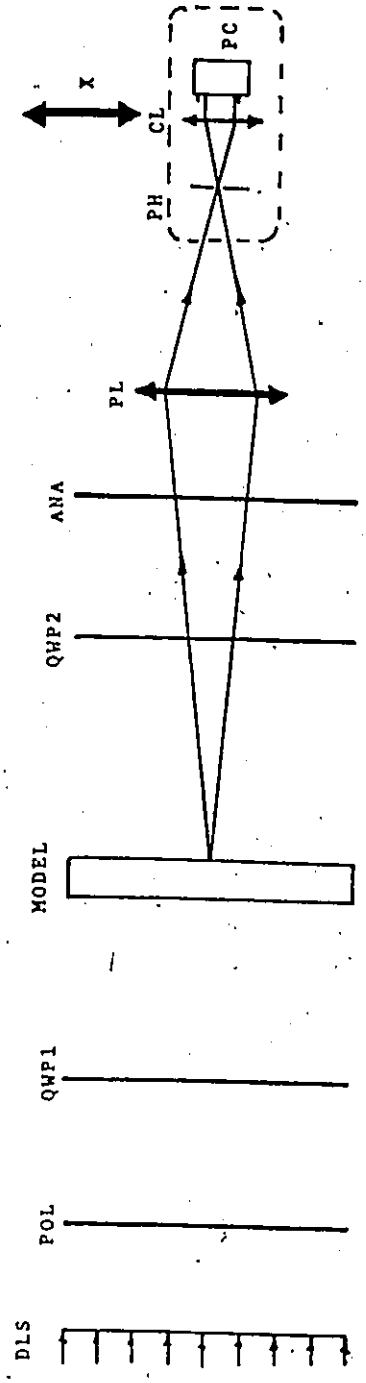

FIGURE A.11 SET-UP FOR STATIONARY LENS AND MOVING SCANNING DEVICE

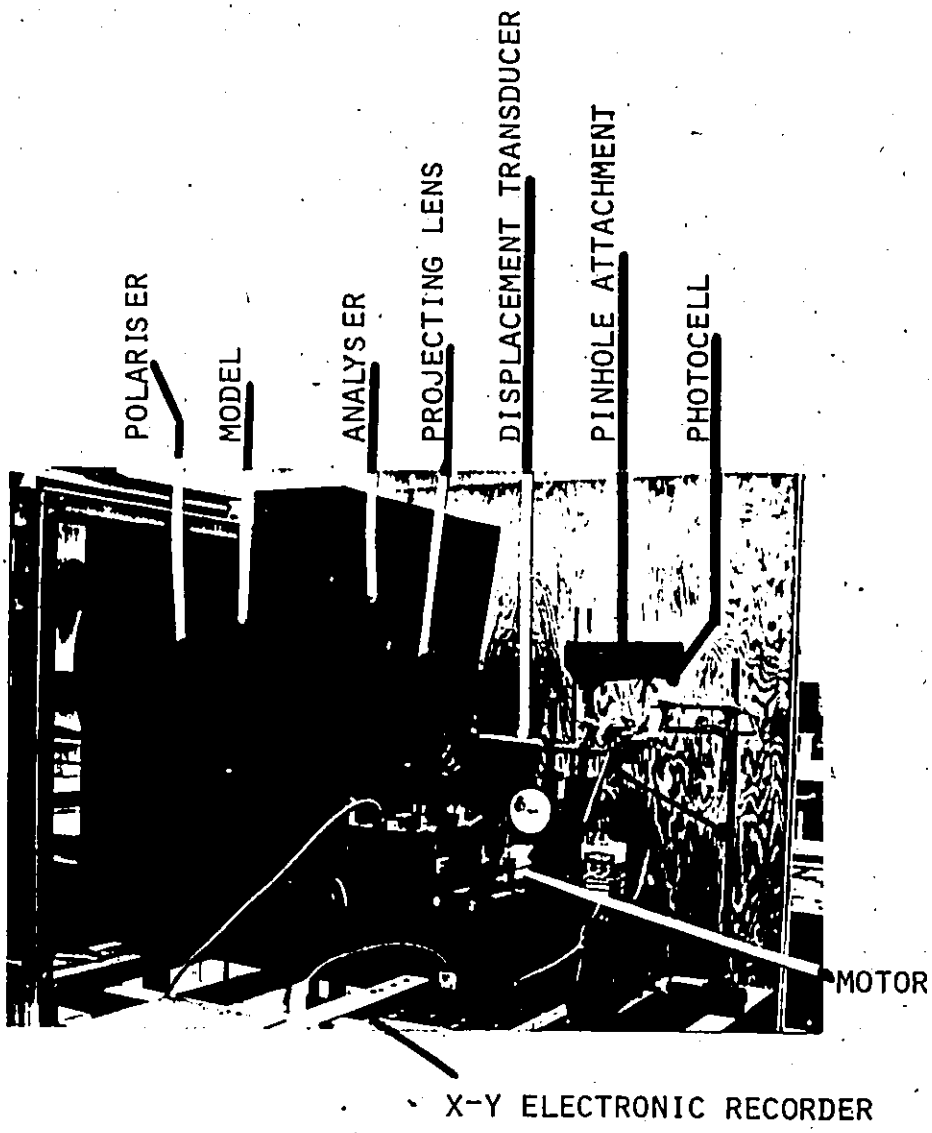

FIGURE A.12 GENERAL LAYOUT OF APPARATUS

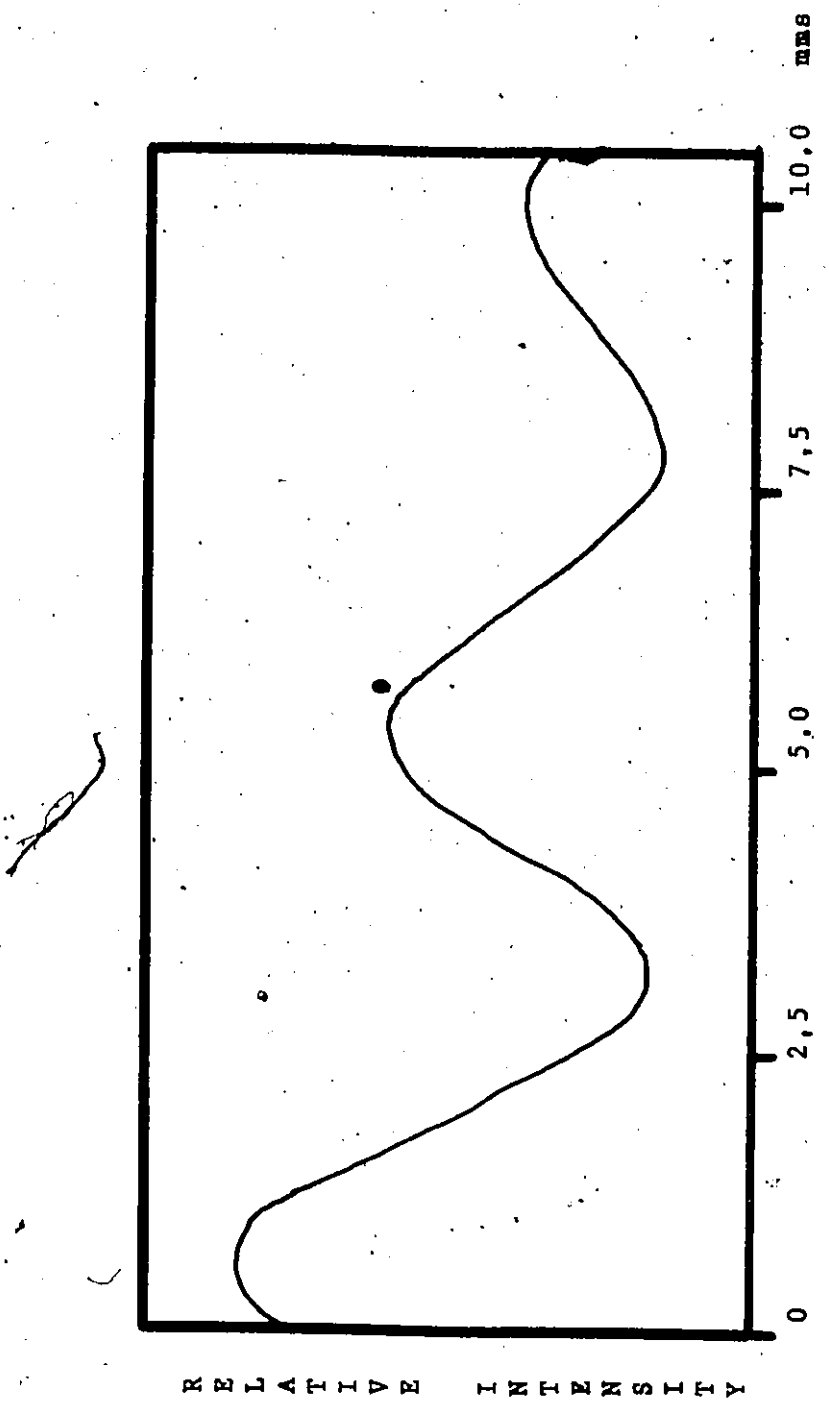

FIGURE A.13 RESULTING SCAN OF A STRESSED PHOTOELASTIC MODEL

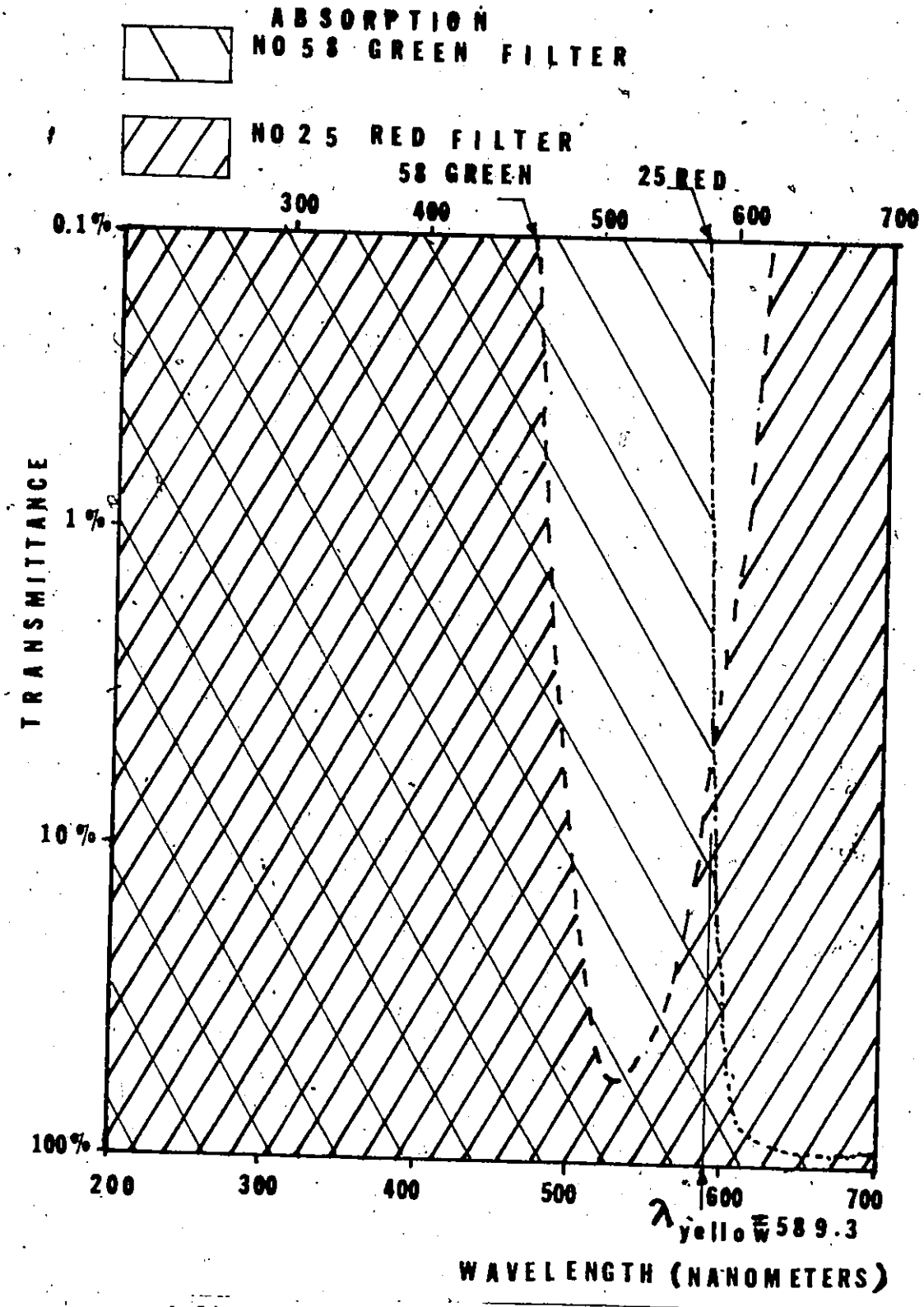

FIGURE A.14 SPECTROPHOTOMETRIC CURVES FOR GREEN AND RED FILTERS SUPERIMPOSED

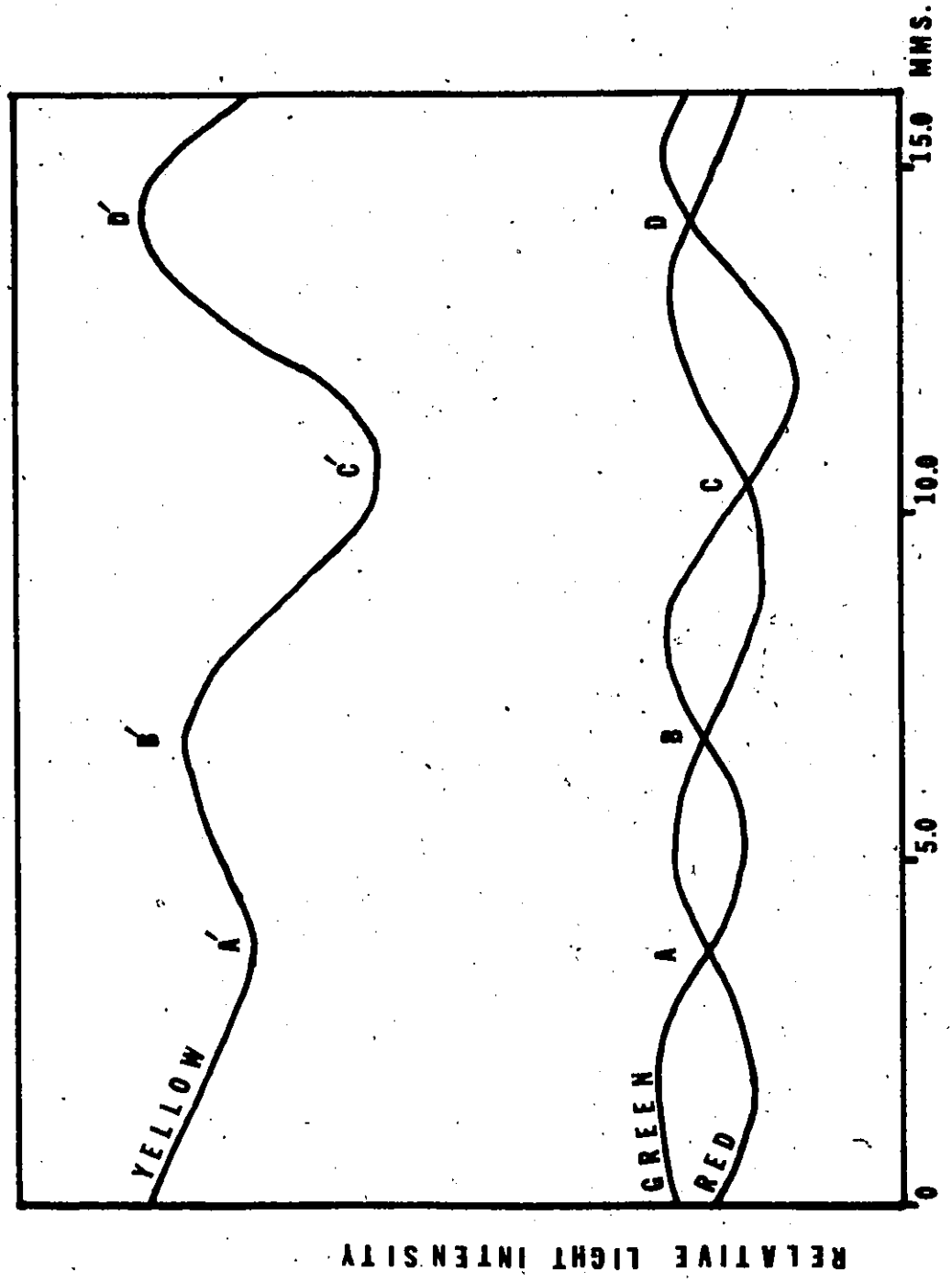

FIGURE A.15 SCANS OF A STRESSED MODEL USING DIFFERENT FILTERS

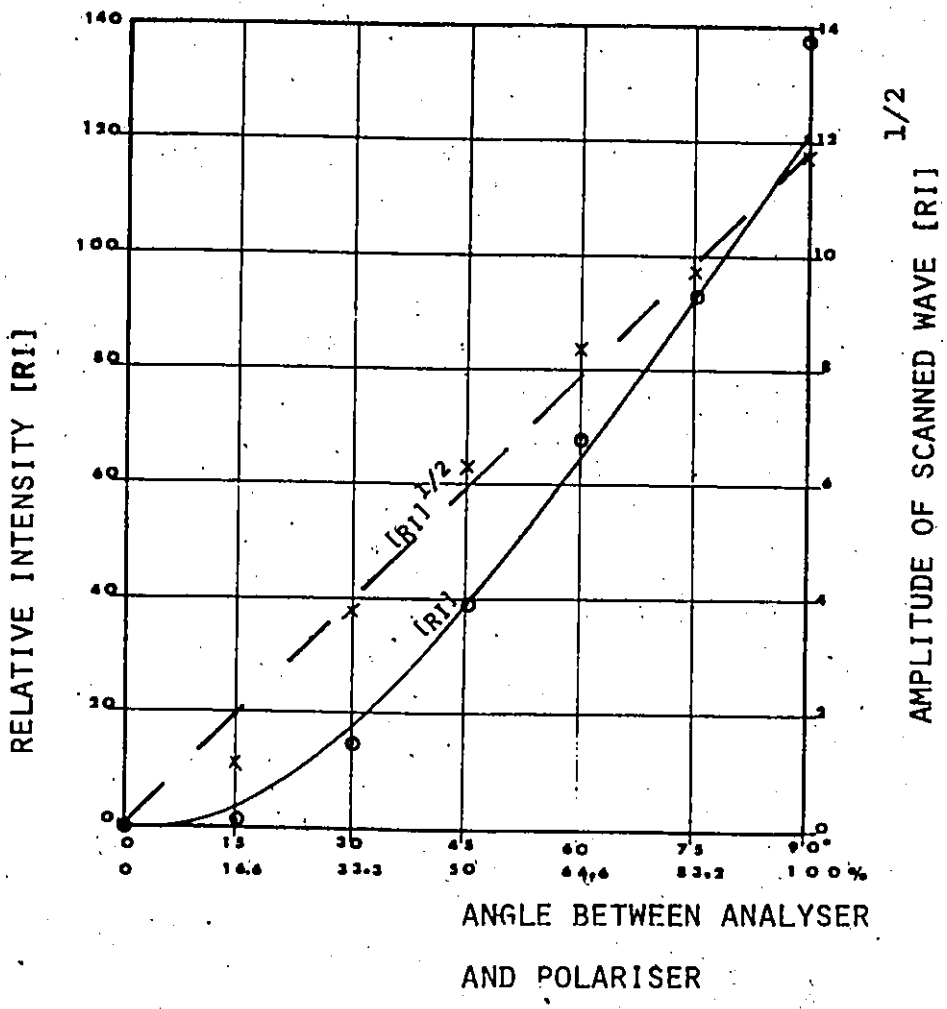

FIGURE A.16 EFFECT OF ROTATING THE ANALYSER TO THE POLARISER

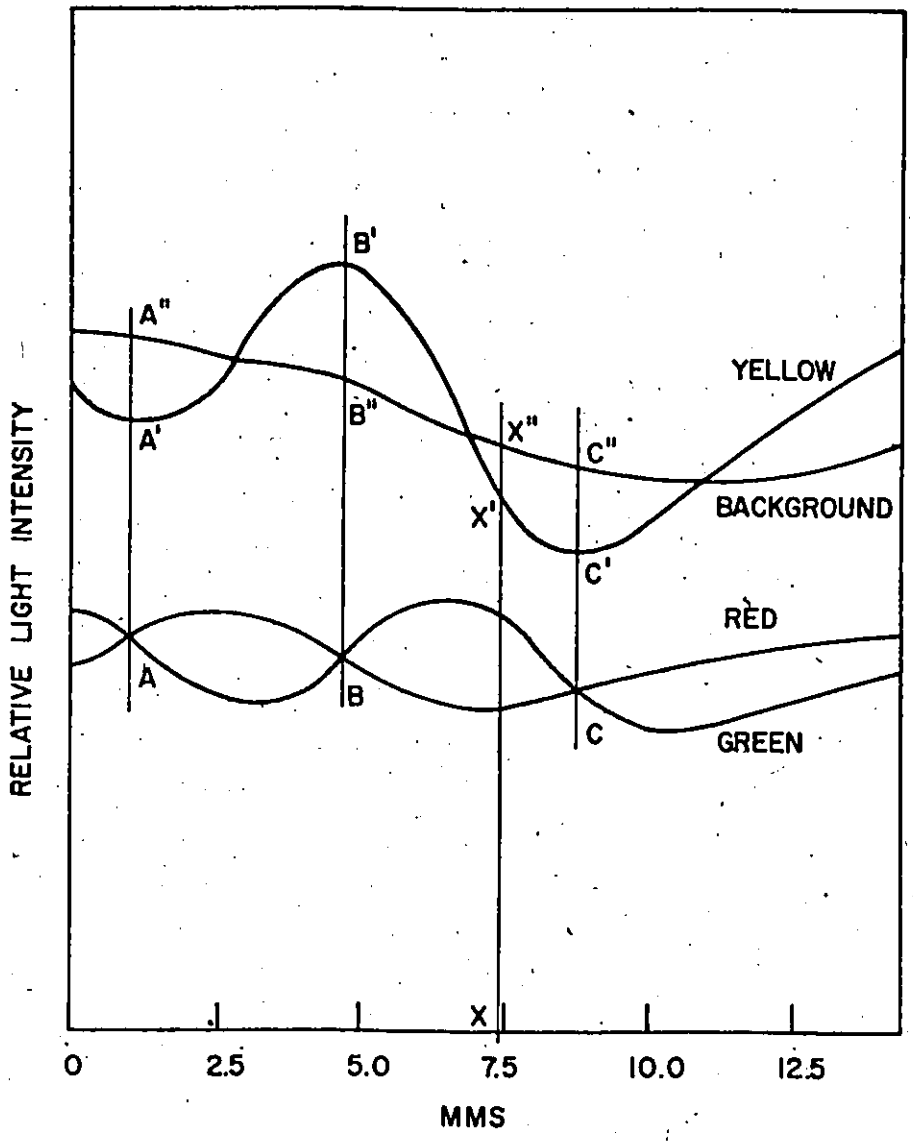

FIGURE A.17 SUPERIMPOSED SCANS